EXAMINATION OF THE LATERAL RESISTANCE OF CROSS-LAMINATED TIMBER PANEL-TO-PANEL CONNECTIONS

Benjamin Lee Richardson

Thesis submitted to the faculty of the Virginia Polytechnic Institute and State University in partial fulfillment of the requirements for the degree of

MASTER OF SCIENCE

IN

FOREST PRODUCTS

Daniel P. Hindman, Chair

Matthew R. Eatherton

Earl D. Kline

24 September, 2015

Blacksburg, Virginia

Keywords: Cross-Laminated Timber, Lateral Resistance, Shear Resistance, Wood Connections

EXAMINATION OF LATERAL RESISTANCE OF CROSS-LAMINATED TIMBER CONNECTIONS IN PANEL-PANEL CONNECTIONS

Benjamin Lee Richardson

Abstract

Cross-Laminated Timber (CLT) combines layers of dimension lumber in alternating grain direction to form a mass timber panel that can be used to create entire wall, floor and roof elements. The viability of CLT as an element to resist lateral forces from racking has been of great interest (Dujic et al. 2004, Blaß and Fellmoser 2004, and Moosbrugger et al. 2006). However, most research to date has been conducted on full-scale wall panels connected with proprietary fasteners according to European Test Methods. Little research has focused on non-proprietary connections, including nails, bolts and lag screws. The behavior of CLT full-scale wall panels is dependent upon the individual connection properties including the panel-panel connections between adjoining CLT panels within the wall.

The purpose of this research is to evaluate the behavior of three small-scale CLT connection configurations using non-proprietary fasteners. Three different connections -LVL surface spline with lag screws, half-lap joint with lag screws, and butt joint with a steel plate fastened with nails – were tested in both monotonic and cyclic tests. In all, 30 connection tests were conducted, with 15 monotonic test and 15 cyclic tests. Connection strength, stiffness, and ductility were recorded for each connection. Experimental values were compared to *National*

Design Specification for Wood Construction, or NDS (AWC 2012) predictions for connection strength.

Nailed steel plate connections yielded much greater loads and behaved in a more ductile manner than did the lag screwed connections. The surface spline and half-lap connections often failed in a catastrophic manner usually due to splitting of the spline and fastener failure. Experimental results were generally lower than predicted by the yield models for the surface spline and steel plate connections. The half-lap connection resulted in higher experimental results than predicted. A discussion of the connection strength for materials with a non-homogeneous grain direction is also included.

Acknowledgements

I would like to thank all of my committee members for their invaluable input and most of all, for their patience and understanding. I want to thank Dr. Hindman for our talks and words of encouragement at times when I thought the world had ended. You motivated me at times when I wanted to throw in the towel. I want to thank Dr. Loferski, who was originally on my committee. Your advice was integral to the research. Thank you to Dr. Kline who stepped up at the last minute to join my committee. I'll never forget that. Thank you to Dr. Eatherton who agreed to join a committee for a Forest Products student. I'm still not sure how I convinced you to do that.

I also want to thank Rick Caudill for the countless hours he spent setting up the test machines. You are a major part of the success of this research, and thank you for being around to complain to. Thank you to David Jones for letting me annoy you in the wood shop. I apologize if I still have any CLT pieces lying around in there.

I also want to thank my fellow students Milad Mohamadzadeh, Thomas McNicol, Khris Beagley and everyone else in our student office for the jokes and laughter that helped keep me sane during the process. I'll miss all of you.

Table of Contents

List of Figures

List of Tables

Chapter 1: Introduction

1.1 Introduction

Few building materials possess the numerous advantages that can be associated with wood. Not only has wood found uses in aesthetic applications in buildings, but also use in structural capacities all over the world. This widespread use can be attributed to the availability, low-cost of production, good strength to weight ratio, and identity as a renewable resource. Traditional structural elements made from wood were restricted to shapes and geometries that could be sawn or carved directly from the bole of the tree. However, advancements in wood machining and resin technology allowed for smaller pieces of wood with fewer defects to be glued together into larger structural wood elements. These new wood materials, called engineered wood products, allowed manufacturers to create wood panels like plywood and oriented strand board (OSB), as well as higher quality beams and columns that can span much larger distances than any solid sawn member could.

Until recently, larger structural engineered wood elements consisted of layers of wood with a homogeneous grain direction, limiting the direction of loading to a single axis. Engineered wood products that alternate grain direction, such as plywood and OSB, give the material the advantage of having strength along two axes, but are limited in size and are required to be attached to structural framing members for support. Manufacturers sought to create a high strength product that also had the advantage of strength along two axes. That effort resulted in a new product known as cross-laminated-timber.

Cross-laminated-timber is a mass timber panel that is created by laminating strips of lumber into alternating layers (according to grain direction). CLT was conceived in Austria and

Germany in the 1990s and has grown significantly in popularity in Europe ever since. CLT in North America is very much in its infancy but is beginning to gain more and more attention. The gain in popularity of this material is due partially to the "green movement" or the shift to sustainable building methods and materials, as well as the inherent advantages that are intrinsic to the material. Since CLT is a prefabricated material, there is greater attention to quality control during the manufacture process than what is seen in traditional on-site wood frame construction. The perception of CLT as a heavy timber or "non-light" construction material makes it comparable to precast concrete and masonry. Unlike precast concrete, the machinability of wood allows for easier alterations on-site. Since CLT panels are much lighter in weight when compared to precast concrete, material handling is easier in terms of transportation and manipulation in the field. The ease of material handling and the high degree of prefabrication allow for greatly reduced erection times in the field. Good thermal insulation and fair sound insulation are also added benefits of the material.

The hope for the future of CLT is use as a primary building material in multi-story construction. As population and urbanization increases, the demand for high rise multi-family dwellings also increases. Increased awareness of the need for structures that are more sustainable and less damaging to the environment has positioned CLT in a very opportunistic place in the world of structures. One hurdle for the use of CLT in multi-story construction is understanding the effects of alternating grain direction on connection design. Current connection design methodologies presented in the *National Design Specification for Wood Construction*, or NDS (AWC 2012), only consider a homogeneous grain direction in the wood material.

Current research into lateral resistance of CLT connections has largely focused on proprietary, long self-tapping screws (Uibel & Blass 2007, Muñoz *et al.* 2010). Another study

utilized numerous fastener types including proprietary and common dowel-type fasteners in full-scale wall sections (Popovski *et al.* 2010). However, failure quickly occurred in the joints that connected the wall panels to the foundation, preventing further measurements of shear deformations between the vertical wall panels. Given the popularity of CLT in Europe, and since the use of CLT in the United States is still in its infancy, little to no research on the lateral resistance of CLT connections has been performed utilizing ASTM test methods and very little research on non-proprietary fasteners has been conducted.

1.2 Objectives

The purpose of this research project is to quantify the strength and stiffness of several selected CLT connection configurations and compare them against predicted values from the NDS (AWC 2012). Currently, all research conducted on CLT connections have been conducted according to European standards (EN) and mostly full-scale testing, and using proprietary fastening systems. This research will utilize procedures based on ASTM methods to evaluate CLT connections fastened with non-proprietary fasteners, and investigate the validity of the NDS for predicting connection strengths. The objectives of this project were:

(1) Evaluate connection shear strength and shear stiffness of selected CLT joints through monotonic mechanical testing.
(2) Compare results of monotonic testing to predicted values from the NDS.
(3) Evaluate connection shear strength, shear stiffness and ductility of selected CLT joints through cyclic mechanical testing.

1.3 Significance

Attainment of the goals of this research will provide insight into the behavior of the lateral resistance of CLTs mechanically fastened with non-proprietary dowel-type fasteners. The results of this research may influence the need for new models to predict design loads for CLT connections. This research may provide further insight into the effects of cyclic loading on CLT panels and is therefore valuable for lateral wall design.

Chapter 2: Literature Review

2.1 Introduction

Understanding the characteristics of connections is essential to designing a functional and safe structure. Connections must be able to carry loads from attached structural elements and transfer those loads to the supporting structure and ultimately through the foundation into the ground. Connections are crucial to providing strength, rigidity, and ductility to the structure. Inadequate design of connections can lead to catastrophic failure of the structure. This chapter discusses current design methodologies for conventional wood connections and possible shortcomings for designing CLT connections. Also included in this chapter is a summary of the current research on the lateral resistance of CLT connections.

2.2 Wood Connection Design Methods

The *2012 National Design Specification for Wood Construction* (NDS) (AWC 2012) defines the methods for the structural design of wood products and is the reference manual for designing wood connections. The 2012 NDS utilizes the European Yield Model (EYM) to determine connection strength for dowel-type fasteners. The EYM is a mechanics based model (Johansen 1949) and is used to predict the yield behavior in dowel-type connections. Prior to Johansen, Trayer (1932) conducted testing on lateral loading of single fastener, dowel-type connections. Trayer (1932) concluded that connection strength was primarily influenced by bolt-bearing stress and was a function of the bolt diameter and length. The design values from Trayer (1932) testing formed the basis for many of the fastener spacing requirements presented in the 2012 NDS (AWC 2012).

Johansen (1949) investigated the yield behavior in dowel-type connections, and created a yield model incorporating the effects of dowel bearing strength and dowel bending strength to predict yielding of dowel-type connections. The current European Yield Model includes the formation of multiple plastic hinges and the effects of wood crushing, and also switched from a proportional limit based design to a yield based design (Soltis and Wilkinson 1987).

2.2.1 Yield Limit Equations

The yield limit equations presented in the 2012 NDS (AWC 2012) are used to predict yield behavior in single and double shear connections. Four main yield modes are defined by the equations in Table 2-1. The yield modes are characterized by: bearing in the main or side members (Mode I), fastener rotation without bending (Mode II), development of a single plastic hinge (Mode III), and development of two plastic hinges in both the main and side members (Mode IV). The yield modes are depicted in Figure 2-1.

Table 2-1: NDS Yield Limit Equations for Single Shear (AWC 2012)

Yield Mode	Single Shear
I_m	$Z = \frac{D\ l_m F_{em}}{R_d}$
I_s	$Z = \frac{D\ l_s F_{es}}{R_d}$
II	$Z = \frac{k_1 D\ l_s F_{es}}{R_d}$
III_m	$Z = \frac{k_2\ D\ l_m\ F_{em}}{(1 + 2R_e)R_d}$

III_s	$Z = \frac{k_3 \, D \, l_s \, F_{em}}{(2 + R_e)R_d}$
IV	$Z = \frac{D^2}{R_d}\sqrt{\frac{2 \, F_{em} \, F_{yb}}{3(1 + R_e)}}$

Where,

$$k_1 = \frac{\sqrt{R_e + 2{R_e}^2\left(1 + R_t + {R_t}^2\right) + {R_t}^2{R_e}^3} - R_e(1 + R_t)}{(1 + R_e)}$$

$$k_2 = -1 + \sqrt{2(1 + R_e) + \frac{2F_{yb}(1 + 2R_e)D^2}{3F_{em}{l_m}^2}}$$

$$k_3 = -1 + \sqrt{\frac{2(1 + R_e)}{R_e}} + \frac{2F_{yb}(2 + R_e)D^2}{DF_{em}{l_s}^2}$$

And,

D = diameter, in.

F_{yb} = dowel bending strength, psi.

R_d = reduction term

$R_e = F_{em}/F_{es}$

$R_t = l_m/l_s$

l_m = main member dowel bearing length, in.

l_s = side member dowel bearing length, in.

F_{em} = main member dowel bearing strength, psi

F_{es} = side member dowel bearing strength, psi

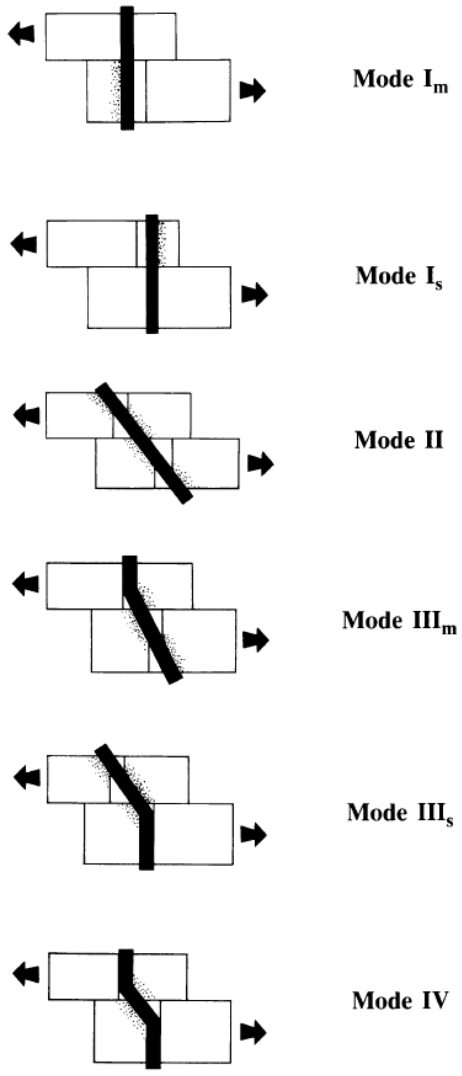

Figure 2-1: 2012 NDS Single Shear Yield Modes (AWC 2012)

One consideration for grain direction presented in these equations is for the term θ, which is used to calculate the Reduction Term (R_d) as presented in Table 2-2. Here, θ is defined as the maximum angle between the direction of load and the direction of grain for the connected members. Therefore, θ only accounts for a material with a consistent grain direction. The only other consideration for grain direction is in the dowel bearing terms for the main member (F_{em}) and the side member (F_{es}). Since CLT consists of layers of material with alternating grain

direction, θ may not be adequate to define the material. Seemingly, assuming one grain direction would yield lower experimental results than predicted for loads applied parallel to grain, and higher experimental results than predicted for loads perpendicular to grain for CLT. Further experimentation to validate the ability of θ to describe a material with a non-homogeneous grain direction is necessary.

Table 2-2: 2012 NDS Reduction Term, R_d (AWC 2012)

Fastener Size	Yield Mode	Reduction Term, R_d
0.25" ≤ D ≤ 1"	I_m, I_s	4 K_θ
	II	3.6 K_θ
	III_m, III_s, IV	3.2 K_θ
D < 0.25"	I_m, I_s, II, III_m, III_s, IV	K_D

Where,

$K_\theta = 1+0.25(\theta/90)$

θ = maximum angle between the direction of load and the direction of grain ($0° \leq \theta \leq 90°$) for any member in a connection

D = diameter, in.

$K_D = 2.2$ for $D \leq 0.17$"

$K_D = 10D + 0.5$ for 0.17" < D < 0.25"

2.2.2 Dowel Bearing Strength

Dowel bearing strength is the ability of wood to resist forces imposed by the length of a dowel pressing into the wood. Dowel bearing strength is based on the yield strength of wood and is found by offsetting a line parallel to the slope of the proportional limit of the load-deformation curve by 5% off the fastener diameter, and is taken as the point where that offset line intersects the load-deformation curve. This method for determining dowel bearing strength stemmed from the work of Soltis and Wilkinson (1991). Dowel diameter was determined to only be a significant factor in dowel bearing strength when the specimen was loaded perpendicular to the grain (Soltis and Wilkinson 1991). This is evidenced by the equations for determining dowel bearing strength according to Equation 2-1, relating to parallel to grain loading, and Equation 2-2, relating to perpendicular to grain loading, as presented in the 2012 NDS (AWC 2012).

$$Fe_{\parallel} = 11200G \qquad (2\text{-}1)$$

Where,

$Fe_{\parallel}$ = Dowel bearing strength parallel to grain, psi.

G = Specific Gravity

$$Fe_{\perp} = 6100G^{1.45}/\sqrt{D} \qquad (2\text{-}2)$$

Where,

$Fe_{\perp}$ = Dowel bearing strength perpendicular to grain, psi.

G = Specific Gravity

Uibel and Blaß conducted 620 embedment tests on CLT according to EN 383 (EN 383 1993) with loads being applied at 0°, 45° and 90° to the grain direction of the outer layers and at different locations within the CLT (Uibel and Blaß 2006). Uibel and Blaß (2006) found good correlation between experimental results and predictions for nails and screws from their model based on fastener diameter and wood density. However the validity of this approach was limited to panels with layers less than 7mm thick.

Kennedy *et al.* (2014) conducted 720 dowel-bearing strength tests utilizing ASTM D5764 (ASTM 2007) with lag screws on CLT and compared the results to different design approaches including those presented in the 2012 NDS (AWC 2012). From this testing, it was concluded that a poor level of safety was achieved with many of the predicted values from the 2012 NDS being non-conservative (Kennedy *et al.* 2014).

2.2.3 Fastener Spacing

Fastener spacing requirements presented in the 2012 NDS (AWC 2012) are based on early research by Trayer (1932). The geometry factor, C_Δ, is the result of edge, end, and spacing considerations. When $C_\Delta = 1.0$, all minimum edge, end and spacing requirements have been fully incorporated, C_Δ is reduced when these conditions aren't met, or are partially met. Figure 2-2 below is an illustration of fastener spacing nomenclature.

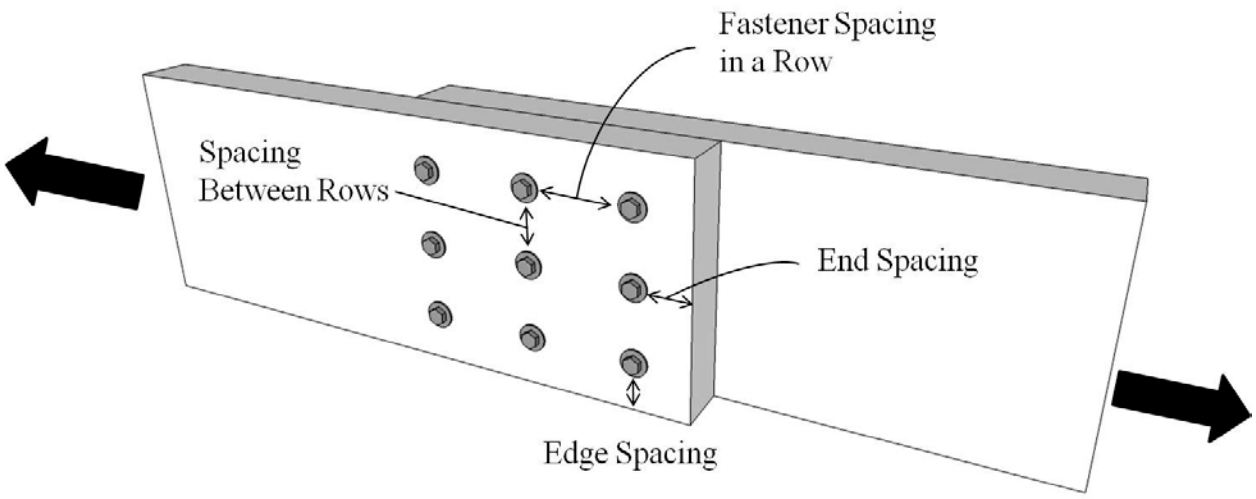

Figure 2-2: Fastener Spacing Illustration

End distance is a measurement of the length between the end of a member and the center of the nearest fastener parallel to the direction of loading. For bolted connections in compression parallel to grain, C_Δ = 1.0 when the end distance is 4 times the diameter (*D)*. When loaded in tension parallel to the grain, end distance must be 7*D* for softwoods and 5*D* for hardwoods. Perpendicular loading requires 4*D* spacing for both tension and compression. For nailed connections with steel side members, end distance is 10*D* and 5*D* for tension and compression parallel to the grain respectively (not prebored). End distances less than 50% of those required for C_Δ=1.0 are not allowed (AWC 2012).

Edge distance is described as the distance from the edge of the connected member to the center of the nearest fastener in the connection. For bolted connections loaded parallel to grain and having a length to diameter ratio less than or equal to 6, minimum edge distance is 1.5*D*. When the length to diameter ratio is greater than 6, minimum edge distance is taken as 1.5*D*, or half the distance between rows, whichever is greater. The length to diameter ratio is the lesser of

the length of the fastener in the wood main member, or the total length of the fastener in wood side members. Perpendicular to grain loading in relation to edge distance, is categorized by the loaded edge or unloaded edge. Load applied perpendicular to grain, requires an edge spacing of 4*D* at the loaded edge and 1.5*D* at the unloaded edge in bolted connections. In nailed connections with steel side members, edge distance is 2.5*D* (AWC 2012).

Fasteners in a row are considered to be fasteners in a line and are parallel to the direction of load. Spacing requirements for fasteners in a row for parallel to grain loading is 4*D* to reach a $C_{\Delta} = 1.0$ in a bolted connection. Spacing below 3*D* is not allowed in bolted connections. For nailed members with steel side members, minimum spacing between fasteners in a row is 10*D* parallel to grain, and 5*D* for perpendicular to grain loading (AWC 2012).

Spacing requirements between rows is the minimum distance between the on-center spacing of fasteners perpendicular to the direction of load. In bolted connections, minimum spacing is 1.5*D* parallel to grain. When load is applied perpendicular to the grain in bolted connections, spacing is based on the length to diameter ratio. Where the length to diameter ratio is less than or equal to 2, minimum spacing is 2.5*D*. When length to diameter ratio is greater than 2 but less than 6, minimum spacing is between rows is $(5l + 10D)/8$. For ratios greater than or equal to 6, fastener spacing is 5*D*. For nailed connections with steel side members, the minimum spacing for fasteners between rows is 3*D* when fasteners are in line, and 2.5*D* when staggered (AWC 2012).

2.3 Typical CLT Connections

Currently, there exist many different methodologies for adjoining CLT panels to create continuous members such as walls and floors or to create intersections such as those that would

occur at wall to wall, wall to floor, and roof to wall corners. These connections may be to other CLT panels, wood based systems, concrete or steel. While proprietary and more elaborate connection systems are available, most CLT to CLT connections are created mechanically through the use of dowel-type fasteners such as nails, screws and bolts.

The Canadian *CLT Handbook* from FP Innovations identifies five different types of connection details that are created by joining CLT panels to other panels and the foundation; they are: panel-to-panel, wall-to-wall, wall-to-floor, wall-to-roof, and wall-to-foundation (FP Innovations 2011). This thesis focuses on panel-to-panel connections.

2.3.1 Panel-to-Panel Connections

The panel-to-panel connection is the most basic form of connection is used to create wall and floor assemblies. Connections of this type are characterized by the joining of panels along their edges in order to create continuous wall or floor sections. When used in a wall, panel-to-panel connections are responsible for transferring shear forces from lateral loads. The *CLT Handbook* identifies several different methods for creating panel-panel connections, such as the internal spline, surface spline, half-lap joint and others (FP Innovations 2011).

2.3.1.1 Internal Spline

An internal spline connection is created by inserting a piece of solid lumber or structural composite lumber into a void that has been milled into edge of the CLT panel at the factory. The spline is then secured in place with fasteners such as wood screw or self-tapping screws (Figure 2-3).

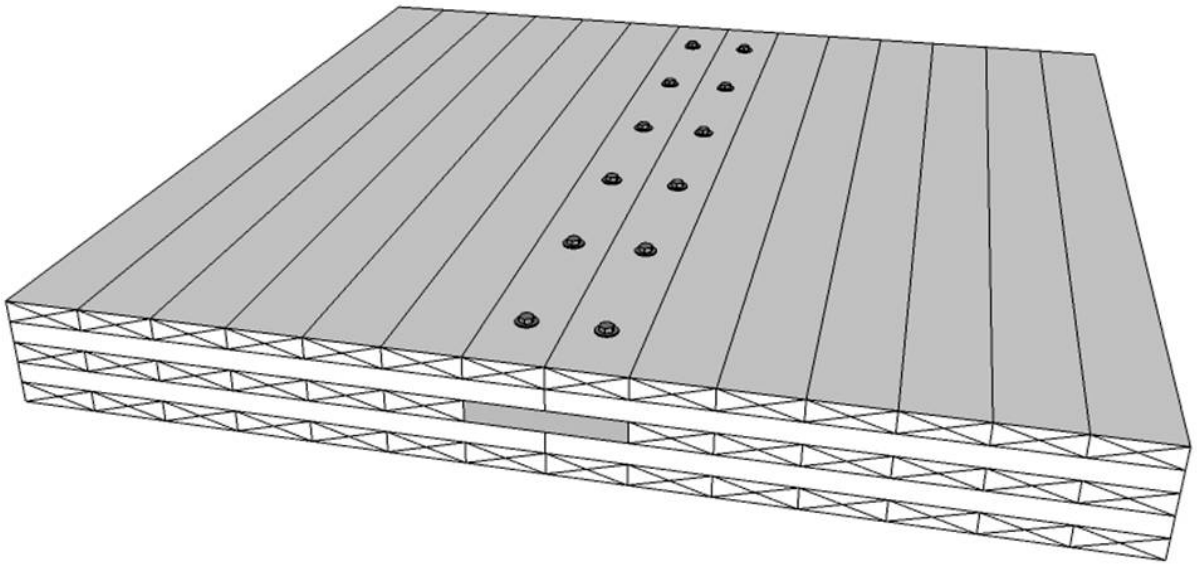

Figure 2-3: Illustration of the Internal Spline Joint

2.3.1.2 Surface Spline

A surface spline connection can be located on two faces (double surface spline) or on a single face (single surface spline). This connection is similar to an internal spline, except that the spline is located on the face or faces of the CLT panel (Figure 2-4). The splines are then held in place with dowel-type fasteners. Surface spline connections require the panel to be profiled for the connection during manufacture. Exposure of the surface spline makes this connection easier and quicker to do on site when compared to the internal spline.

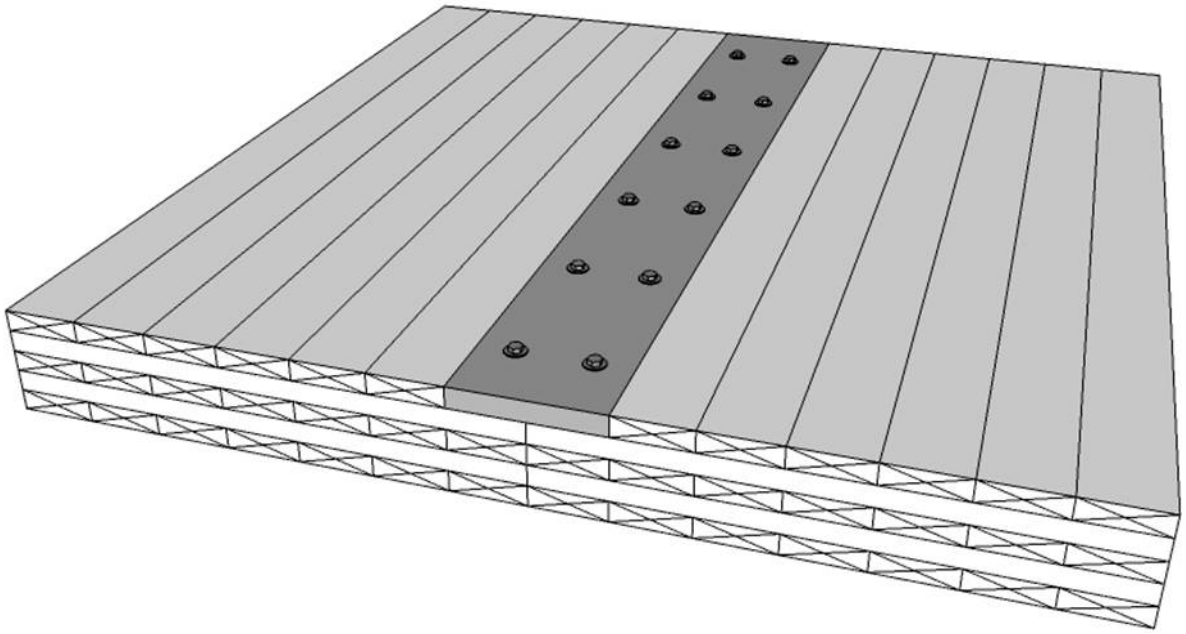

Figure 2-4: Illustration of Single Surface Spline Joint

2.3.1.3 Half-lapped Joint

A half-lap joint is created by removing half of the material at the edge of the panel to a specified depth into the sides of the panels that are to be joined. The remaining half of the material then overlaps the remaining half of the material of the adjoining panel (Figure 2-5). The panels are then screwed into place with wood screws or self-tapping screws.

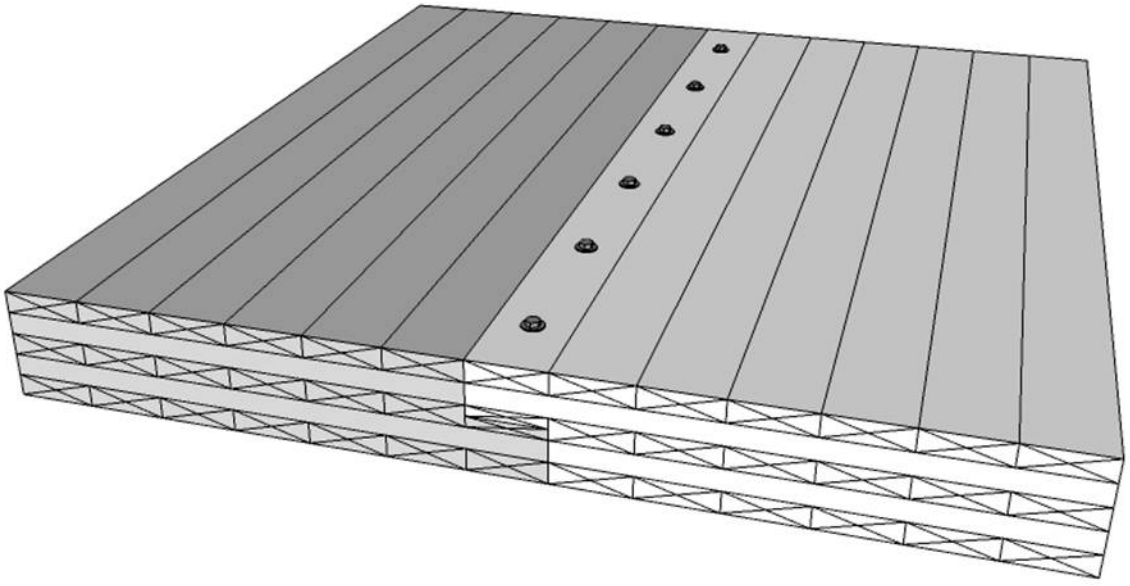

Figure 2-5: Illustration of the Half-Lap Joint

2.4 CLT Connection Research

In the US, many houses and buildings are created by erecting a frame of dimension lumber and sheathed with either OSB or plywood. This sheathing acts to stabilize the structure against racking due to horizontal loads generated by wind or seismic events. In structures that contain many openings for windows and doors, this method of mechanically fastening sheathing to stud framing may not provide enough shear resistance. In such structures, the viability of CLT in intermittent wall segments or as entire wall constructions was explored (Dujic et al. 2004, Blaß and Fellmoser 2004, and Moosbrugger et al. 2006). As interest in CLT grows, the need for a better understanding of how to connect panels will increase in importance.

2.4.1 Vessby et al. 2009

Vessby et al. (2009) investigated the structural performance of five-layer CLT elements. Two connection types were tested and compared to solid CLT specimens that contained no joinery. The first was a purely mechanical connection using hex-head screws to secure a single spline placed in the center of the two panels and screwed from both sides. The second utilized both screws and glue to secure fiber board to the outsides of the panels from the front and the back. Two tests were conducted. The first test utilized the two upright connected panels secured at the bottom, just as they would be in a building, and applied a load at the top corner of the connected panel (shear). Since the specimens were short deep beams, the second test laid the panels flat on the ground, supported on the left and right edge and applied a load in the center of the connected panel at the connection to induce shear from bending. (Vessby et al. 2009)

Catastrophic failures were observed for the solid sawn internal spline connection. This type of connection was half as stiff and yielded a much lower ultimate load than the glued and screwed fiberboard surface spline. The fiberboard surface spline specimens yielded nearly identical results to the non-jointed control group. The authors speculate that the high level of stiffness obtained for the surface spline connections, indicates a strong potential for use of CLT in structures (Vessby et al. 2009).

2.4.2 Joyce et al. (2011)

Joyce et al. (2011) conducted research in order to better understand the performance of wall-to-wall connections by investigating the static and dynamic properties of common connections. These connections were subjected to tensile and in-plane shear forces. Two connections were investigated, a double spline and angled screws in two different fastener

variations. The CLT used was 3 layers thick at 112mm. The boundaries were notched to allow the Douglas fir plywood spline to sit flush. (Joyce et al. 2011)

From monotonic testing, a relatively high degree of correlation was seen for all of the connections except the partially threaded angled screws. Angled screws yielded higher stiffness values than the double spline. The failure of the double spline was determined to be due to the formation of plastic hinges. Consistent pull through of the screw head through the plywood was seen. In the angled screws the failure was found to be due to the splitting of the outer lamination of the CLT due to forces acting perpendicular to the grain. This was slightly mitigated by the use of fully threaded screws which provided additional embedment strength. Results from cyclic testing showed significant agreement with monotonic testing and a clear pinching effect at high displacements. Fully threaded screws provided the highest stiffness values compared to any other test. (Joyce et al. 2011)

2.4.3 Gavric et al. 2012

Early seismic testing of a full scale one story CLT building (Lauriola and Sandhaas 2006) and a three story CLT building (Ceccotti 2008) demonstrated that CLT structures were able to survive a series of strong earthquakes with virtually no damage to the structure. However, the authors felt that further research was needed in order to better characterize the seismic behavior of CLT connections. The study used 20 different specimens in four different set ups. The tested connections were lap joints and spline joints made from LVL. The connections were then tested in parallel and perpendicular configurations. Additionally, panels simulating perpendicularly connected walls (wall-wall), panels simulating wall -floor connections, and panels simulating floor-floor connections were tested. Each specimen was subjected to at least one monotonic test

and several cyclic tests. The authors found that the lap joints yielded a higher stiffness than the LVL spline, but often resulted in catastrophic failure. Results showed that LVL spline joints could resist greater forces at higher displacements than the lap joints. (Gavric et al. 2012)

Chapter 3: Methods and Materials for CLT Connection Testing

This section describes the methods and materials used for CLT panel-panel connection testing. The purpose of this research is to quantify the strength and stiffness of several selected CLT connection configurations connected with non-proprietary fasteners and compare the experimental results against predicted values from the NDS (AWC 2012).The following sections detail monotonic testing, a comparison of experimental results to the *National Design Specification for Wood Construction,* NDS (AWC 2012), and cyclic (reversed) testing of CLT connections.

3.1 Materials and Connections Tested

CLTs were made up of 5 layers of No. 2 Southern Pine (*Pinus spp.*) bonded with a single component polyurethane adhesive, and manufactured at the Southern Virginia Higher Education Center in South Boston, VA (Hindman et al. 2015). Since restrictions on test specimen size existed due to limitations of testing apparatuses, full scale testing was not possible. Therefore, specimen size was scaled down and each connection studied was a localized area around the connection. Each connection configuration consists of mechanically connecting a 12” by 12” by 6 7/8” CLT block to either a 12” by 18” block for monotonic testing, or a 12” by 24” block for cyclic testing (Figure 3-1). The extra length of the cyclic specimen allowed the crosshead to move up and down without contacting the 12” by 12” test specimen. The CLT blocks were positioned to be flush at the bottom for monotonic testing and centered to to allow for overhang at the top and bottom for cyclic test specimens (Figure 3-1). Three separate panel-to-panel connections were selected for this study, including a single surface spline, a butt joint with a steel plate connector, and a half-lap joint. Since one objective of this thesis was to determine the

validity of the NDS to predict the strength of these CLT connections, all fasteners used were non-proprietary and capable of being specified by the NDS. Direction of grain when connecting the CLT blocks runs top to bottom in in the face layer in order to simulate the orientation of the block within a full size CLT panel.

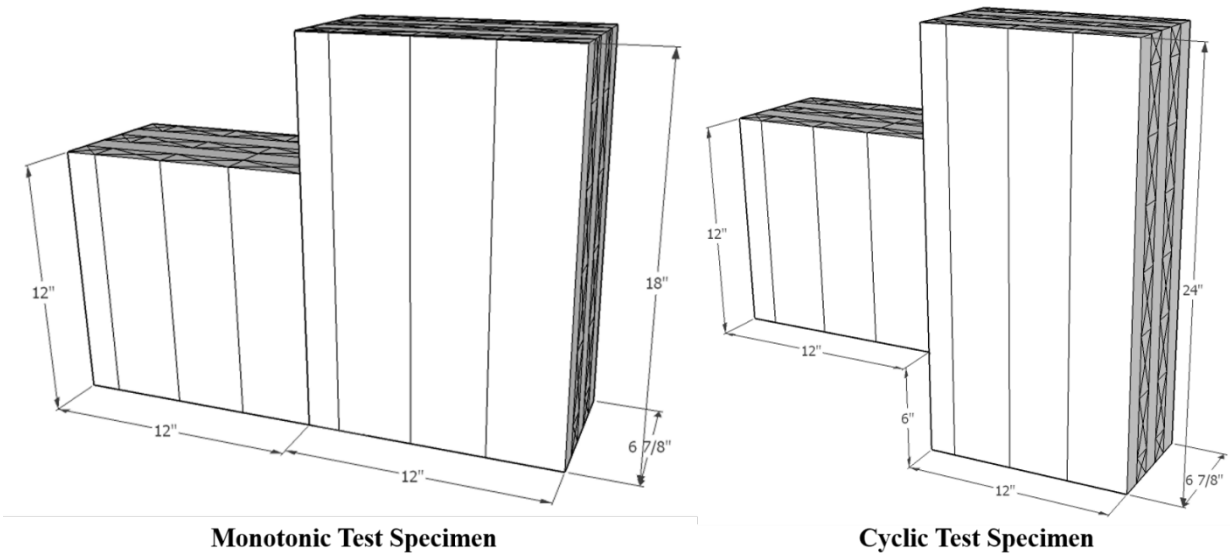

Figure 3-1: CLT Block Specimens

Figure 3-2 is a schematic drawing of the surface spline connection used for monotonic testing. First, a slot 1.75 inches deep and 4 inches wide was removed from the front face of each CLT block. Then, a 1.75 inch x 8 inch 2.0E RigidLam LVL measuring 12 inches long was used as the spline member and attached with ¼ inch diameter x 6 inch long lag screws and standard cut washers according to the fastener spacing diagram in Figure 3-2. Fastener spacing is in accordance with the minimum requirements set forth by the NDS (AWC 2012). Lag screws were installed by the pre-boring method described in Section 11.1.4.2 of the NDS (AWC 2012). Cyclic test specimens were created in the same fashion. Fastener spacing and spline dimensions were identical to monotonic specimens. The CLT blocks were positioned as shown in Figure 3-1.

To allow for a greater sample size for monotonic and cyclic testing, an additional joint was added to the face of the larger specimen allowing the specimen to be tested twice. Since failure was predicted to occur in the fastener and a localized area of the wood around the fastener, the wood at the location of the second joint remained unstressed permitting further testing.

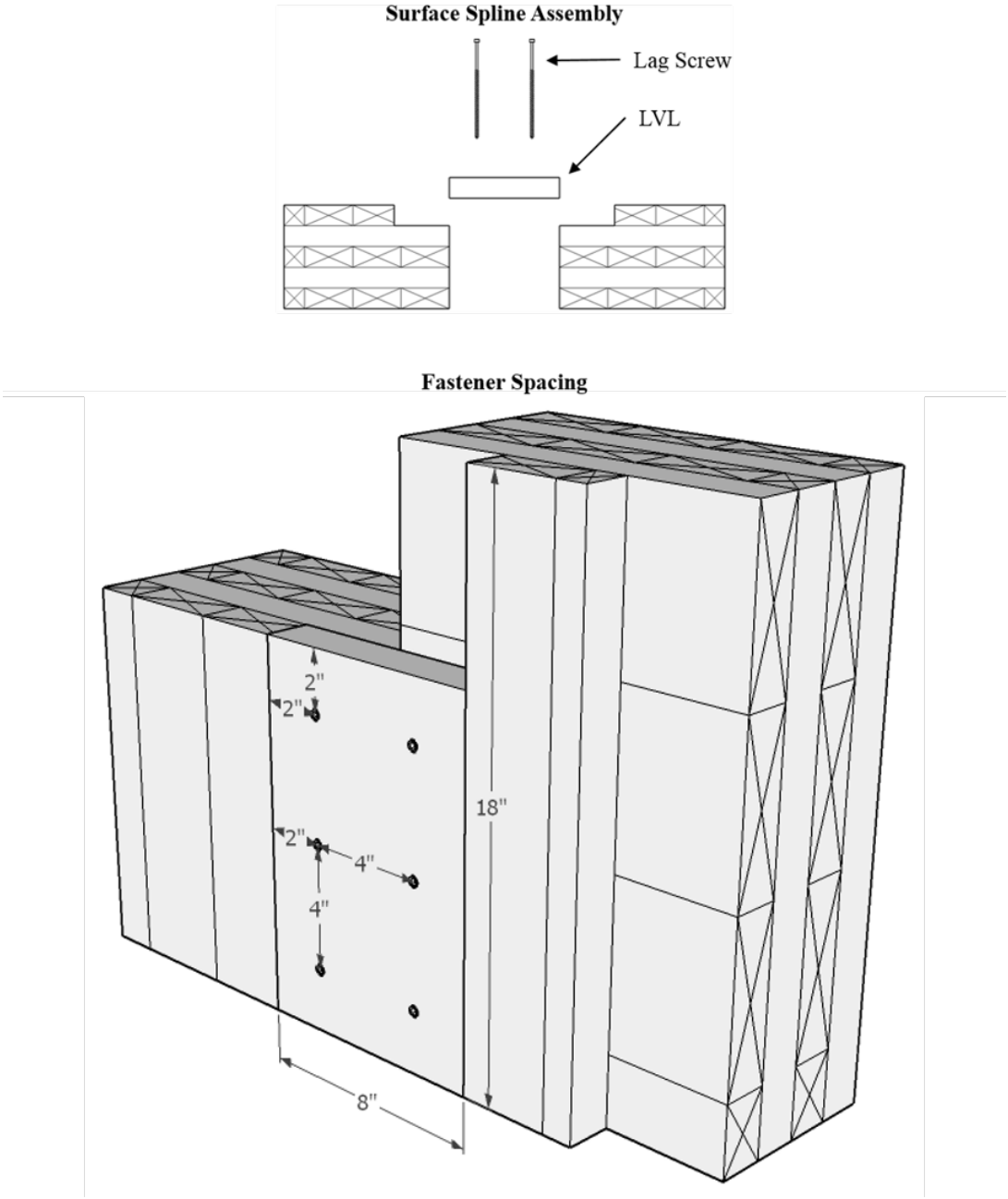

Figure 3-2: Surface Spline Assembly and Fastener Spacing

Figure 3-3 is a schematic of the butt joint with a one-sided steel plate connector for monotonic testing. CLT blocks were simply “butted” together and joined by a steel plate fastened with nails. The steel plate used was an 11 gauge (0.120”) ASTM-653, Grade 33 galvanized steel plate. Holes were drilled in the plate for eight 16d common wire nails measuring 0.162 inches in diameter by 3.5 inches in length to be inserted into each panel face for a total of sixteen nails. Fastener spacing is depicted in Figure 3-3 and all spacing meets the requirements of the NDS (AWC 2012). Cyclic test specimens were created in the same fashion. Fastener spacing and steel plate dimensions were identical to monotonic specimens. The CLT blocks for cyclic testing were positioned as shown in Figure 3-1. To allow for a greater sample size for monotonic and cyclic testing, the larger specimen was retested at an area not affected by previous testing. Since failure was predicted to occur in the fastener and a localized area of the wood around the fastener, the wood at the location of the second joint remained unstressed after initial testing, permitting a second test.

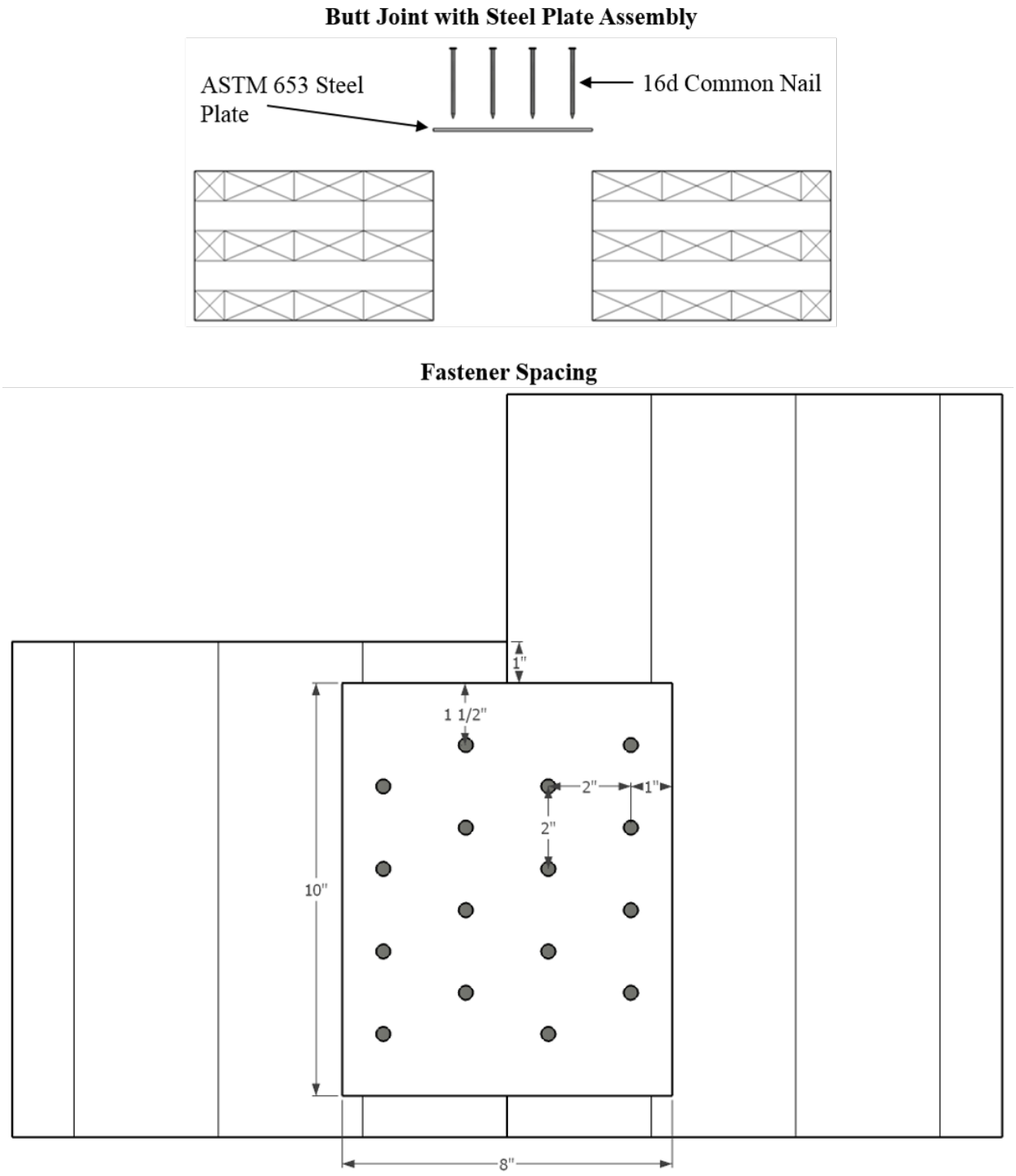

Figure 3-3: Butt Joint with Steel Plate Assembly and Fastener Spacing

Figure 3-4 is a schematic of the half-lap joint. A section 4 inches long by 3 7/16 inches deep was removed from each of the CLT blocks to create an interlocking joint. The two blocks were then fastened with ¼ inch diameter by 6 inch long lag screws and standard cut washers according to the fastener spacing shown in Figure 3-4. Fastener spacing meets the requirements detailed in the NDS (AWC 2012). Lag screws were installed by the pre-boring method described in Section 11.1.4.2 of the NDS (AWC 2012). Cyclic test specimens were created in the same fashion. Fastener spacing and joint details were identical to monotonic specimens. The CLT blocks for cyclic testing were positioned as shown in Figure 3-1. To allow for a greater sample size for monotonic and cyclic testing, an additional joint was added to the face of the larger specimen allowing the specimen to be tested twice. Since failure was predicted to occur in the fastener and a localized area of the wood around the fastener, the wood at the location of the second joint remained unstressed permitting further testing.

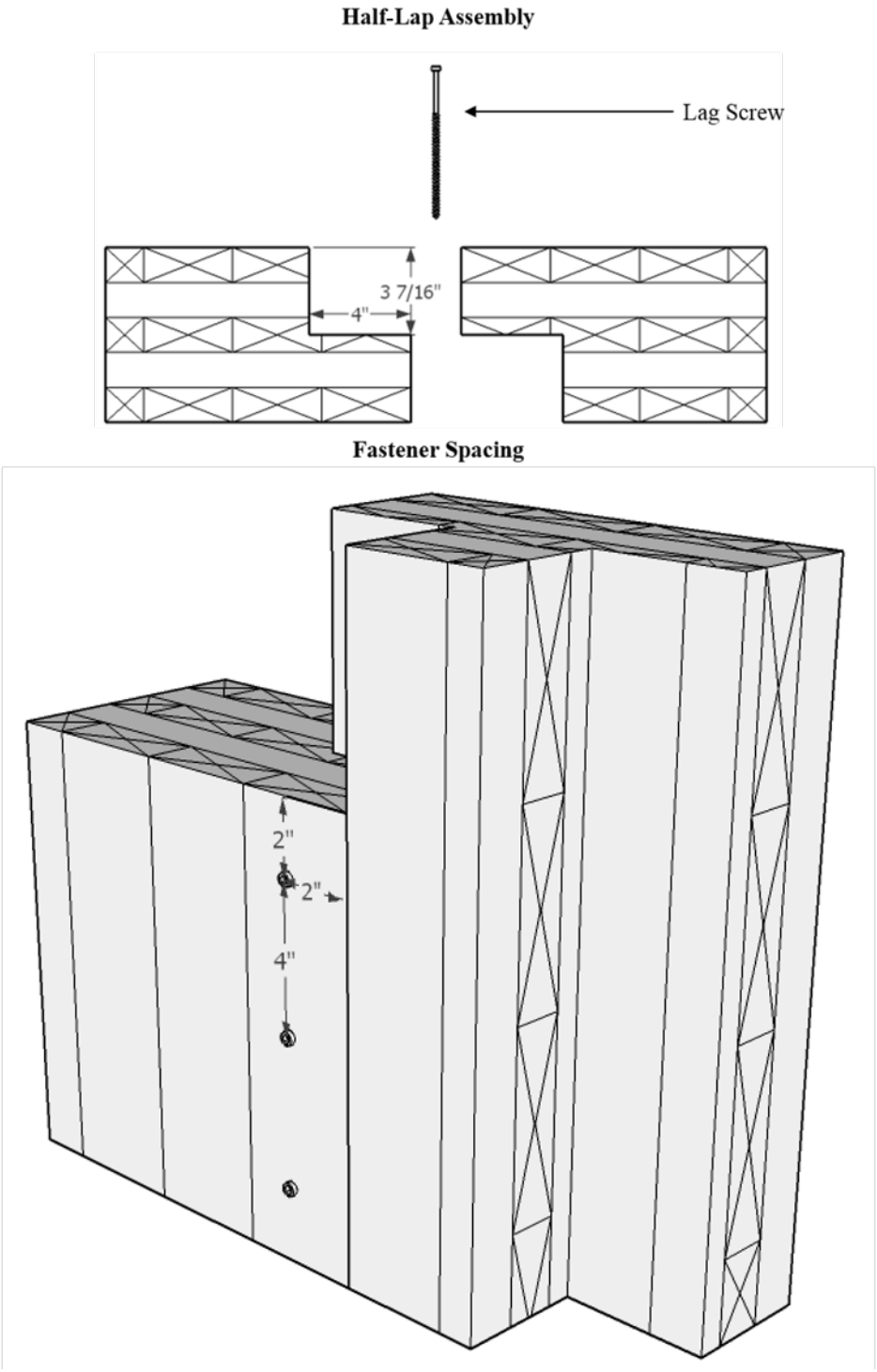

Figure 3-4: Half-Lap Assembly and Fastener Spacing

The treatments and sample size for monotonic and cyclic (reversed) shear testing of CLT connections are shown in Table 3-1. For each testing type, static and cyclic, five specimens were tested for each of the three CLT connection types resulting in thirty total tests.

Table 3-1: CLT Connection Test Schedule

Connection Type	Fastener	No. of Fasteners in Each Panel Face	Total No. of Fasteners	Number of Monotonic Specimens	Number of Cyclic Specimens
Surface Spline	¼" x 6" Lag Screw	3	6	5	5
Butt Joint w/ Steel Plate	16d common nail (0.162 x 3.5")	8	16	5	5
Half-Lap	¼" x 6" Lag Screw	3	3	5	5
			Total	15	15

3.2 Objective 1: Monotonic Connection Testing

All testing was conducted in the Wood Engineering Lab at the Thomas M. Brooks Forest Products Center at Virginia Tech. Connection test procedures were modelled after ASTM D1761-12, *Standard Test Methods for Mechanical Fasteners in Wood* (ASTM 2012).

3.2.1 Monotonic Test Set-up

Figure 3-5 is a photograph of the test set-up to apply a monotonic shear force to a CLT panel-panel connection test specimen. For better clarity, the set-up was modelled in Figure 3-6 and Figure 3-7. The test specimen is supported at one end by a solid, rigid base with enough height to allow for deflection of the connected CLT block. The base was positioned far enough away from the connection to prevent any part of the connection from contacting the base, but not

so far away that an excessive moment was produced by the cantilever section. The specimen was then clamped securely to the base of the test machine utilizing hold-downs across the top of the specimen fastened by threaded rods attached to the test machine base to prevent rotation of the specimen during testing. To reduce in-plane rotation and damaging the hydraulic ram, steel brackets fitted with low friction High Density Polyethylene (HDPE) sheets, and cross-head guides were added to the sides and front and back respectively (Figure 3-6). For simplicity, the test set-up was simplified in Figure 3-7. The test machine used was an MTS Servo-Hydraulic Test Machine outfitted with a 50 kip load cell capable of reporting loads with a range of error of less than 1% of the load. Linear variable differential transducers (LVDTs) with a sensitivity of 0.001 inches were attached to the front and back faces of the specimen. An aluminum yoke allowed the deflection to be measured relative to the two CLT blocks. Load was applied vertically to the top edge of the specimen to induce shear between the two CLT blocks.

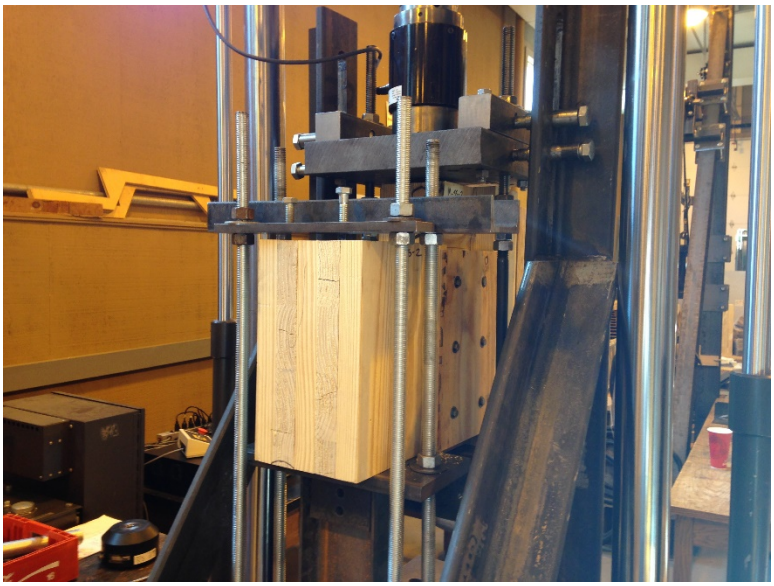

Figure 3-5: Photograph of Monotonic Test Set-Up

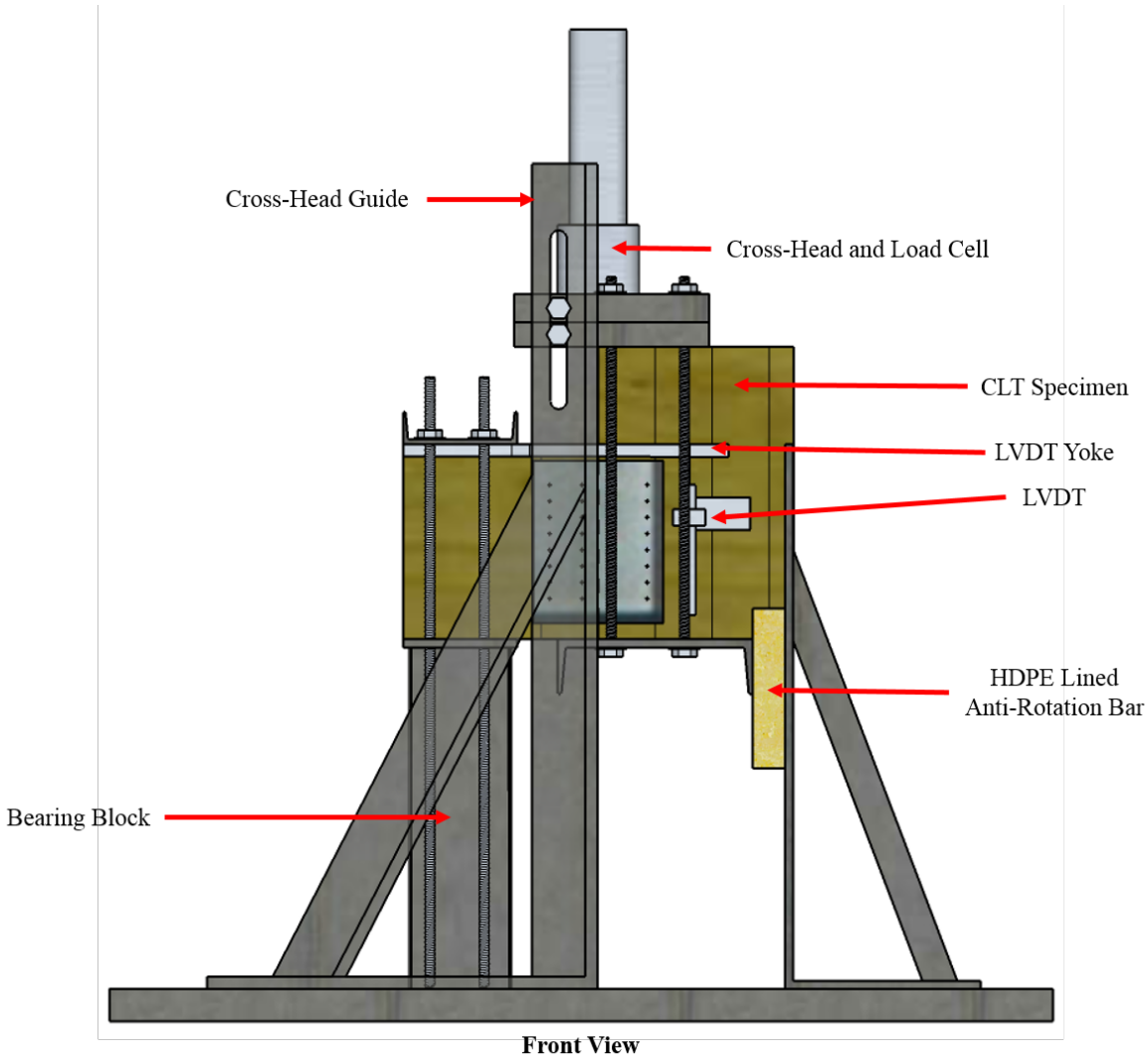

Figure 3-6: Front View Schematic of Monotonic Test Set-Up

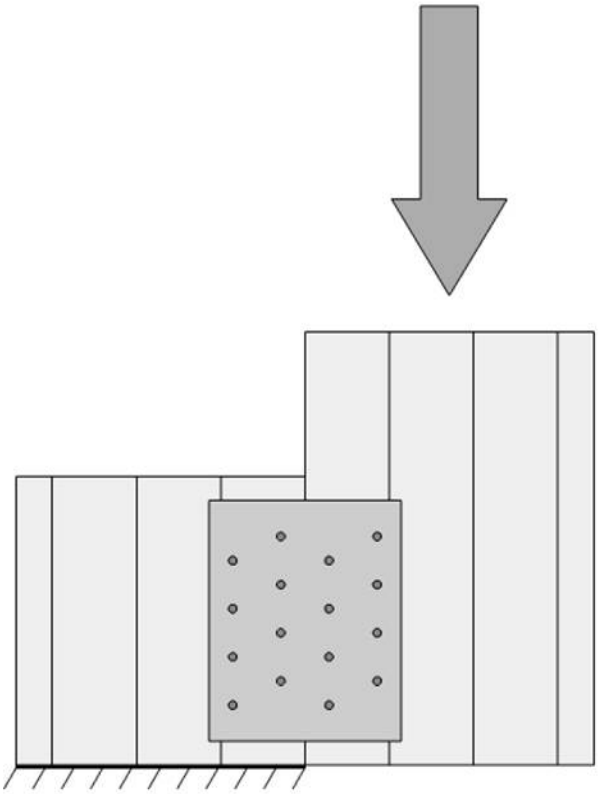

Figure 3-7: Simplified Drawing of Monotonic Test Set-Up

3.2.2 Monotonic Testing Procedure

All CLT specimens had been stored in the Wood Engineering Lab of the Thomas M. Brooks Forest Products Center at Virginia Tech prior to testing. This helped to ensure that all tested specimens were subjected to the same environment and allowed to season in a similar manner. In order to mitigate bias, CLT blocks were paired at random. Load was applied at a uniform rate of 0.10 in (2.54mm)/min. Displacement was measured at the nearest 0.001 in (0.025 mm). Testing was concluded once the load dropped 20% of the ultimate load and no signs of recovery were observed, or when deflection reached 3 inches. Load and displacement were

continuously monitored throughout the test. The maximum load and shear stiffness of the linear portion of the load-deflection curve were reported. Five percent offset values were taken as the point where a line parallel to the initial load/displacement curve, and offset by 5% of the fastener diameter, intersects the original load displacement curve. Figure 3-8 is an example of how 5% offset values were found.

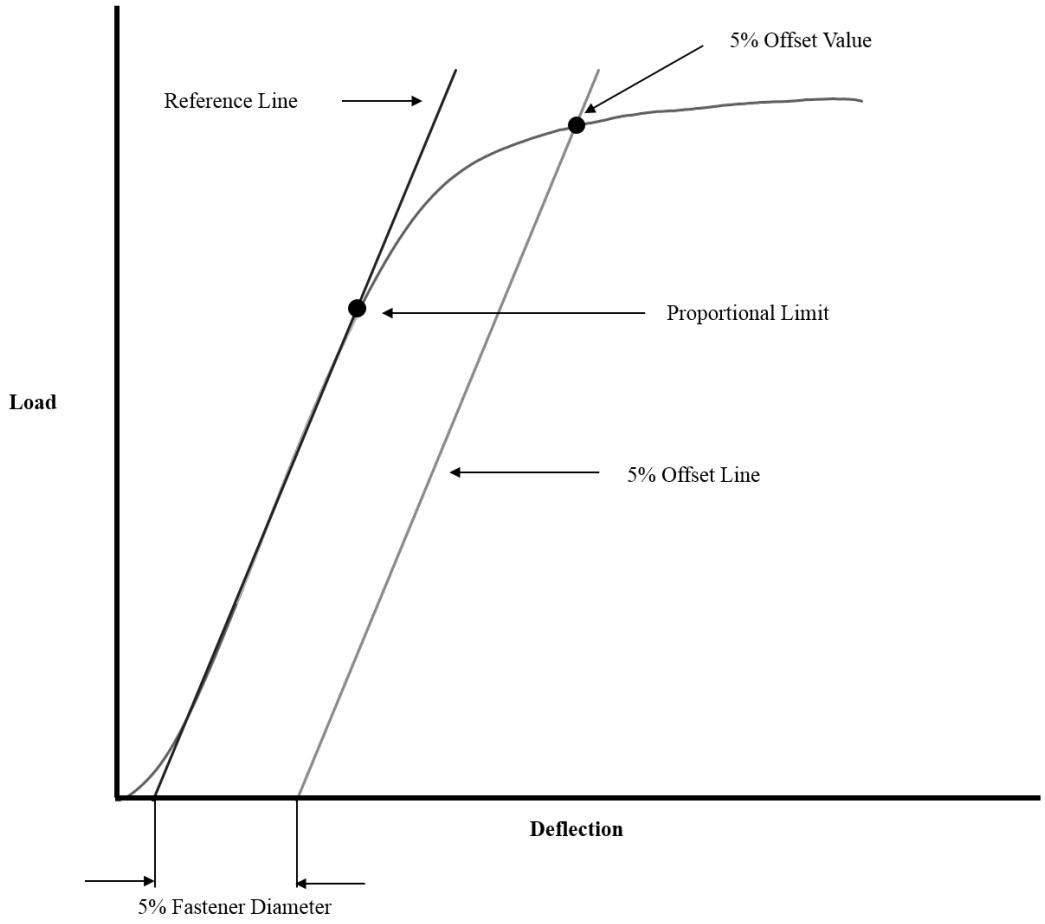

Figure 3-8: 5% Offset Example

Upon completion of testing, a test sample approximately 1 inches in length was cut from the center of the body of both CLT blocks in the connection, and the LVL spline when applicable, to determine the specific gravity and moisture content according to the methods

described in ASTM D 2395-14 (ASTM 2014) and ASTM D 4442-07 (ASTM 2007), respectively.

3.3 Objective 2: NDS Prediction

One of the objectives for this research was to compare the experimental results from monotonic testing to lateral design values predicted by the NDS (AWC 2012). Yield limit equations from the NDS (AWC 2012) were used to calculate predicted yield mode values for each of the selected CLT connection configurations described in Section 3.1. The minimum yield value of each CLT configuration was chosen as the governing lateral design value, *Z*. This lateral design value, *Z*, was then multiplied by the applicable adjustment factors for dowel-type fasteners from Table 10.3.1 of the NDS (AWC 2012) to include the Format Conversion Factor (K_F), Resistance Factor (ϕ), and Time Effect Factor (λ), required for the Load and Resistance Factor Design (LRFD) method, to obtain the adjusted lateral design value, *Z'*.

Yield limit equations assume a homogenous grain direction in each connected member. Since CLT contains layers of material in alternating grain directions, both $Z_{\parallel}$ and $Z_{\perp}$ were calculated for the half-lap connection. For the spline connection $Z_{\parallel}$ and $Z_{\perp}$ were calculated for the CLT only, since the LVL spline was only loaded parallel to grain. Prediction inputs were based on the net area of the CLT at the connection, and not the gross area of the CLT block specimen. To predict the strength of the connection, *Z'* was multiplied by the number of fasteners occurring in one CLT panel face. For the surface spline, steel plate, and half-lap, *Z'* was multiplied by 3, 8, and 3, respectively, to obtain predicted connection strength of the total connection.

For comparison to predicted values, 5% offset values from monotonic testing were divided by the appropriate reduction term (R_d) from the NDS (AWC 2012) and *Technical Report 12* (AWC 2014). The formula used for format conversion is given in Equation 3-1.

$$Z = \frac{P}{R_d} \tag{3-1}$$

Where,

Z = Reference lateral design value

P = 5% offset yield value from monotonic testing

R_d = NDS reduction term for dowel type fastener connections, NDS Table 11.3.1B.

A Reduction Term (R_d) of 2.28 was used for parallel comparisons while an R_d 2.85 was for perpendicular comparison for connections containing lag screws. An R_d of 2.2 was used for the nailed connections.

3.4 Objective 3: Cyclic (Reversed) Connection Testing

All testing was conducted in the Wood Engineering Lab at the Thomas M. Brooks Forest Products Center at Virginia Tech. The testing conducted in this section was based on ASTM E2126-11, *Standard Test Method for Cyclic (Reversed) Load Test for Shear Resistance of Vertical Elements of the Lateral Force Resisting Systems for Buildings: Test Method C (CUREE Basic Loading Protocol)* (ASTM 2011). Since this standard describes a method for testing of full-scale wall panels, it was adjusted to account for the scaled-down specimens used in this

study. The treatments and sample size for cyclic shear testing of selected CLT connections are listed in Table 3-1. Three different connection configurations were examined, each connection configuration was tested five times for a total of fifteen tests.

3.4.1 Cyclic (Reversed) Test Set-up

Figures 3-9 and 3-10 are schematics of the test set-up to apply a full-reversal cyclic shear force to the specimen. The test specimen rests at one end on a rigid bearing base with enough height to allow for adequate deflection of the connected CLT block. The base was positioned far enough away from the connection to prevent any part of the connection from contacting the base during testing, but close enough to the connection that an excessive moment was not produced. To prevent rotation of the specimen during testing, the specimen was clamped to the test machine base by connecting hold-downs across the top of the specimen to the base with threaded rods. Roller bars covered with high density polyethylene (HDPE) sheets to reduce friction, were positioned at the end of the cantilevered section in order to prevent any load eccentricity. The cross-head was clamped above and below the cantilevered section to allow the test machine to push and pull the specimen. The test machine used was an MTS Servo-Hydraulic Test Machine outfitted with a load cell with a range of 50 kips and the capability of reporting loads with an error of less than 1% of the load. A linear variable differential transducer (LVDT) with a sensitivity of 0.001 inches was attached to the bottom of the cantilevered section in line with the cross head to record displacement. Load was applied vertically to the top edge of the specimen to induce shear between the CLT blocks.

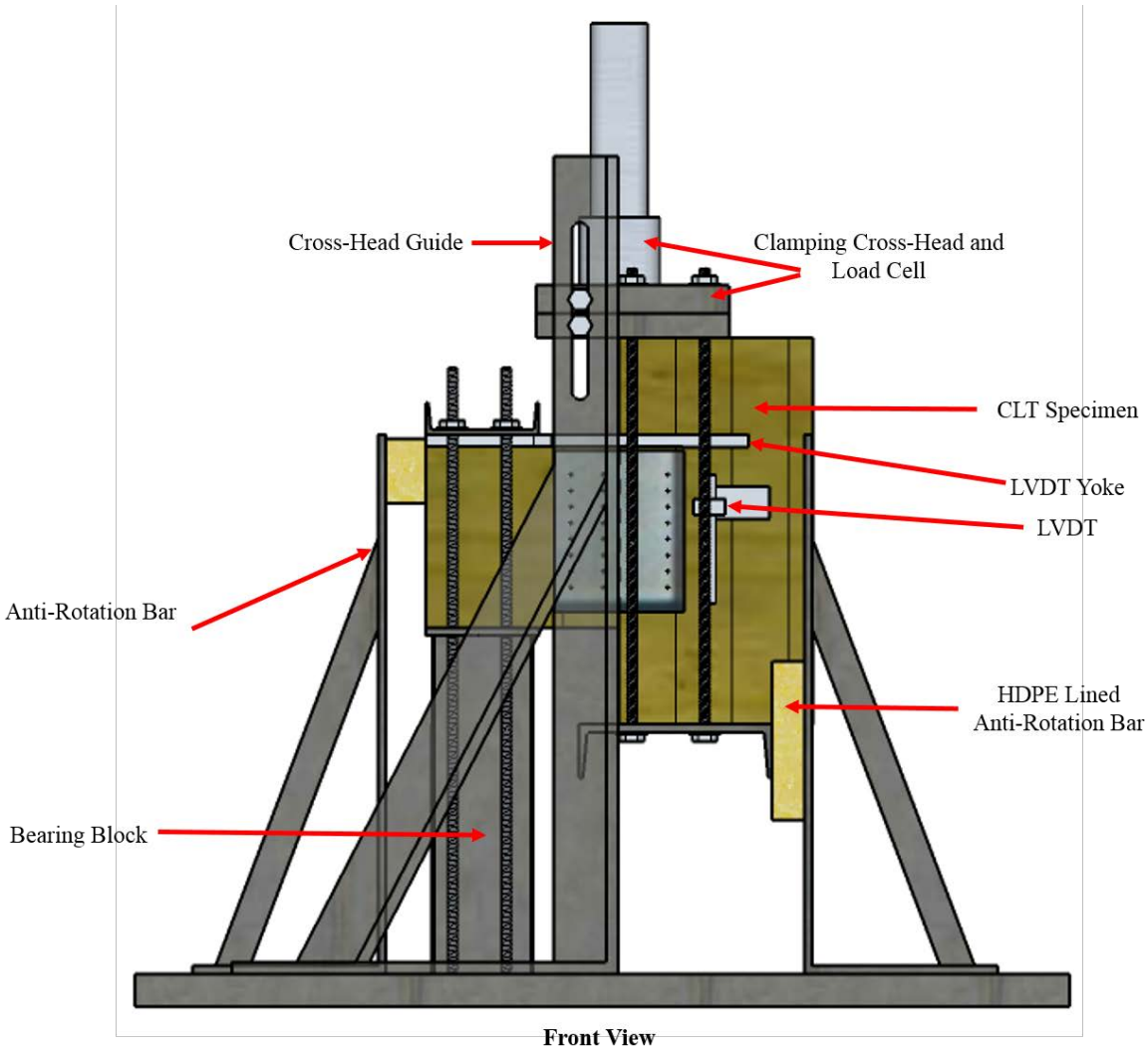

Figure 3-9: Front View Schematic of Cyclic Test Set-Up

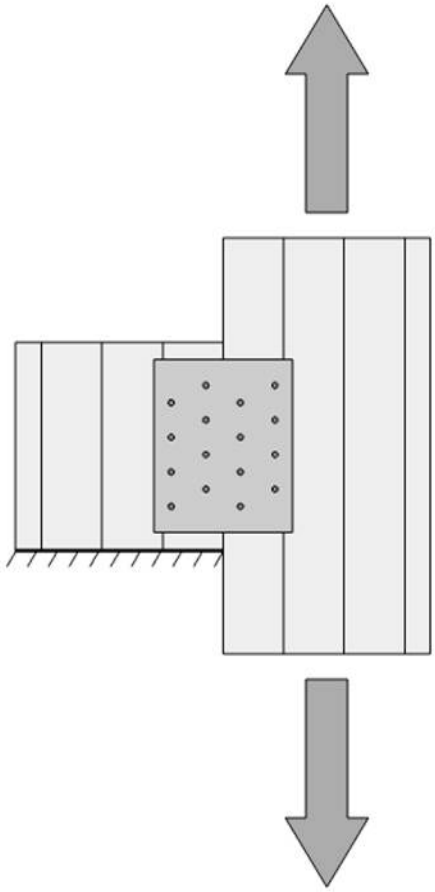

Figure 3-10: Simplified Drawing of Cyclic Test Set-Up

3.4.2 Cyclic (Reversed) Testing Procedure

All CLT block specimens had been stored in the Wood Engineering Lab of the Thomas M. Brooks Forest Products Center at Virginia Tech, in Blacksburg VA prior to testing to ensure that all specimens were allowed to season in the same manner. Pairing of CLT blocks was randomized to reduce bias. Shear stiffness, strength and ductility of tested connections were determined by subjecting the specimens to full-reversal cyclic shear loads. Shear loads and displacements were continuously monitored throughout the test. The cyclic displacement of the actuator followed Test Method C (CUREE Basic Loading Protocol) prescribed in ASTM E2126-

11 (ASTM 2011). The actuator displacement was controlled at a constant rate of 1 inch (25.4mm)/second. Testing was terminated once the applied load dropped below 20% of the peak load. Envelope curves, shear strength, and mean values of load (*P*), displacement (Δ), and shear stiffness, were drawn or calculated according to the methods described in ASTM E2126-11 (ASTM 2011).

Upon completion of testing, a test sample approximately 1 inches in length was cut from the body of both CLT blocks in the connection, and the LVL spline when applicable, to determine the specific gravity and moisture content according to the methods described in ASTM D 2395-14 (ASTM 2014) and ASTM D 4442-07 (ASTM 2007), respectively.

3.5 Materials Testing

This section describes the procedures used to determine the fastener yield bending strength (F_{yb}) and the dowel embedment strength (F_e) of the fasteners and wood material used in monotonic and reversed cyclic testing described in sections 3.2 and 3.4.

3.5.1 Fastener Yield Bending Strength Test

Fastener bending strength tests were conducted for the 0.25-in. by 6-in. lag screws and the 16d common wire nails used for the CLT connection testing proposed in this chapter. Bending strength of nails followed the procedure as defined by ASTM F1575-03, *Standard Test Method for Determining Bending Yield Moment of Nails* (ASTM 2013). The test set-up for determining the bending strength of nails is shown in Figure 3-11. The base of the apparatus consists of a flat steel base that screws into the test machine for added stability during testing. Two steel bars with rounded recesses cut into the top, sit on an aluminum block with slots that

allow for the spacing of the upright steel bars to be adjusted to various spans. Atop the upright bars are two free-rotating, cylindrical bearing points measuring 0.370-in. in diameter and spaced 1.9-in. apart as defined by the requirements of ASTM F1575. A cylindrical crosshead attachment measuring 0.370-in. in diameter was placed in the center of the 1.9-in. span of the cylindrical bearing points and used to apply a bending load to the nails. The mid-point of the length of the nails were marked and positioned directly centered under the crosshead. Load was applied at a constant rate of 0.25-in./min and testing was concluded once deflection reached 0.25-in. Load and deflection were constantly monitored and recorded throughout the duration of the test in order to generate a load-deflection curve.

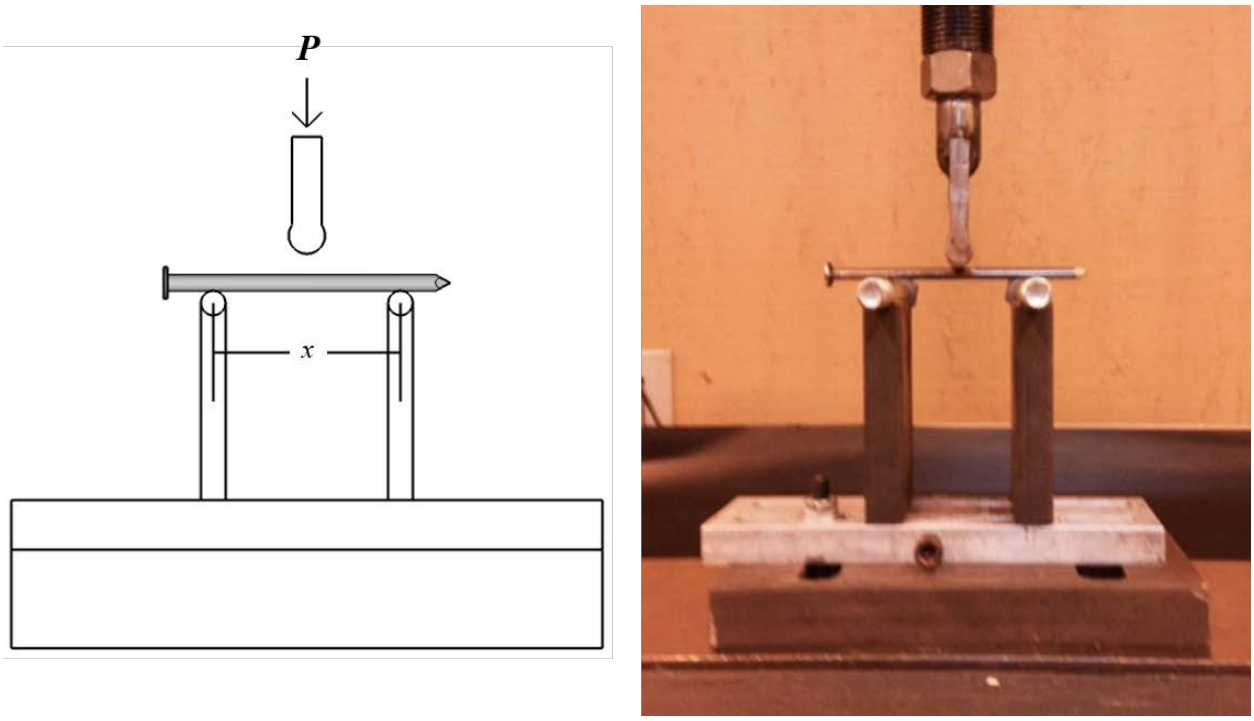

Figure 3-11: Model and Photograph of Nail Bending Test Set-Up

From the recorded data a load-deflection curve was generated and a 5% offset line was drawn to determine the yield load. The nominal yield bending strength was determined by the following:

$$F_{yb} = \frac{M}{S} \qquad (3\text{-}2)$$

where,

F_{yb} = nominal fastener yield strength, psi.

S = plastic section modulus (in.^{3}) for plastic hinge ($S = D^3/6$, where D = nail diameter)

M = calculated moment based on test load, in.-lb ($M = P * x/4$)

P = 5% offset yield load, in.

x = cylindrical bearing point spacing, in.

Since no standard test method exists for determining bending yield moment of lag screws, the testing procedure of ASTM F1575-03, *Standard Test Method for Determining Bending Yield Moment of Nails* was adapted for the testing of lag screws (ASTM 2013). This was permissible under section 11.3.6.2 of the NDS (AWC 2012). Since the binding of the coarse lag screw threads on the cylindrical bearing points during testing was a concern, a cantilever test set-up, as seen in Figure 3-12, was used in lieu of the three-point bending test used for nails. The cantilever test method followed a procedure similar to those used by Billings (2004) and Albright (2006). Albright's research found similar results between three-point bending and cantilever bending configurations (Albright 2006). The test fixture consisted of a vertical steel plate welded

securely to a steel base-plate. Two angled steel side plates were outfitted to either side of the rear vertical steel plate for added rigidity. A series of supporting steel blocks was fitted to the face of the fixed rear vertical block and secured in place with threaded bolts. Each of these steel blocks had a hole drilled through them and positioned so that the holes would line up when stacked together. These holes were drilled at a diameter that allowed for a snug fit of the threads of the lag screws. Load was applied at a known distance (x) from the face of the support by a cylindrical bearing block outfitted to the crosshead. All lag screws were loaded at a uniform distance of 3-in. from the support fixture. Load was applied at a constant rate of 0.25-in./min and was monitored and recorded in tandem with deflection. Testing was terminated when an adequate amount of data points on the load-deflection curve were recorded that permitted a 5% offset line to intersect the load-deflection curve. A total of ten lag screws were tested in all.

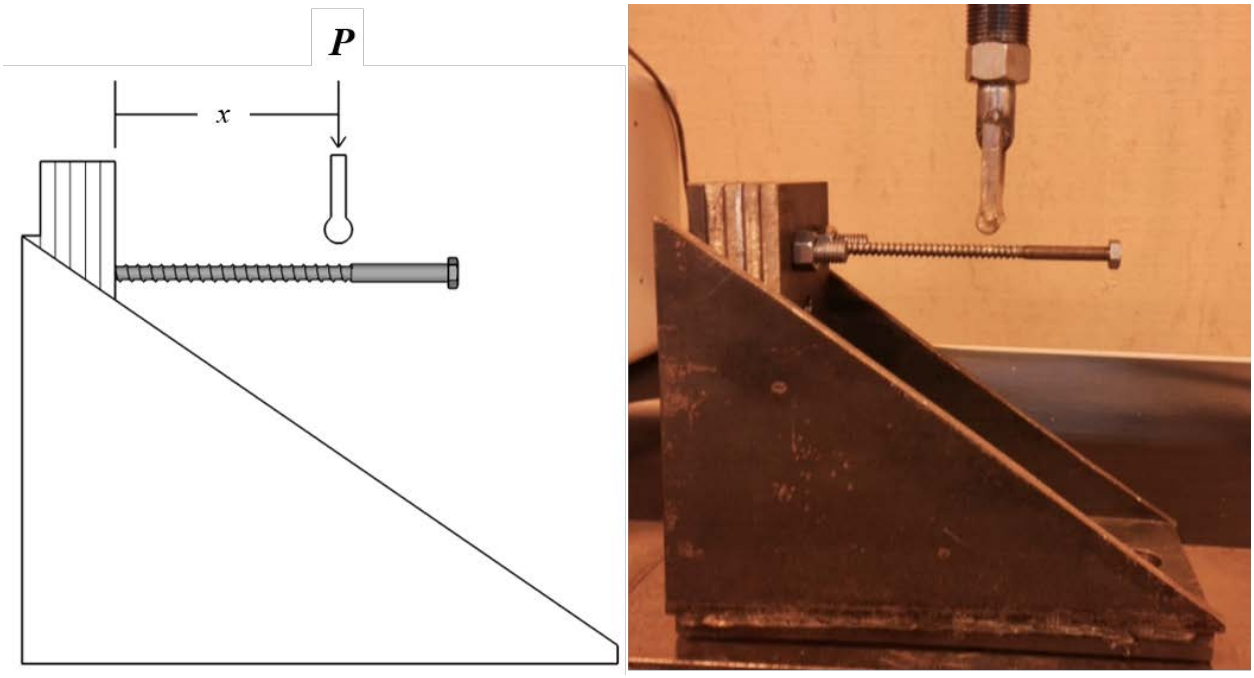

Figure 3-12: Model and Photograph of Cantilever Test Set-Up

From the recorded data a load-deflection curve was generated and a 5% offset line was drawn to determine the yield load. The nominal yield bending strength was determined by the following equation:

$$F_{yb} = \frac{M}{Z} \quad (3\text{-}3)$$

where,

F_{yb} = nominal fastener yield strength, psi.

Z = plastic section modulus (in.^{3}) for plastic hinge ($Z = D^3/6$, where D = lag screw diameter)

M = calculated moment based on test load, in.-lb ($M = P*x$)

P = 5% offset yield load (lb)

x = distance from face of support to point of applied load (in.).

Average F_{yb} values were calculated for both the lag screws and nails. These averages were then used as the F_{yb} inputs in the yield limit equations for NDS predictions described in section 3.3.

3.5.2 Dowel Bearing

Due to time and resource constraints, dowel bearing strength test for 0.25” diameter lag screws were not conducted. Separate research on the effects of alternating grain direction of CLT layers on dowel bearing strength was being conducted at the Wood Engineering Lab of the

Thomas M. Brooks Forest Products Center of Virginia Tech in Blacksburg, VA at the time of this thesis study.

Chapter 4: Results and Discussion

This chapter contains the results materials testing, connection testing and NDS predictions described in Chapter 3. Results of fastener yield bending strength and a discussion of dowel bearing strength are included in Section 4.1. Results of monotonic CLT connection testing are reported in Section 4.2. Products of yield limit calculations and a comparison of predicted results to monotonic data can be found in Section 4.3. Section 4.4 includes the results of cyclic testing of CLT connections and brief comparisons to monotonic results.

4.1 Material Tests

4.1.1 Fastener Yield Bending Strength Tests

Lag screws and nails used for connection testing were subjected to a bending test to determine fastener yield bending strength as described in Section 3.5. The lag screws were 0.25-in. in diameter at the shank with a root diameter (D_r) of 0.178-in. as measured with a caliper, and were 6-in. in length including the tapered tip. Nails were 16d common wire nails 0.162-in. in diameter as measured with a caliper and 3.5-in. in length. Ten lag screws and ten nails were tested in all. Lag screws were tested using a cantilever test setup while nails were subjected to a 3-point bending test as described in Sections 3.5.1 and 3.5.2.

Fastener yield bending strengths (F_{yb}) were calculated according to the formula presented in Section 3.5.1 and then averaged to obtain a value to be used as an input in the yield limit equations. The root diameter (D_r) was used to determine F_{yb} for lag screws. The results from testing are given in Table 4-1 below.

Table 4-1: Fastener Yield Bending Strengths

Test Method	Type of Fastener	Average Fyb (psi)	COV
Cantilever	Lag Screw	58,400	15.3%
3-Point	16d Common Nail	92,980	2.80%

Tested lag screws had an average F_{yb} of 58,400-psi, while the 16d common nails averaged around 92,980-psi. These values were used as the material inputs in the yield limit equations. The NDS (AWC 2012) lists an F_{yb} of 70,000 psi and 90,000 psi for lag screws and nails respectively.

4.1.2 Dowel Bearing Strength

Dowel bearing strength (F_e) values were obtained as detailed in Section 3.5.3. Since time and resource constraints prohibited the experimental testing of 0.25-in. diameter dowels, values were estimated from the results of dowel embedment testing of CLTs that was currently in progress at the Wood Engineering Lab of the Thomas M. Brooks Forest Products Center at Virginia Tech in Blacksburg, VA during the time of this study. Dowel bearing testing consisted of two layer and three layer CLT specimens tested with dowel diameters of 0.5, 0.75 and 1.0-in. Single layers were then tested by loading parallel to grain and perpendicular to grain with the same three different dowel diameters for comparison.

Average dowel bearing strengths from testing are plotted in Figure 4-1 (Hindman et al. 2015). Two layer and three layer CLT specimens appear to more closely follow the behavior of F_e parallel when compared to the results for the single layers. Therefore, F_e parallel was assumed as the governing layer in the CLT specimens. Values for F_e parallel were averaged giving a

result of 5,170 psi. The average specific gravity for the CLT test specimens was found to be 0.57 as reported in Section 4.1.3. NDS Table 11.3.3 reports the F_e for a 0.178-in. dowel diameter to be 5,900-psi. at a SG of 0.57. The average 5,170-psi. for F_e parallel from testing was used as the material input in the yield limit equations.

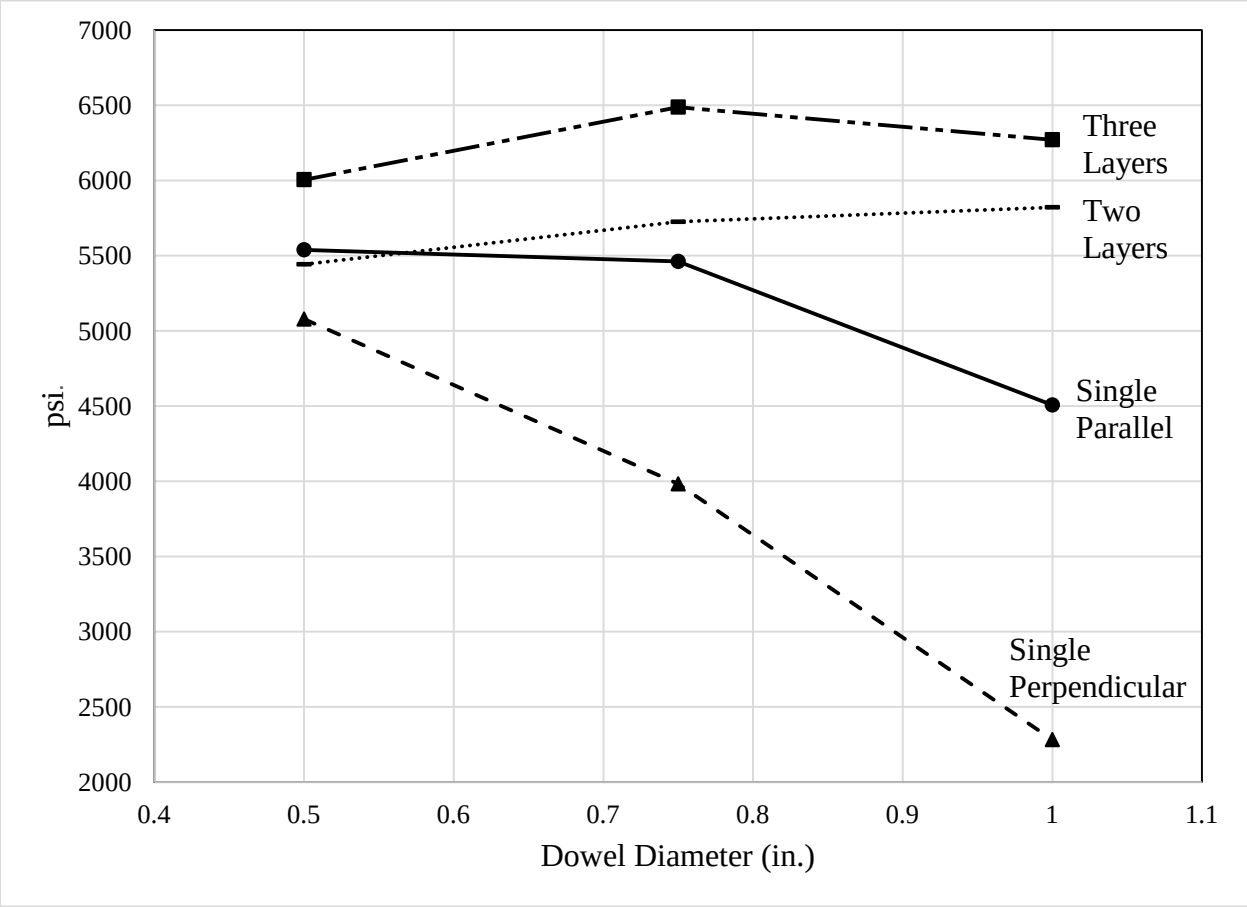

Figure 4-1: Graph of Average Dowel Bearing Strength by Diameter

4.1.3 Moisture Content and Specific Gravity

Moisture contents (MC) and specific gravities (SG) are presented in Table 4-2 below. The mean value of SG for CLT was 0.57 which was 3.63% higher than the NDS listed value of 0.55 (AWC 2012). The mean moisture content for CLT members was 7.7% with a variation of less than 5%. Mean moisture content for LVL was 8.1% also with a COV of less than 5% and a SG of 0.58. All moisture content levels were less than 19%, which precluded the necessity to apply the wet service factor (C_M) to lateral design calculations.

Table 4-2: Moisture Content and Specific Gravity of Materials Tested

Material	Moisture Content		Specific Gravity	
	Mean	COV	Mean	COV
SYP CLT	7.7%	4.5%	0.57	10.7%
LVL	8.1%	4.6%	0.58	11.1%

4.2 Objective 1 Results: Monotonic Connection Tests

This section presents the results of monotonic connection testing as described in Section 3.2. Five specimens were tested for each of the three connection configurations for a total of 15 tests. From test results, the data were analyzed and ultimate load, yield load from 5% offset, shear stiffness, ductility ratio and monotonic reference deformations were found and presented in the following sections.

4.2.1 Load

The average 5% offset yield load values and maximum load for each of the CLT connection configurations are shown in Table 4-3. Each connection was tested until failure occurred or the load dropped 20% below the peak load. Average 5% offset yield values ranged from 885 lbs. to 1,285 lbs. for surface spline specimens, 1,306 lbs. to 1,758 lbs. for half-lap joints, and 1,945 lbs. to 3,692 lbs. for the butt-joint with a steel plate. The surface spline connection yielded the lowest average 5% offset yield load of 1,036 lbs. Yield load values, from 5% offset, showed little similarity between each connection type. The butt-joint with the steel plate connection had an average 5% offset yield load of 2,555 lbs. or nearly 2.5 times the 5% offset obtained for the surface spline connection. The steel plate connection had a mean yield load of more than 1,000 lbs. higher than the half-lap connection and over 1,500 lbs. higher than the spline connection. The half-lap joint had the lowest amount of variation in 5% offset values at 11% while the steel plate had the highest at 27%.

Table 4-3: Average 5% Offset Yield Loads and Maximum Loads from Monotonic Testing

Connection Configuration	5% Offset Yield Load		Maximum Load	
	Mean (lbs)	COV	Mean (lbs)	COV
Spline	1,036	19%	4,054[1]	26.8%
Half-Lap	1,527	11%	4,258	18.2%
Steel Plate	2,555	27%	4,942	6.5%

1. Considering only 4 specimens. One specimen stopped prematurely to prevent test machine damage.

One surface spline connection test was stopped prematurely to prevent the cross-head of the test machine from contacting the anti-rotation bracing. Therefore the specimen was not

loaded to failure and a lower than average maximum value of 2,473 lbs. was obtained. Table 4-3 excludes this value in the calculation of its mean maximum load for the single surface spline.

Average maximum load values ranged from 2,473 lbs. to 4,987 lbs. for spline specimens, 3,370 lbs. to 4,870 lbs for half-lap specimens, and 4,655 lbs. to 5,399 lbs. for the butt-joint with a steel plate connection. Steel plate average maximum values occur within a much smaller range of difference than did the 5% offset yield load values. The surface spline connection and the half-lap connection only differed by 204 lbs., while the difference between the half-lap connection and the steel plate connection was 684 lbs. The surface spline connection demonstrated nearly four times the amount of variation when compared to the steel plate connection which had an approximate COV of 6.5%. Five percent offset yield loads were approximately 26%, 36%, and 52% of the reported maximum load values for the spline, half-lap, and steel plate connections respectively.

4.2.2 Loading Behavior: Load-Deformation Curves

Upon completion of testing, load-deformation curves were generated for each tested specimen. Specimens were tested with two LVDTs, one placed on the front face and one placed on the back face near the connection. Deflection was taken as the average of the two deflections as recorded by the LVDTs. The LVDT located at the back face of the specimen, tended to report higher deflections as the test progressed, than did the LVDT placed at the front face of the specimen. The maximum difference ranged from 0.10 -in. to 0.398 in. for the surface spline connection, 0.028 in. to 0.120 in. for the half-lap connection. The steel plate specimens averaged a difference in deflection of around 0.211 in., with the exception of specimen SP-2, which had a recorded difference in deflection 1.285 in. This is because the rotation of the steel plate contacted

the LVDT yoke and forced the yoke to move providing a false reading. The single surface spline and the half-lap joint averaged a maximum deflection difference of 0.231 in. and 0.052 in. respectively.

Each connection configuration displayed unique loading-deformation relationships. Figure 4-2 is a load-deformation curve for a surface spline connection. The curve did not exhibit a plateau. Instead, the load steadily increased past point *X*. Initially, the shear stiffness of the connection was due to the bearing stress on the wood below the fastener up to the proportional limit. After the proportional limit, the increased bearing stress caused wood crush and bending of the fastener, creating the rounding portion of the curve between the proportional limit and point *X*. Beyond point *X*, increased loading caused screw deformation and tension began to develop in the fastener due to the resistance of withdrawal by the fastener threads. Therefore, the increase in stiffness beyond point *X* was the result of wood bearing stress and the development of axial stress in the fastener.

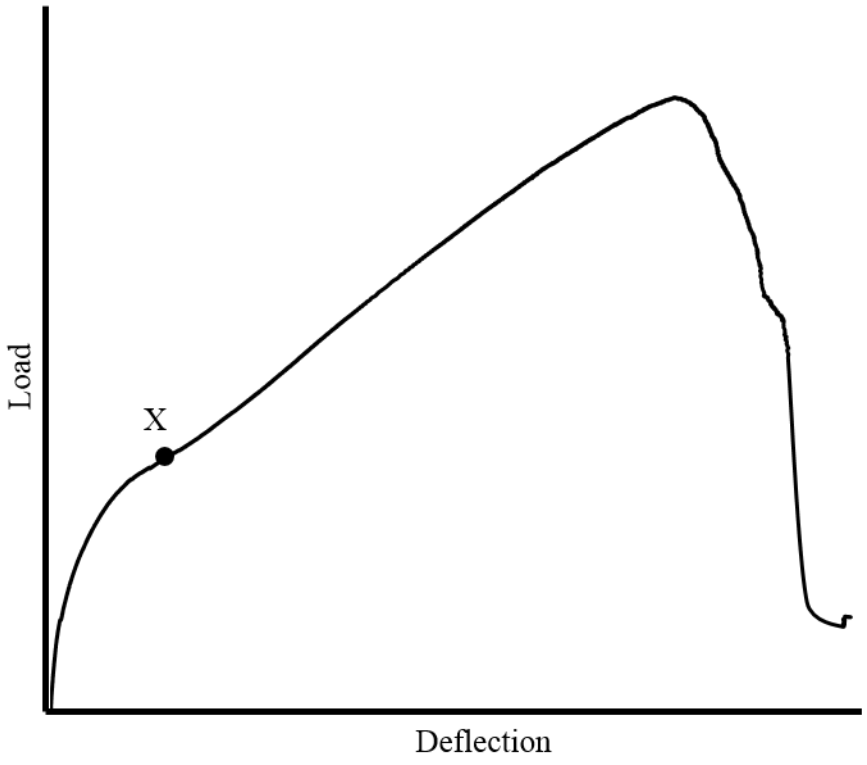

Figure 4-2: Load-Deformation Curve for a Surface Spline Specimen

Figure 4-3 below is a load-deformation curve for a half-lap connection. Unlike the surface spline connection, the half-lap connections demonstrated a slight plateau before the development of axial stress in the fastener caused a second increase in loads similar to the spline connection after the plateau.

Figure 4-3: Load-Deformation Curve for a Half-Lap Specimen

Figure 4-4 is a load-deformation curve for a steel plate specimen. Unlike the surface spline and half-lap connections, the steel plate specimens had a load-deformation relationship similar to what is typically seen in a bending test. This is probably due to the greater dowel bending strength of nails which caused significant wood crush below the fastener. The wood crush caused bending of the fasteners which prevented the fastener from experiencing high withdrawal forces and therefore precluded the second increase in shear stiffness observed for the surface spline and half-lap connections.

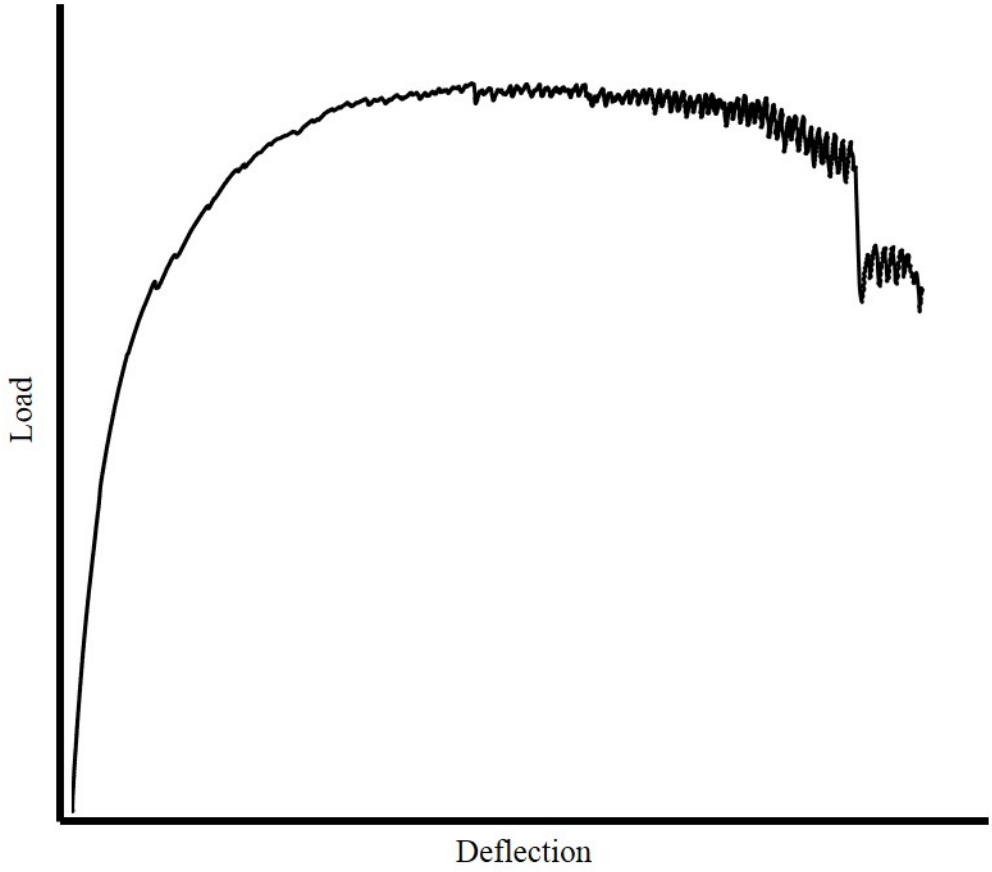

Figure 4-4: Load-Deformation Curve for a Steel Plate Specimen

Figure 4-5 is a graph that combines the load-deformation curves for each connection configuration from monotonic testing. The steel plate typically experienced greater loads compared to the other connections, but the surface spline connection generally produced greater deflections.

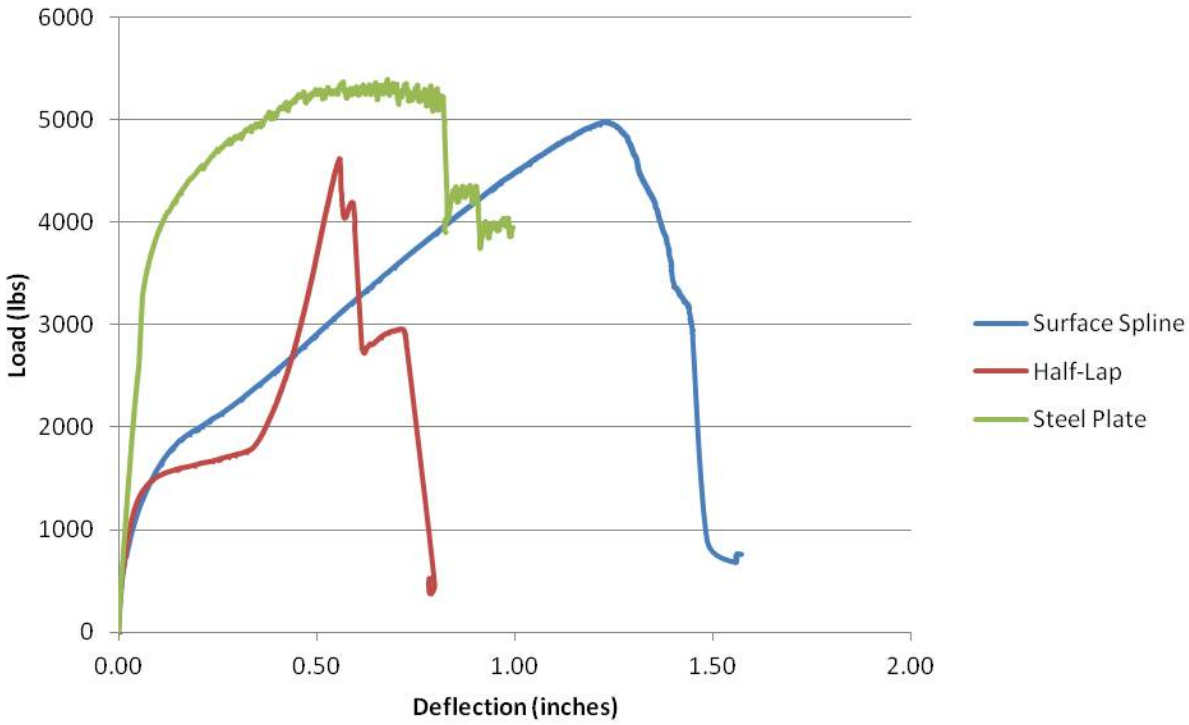

Figure 4-5: Typical Load-Deflection Curves by Connection Configuration

4.2.3 Connection Stiffness

The average stiffness for each of the CLT connection configurations along with COV values is shown in Table 4-4. Stiffness was the slope of the elastic region of the load-deformation curves. Average stiffness values ranged from 33,200 lb/in. to 58,100 lb/in. and COVs ranged from 25% to as high as 56%. The surface spline connections produced the highest COV at over twice the COV produced by the half-lap connection. This is most likely the result of the catastrophic failure of the LVL spline as discussed later in Section 4.2.4.

Table 4-4: Connection Stiffness from Monotonic Testing by Connection Type

Connection Configuration	M-SS-1 (lbs)	M-SS-2 (lbs)	M-SS-3 (lbs)	M-SS-4 (lbs)	M-SS-5 (lbs)	Avg. (lbs)	COV
Spline	23,300	**8,850**	41,100	57,900	34,900	33,200	55.6%
Half-Lap	27,300	44,900	49,900	37,900	53,800	42,700	24.6%
Steel Plate	49,000	47,900	42,300	54,300	**97,200**	58,100	38.2%

The steel plate connection produced the greater average connection stiffness while the surface spline produced the lowest average shear stiffness values. The half-lap connection and the steel plate connection have 28.7% and 75.0% higher average shear stiffness values respectively compared to the surface spline connection. Surface spline specimen M-SS-2 exhibited a much lower shear stiffness value than the other tests of that configuration. M-SS-2 reported a stiffness value of 8,850 lbs/in. which is a reduction of 77.5% of the average of the other four test of that configuration. Excluding this test as an outlier would yield an average shear stiffness of 39,300 lbs/in. and a COV of 36.7%. Similarly, Steel Plate Specimen M-SP-5 yielded an increase in stiffness of 100.8% when compared to the average of the other four tests for that configuration. Excluding this test as an outlier would yield an average stiffness of 48,400 lbs/in. and a COV of only 10.2%.

4.2.4 Connection Failures

A catastrophic or delayed failure was determined by the failure that occurred beyond the ultimate load (Figure 4-6). A delayed failure was determined by a gradual decrease in load, or

the ability to appreciably carry load after ultimate load had been achieved. A catastrophic failure was defined by a sudden drop off of load during testing. Catastrophic failure was also determined by sudden wood or fastener failure such as splitting of the member or fastener shear-off.

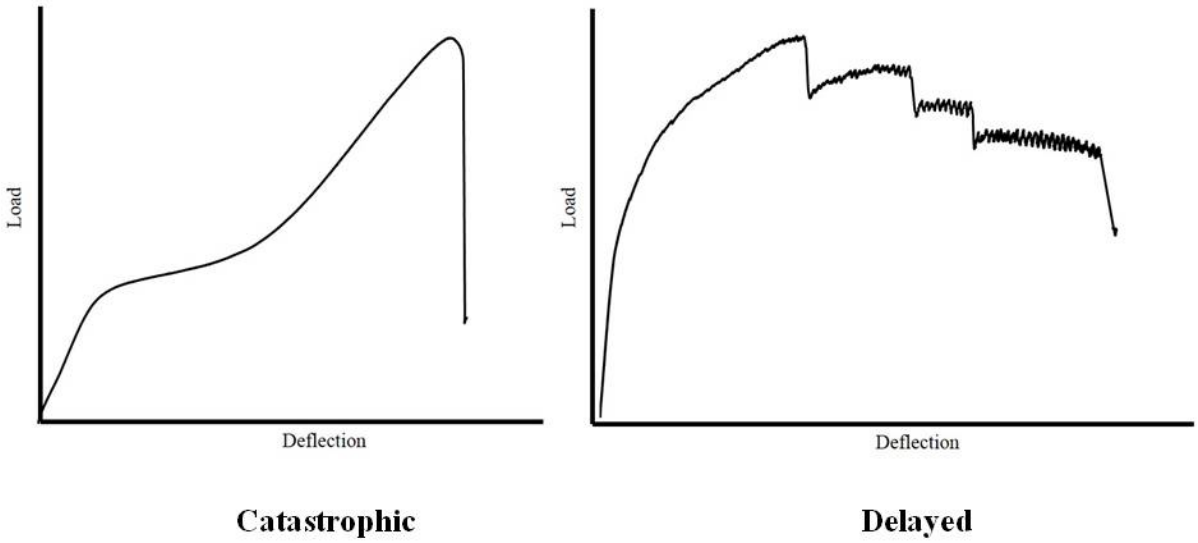

Figure 4-6: Example Catastrophic and Delayed Failures by Load-Deformation Curves

4.2.4.1 Surface Spline Failures

The failures that occurred in the surface spline connections are listed in Table 4-5. Testing of surface spline specimen M-SS-1 was aborted early due to reasons specified in Section 4.2.1. Failure modes were visually inspected and classified according to Figure 2-1, which was taken from NDS Figure I1 (AWC 2012). All surface spline failures exhibited catastrophic failures, either due to a sudden drop off in load, or due to material failure. M-SS-2 failed due to fastener failure. Combined shear and axial stress caused the fastener to shear off at the connection interface. This resulted in a sudden drop in load to near 0-lbs. Figure 4-7 is two photographs of the failure of M-SS-2.

Table 4-5: Failures for Monotonic Surface Spline Specimens

Surface Spline Specimen	Failure Classification	Failure Mode	Failure Details
M-SS-1	Not Available	Not Available	Test aborted prematurely
M-SS-2	Catastrophic	IV	Fastener Failure (axial stress)
M-SS-3	Catastrophic	III_s, IV	LVL split (parallel to grain shear)
M-SS-4	Catastrophic	III_s	LVL split (parallel to grain shear)
M-SS-5	Catastrophic	III_s, IV	LVL split (parallel to grain shear)

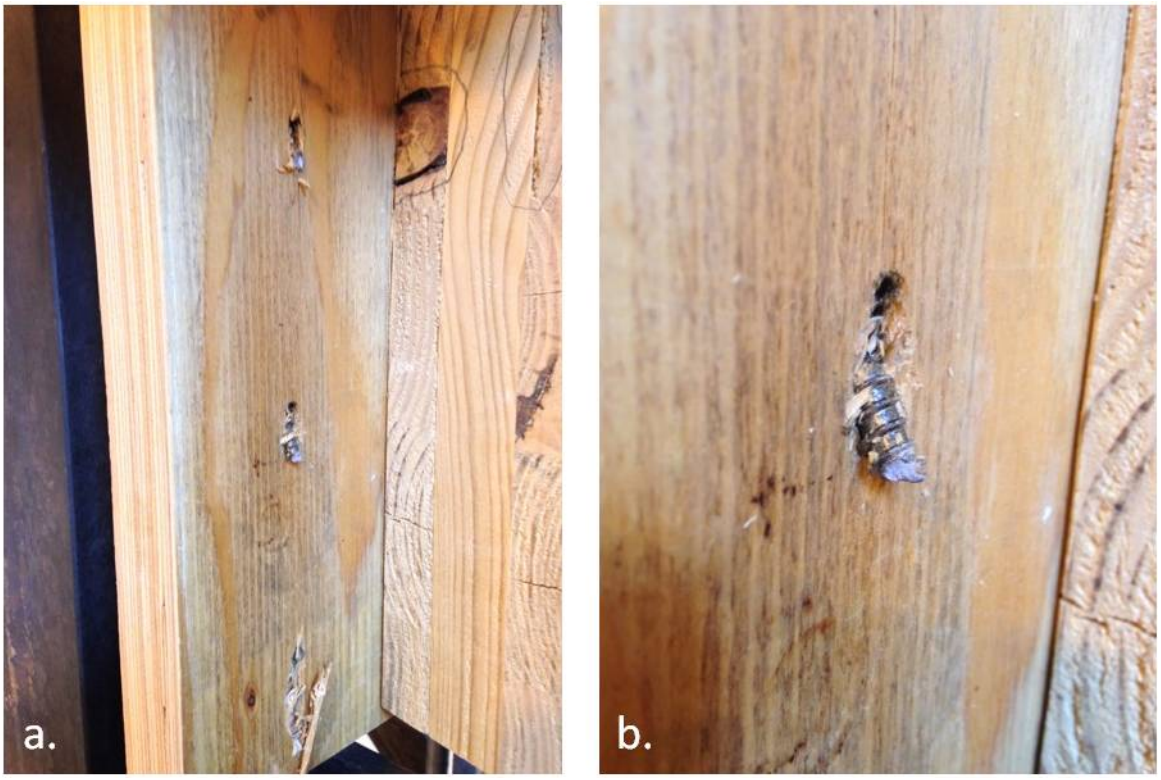

Figure 4-7: Photographs of Observed Failure in M-SS-2

Surface spline specimens M-SS-3 and M-SS-5 exhibited similar failures. Both specimens experienced a significant drop off in load after failure of the LVL spline in shear parallel to grain. This type of failure was expected due to grain direction, results in low shear parallel to grain resistance. M-SS-3 and M-SS-5 appeared to exhibit both Mode III_s and Mode IV failures. Figures 4-8 and 4-9 are photographs of the failures that occurred in specimens M-SS-3 and M-SS-5 respectively.

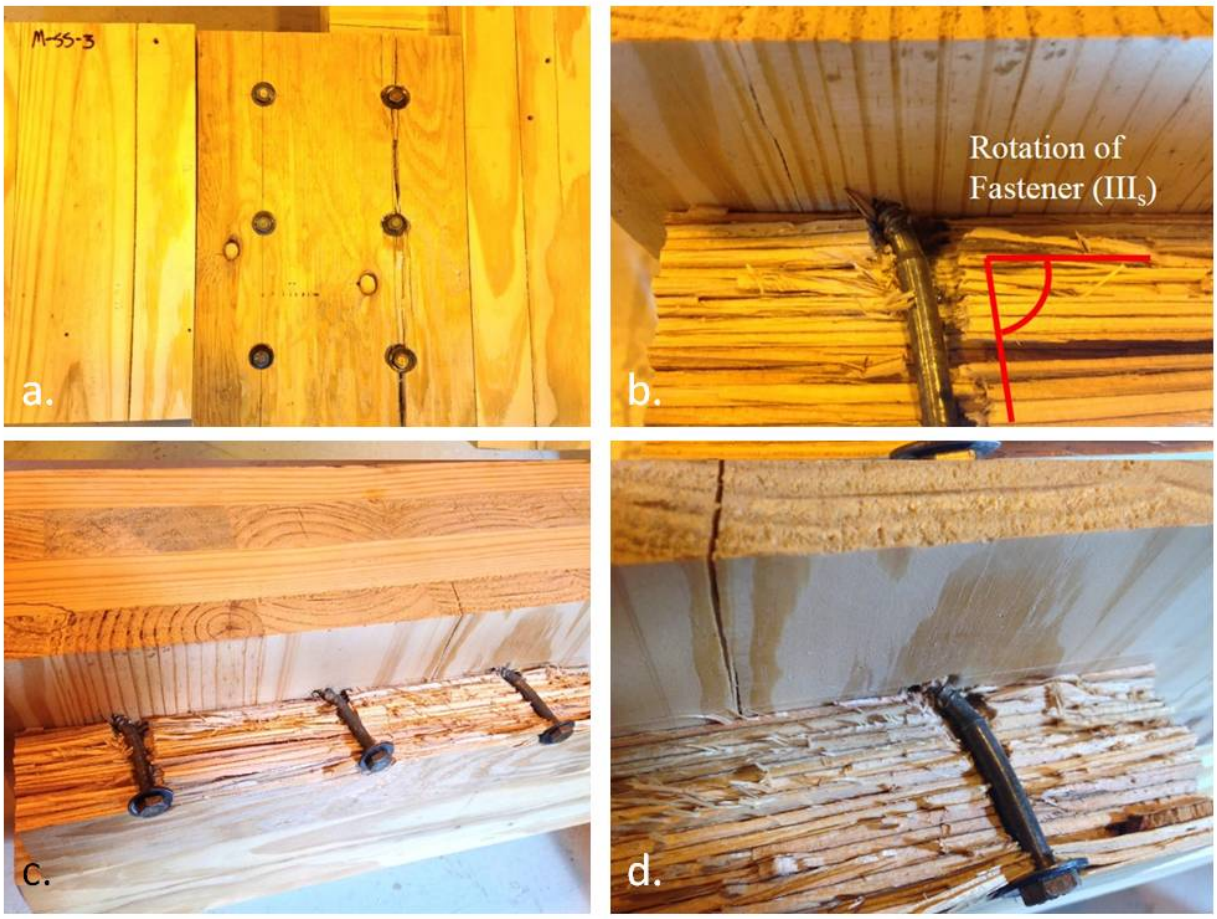

Figure 4-8: Photographs of Observed Failure in M-SS-3

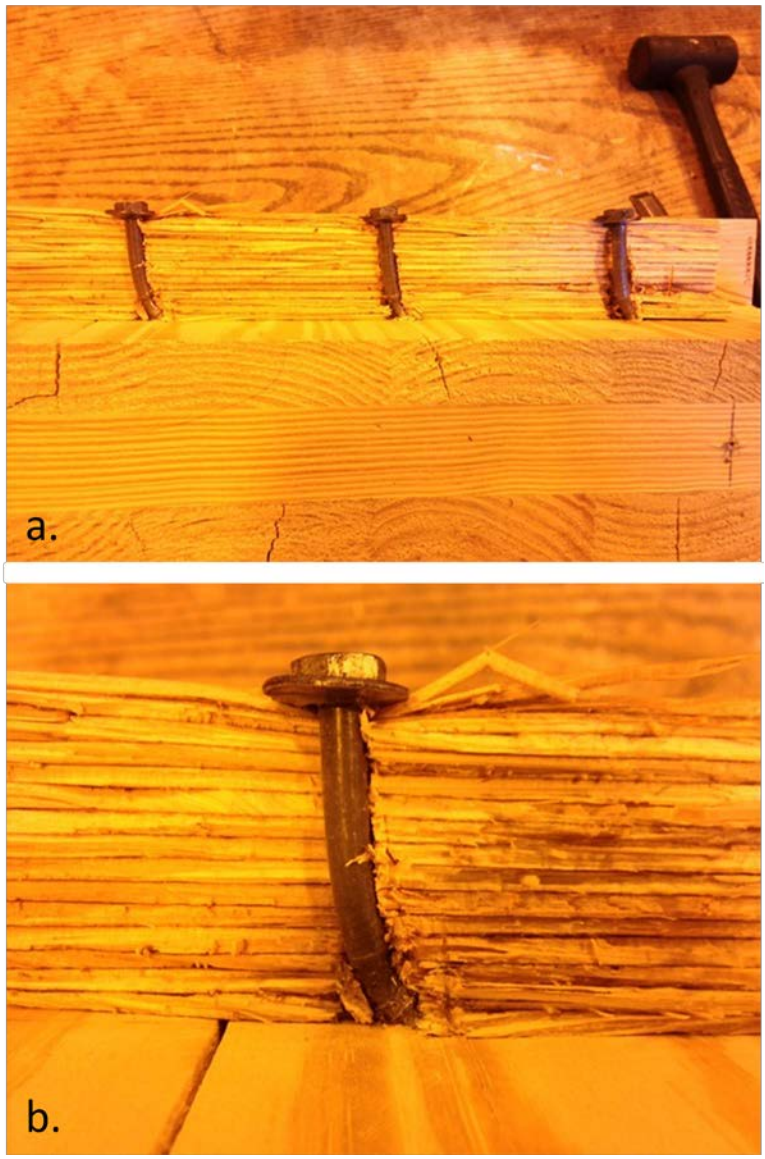

Figure 4-9: Photographs of LVL Spline Failure in M-SS-5

Specimen M-SS-4 also experienced a marked drop of in load after the LVL spline failed in shear parallel to grain. Unlike M-SS-3 and M-SS-5, M-SS-4 appeared to demonstrate a Mode III_s failure only. Figure 4-8 is a photograph of M-SS-4 showing rotation of the fastener in the LVL side member. Pull through of the lag screw is evidenced by the deformation of the washer and wood crush under the washer as shown in Figure 4-10 and Figure 4-11. Axial stress, or

tension, was being applied to the fastener and was a factor in the fastener failure observed for M-SS-2 and the second increase in shear stiffness discussed in Section 4.2.2.

Figure 4-10: Photographs of LVL Spline Failure in M-SS-4

Figure 4-11: Photographs of Fastener Pull Through in the Surface Spline Connection

4.2.4.2 Half-Lap Failures

The half-lap specimen produced the same failures for all specimens tested. All half-lap joints failed in a catastrophic fashion due to fastener failure. Three of the load-deformation curves exhibited a stair stepping effect as the load dropped after ultimate load was reached. Each of these curves had three distinct steps as seen in Figure 4-3. These steps appear to indicate individual fastener failures since three lag screws were used to make the connection. The load-deformation curve for M-HL-3 exhibited only one of these steps while M-HL-5 had none. Connection yield modes were not able to be identified since the connection was not exposed as in the surface spline specimens. Figure 4-12 a. and b. are photographs of the failures that occurred in the half-lap connection during testing. Wood crush is observable above or below the fastener as well as bending of the fastener.

Figure 4-12: Photographs of Observed Failures in Half-Lap Connections

4.2.4.3 Steel Plate Failures

The failures observed in the steel plate specimens are listed in table 4-6. The steel plate connections were more delayed than the surface spline connections and the half-lap connections. In all steel plate specimens tested, testing was terminated when load dropped 20% of the maximum load according to monotonic testing procedures described in Section 3.2.2. Therefore, complete failure was never observed for these specimens.

Table 4-6: Failures for Monotonic Steel Plate Specimens

Steel Plate Specimen No.	Failure Classification	Failure Details
M-SP-1	Delayed	Nail head shear-off. Load dropped by 20% of the maximum load.
M-SP-2	Delayed	Nail head shear-off. Load dropped by 20% of the maximum load. Wood splitting.
M-SP-3	Delayed	Load dropped by 20% of the maximum load.
M-SP-4	Delayed	Nail head shear-off. Load dropped by 20% of the maximum load. Wood splitting.
M-SP-5	Delayed	Wood splitting. Nail head shear-off. Load dropped by 20% of the maximum load.

In, all cases except for M-SP-3, rotation of the steel plate from the applied shear force resulted in the heads of the nails being sheared off. Loss of nail heads during testing did not seem to coincide with the cascading effect of the load due to fastener failure as seen in the half-lap joint. Figure 4-13 is a photograph of the plate rotation that occurred during testing. Figure 4-14 a. and b. are photographs depicting nail head shear-off.

Figure 4-13: Photograph of Plate Rotation

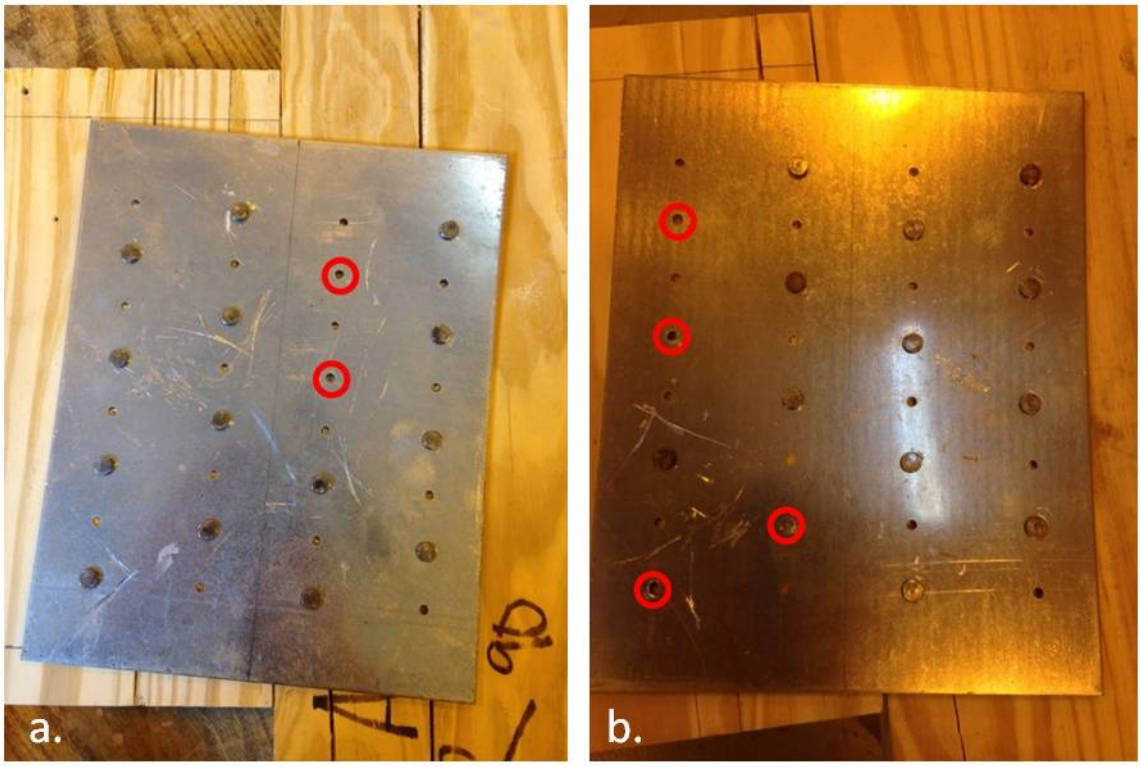

Figure 4-14: Photographs of Nail Head Shear-Off

For steel plate specimens M-SP-2, M-SP-4 and M-SP-5, the applied shear force caused splitting in the face layer of the CLT. This is due to loading parallel to grain in the face layer. This is the same phenomenon that occurred with the LVL member in the surface spline connection. Figure 4-15 is a photograph of splitting in the face layers of the CLT in M-SP-2. Figure 4-16 is a photograph of significant wood splitting in M-SP-5. Propagation of cracks or splits due to shear parallel to grain may be the cause of the cascading or stair stepping effect in the load-deformation curve as load decreases after ultimate load was reached.

Figure 4-15: Photograph of Splitting Due to Shear Parallel to Grain in M-SP-2

Figure 4-16: Photograph of Wood Splitting Failure in M-SS-5

4.2.5 Ductility Ratios

Ductility ratios were calculated from experimental results from monotonic shear testing of CLT connections. Ductility ratio is the ratio between the displacement at ultimate load and the displacement at the 5% offset yield load. Ductility ratios for each specimen tested are presented in Table 4-7 along with the average ductility ratio and COV for each connection configuration. Surface Spline Test No. 1 (M-SS-1) was aborted early, so true deflection at ultimate load was not obtained. Therefore, the ductility ratio for this specimen is not available. The spline connection had the greatest average ductility ratio, contrary to the findings of Gavric et. al (2012) who reported similar ductility ratios between an LVL spline joint and half-lap joint. Furthermore, the average ductility ratios from current testing were much greater than the ratios of 14.43 and 15.98

reported by Gavric for the spline joint and half-lap joint respectively (Gavric, et. al 2012). This may be due to differences in experimental testing since Gavric (2012) used three full-scale CLT panels featuring two connections with bearing at both sides. This type of testing reduced the effect of applied moment which may have led to lower deflection values and thus lower ductility ratios found by this study. Further investigation of the effects of moment from the test set-up on experimental values may be necessary.

Table 4-7: Ductility Ratios from Monotonic Connection Testing

Connection Configuration	Test No. 1	Test No. 2	Test No. 3	Test No. 4	Test No. 5	Avg.	COV (%)
Spline	-	14.1	24.7	37.6	33.4	27.4	37.9
Half-Lap	11.0	9.5	10.1	10.8	12.6	10.8	10.9
Steel Plate	8.3	9.3	8.8	10.5	25.0	12.4	57.1

The steel plate connection yielded low ductility ratios with the exception of test No. 5 (M-SP-5) which had a reported ductility ratio of 25.0, which was 171% higher than average of the other four steel plate specimens. Excluding this test as an outlier would yield an average ductility ratio of 9.23 and a COV of 10.4%.Surface Spline Test No. 2 (M-SS-2) reported a decrease in ductility ratio of 55.8% compared to average of tests M-SS-3, 4 and 5. Eliminating this test as an outlier would yield an average ductility ratio of 31.9 and a COV of 20.6%. Higher and lower ductility ratios for M-SP-5 and M-SS-2 respectively, coincide with the higher and lower shear stiffness values reported in Section 4.2.3.

4.2.6 Monotonic Reference Deformation

Monotonic reference deformations (Δ_m) were calculated from the results of monotonic CLT connection testing. It is necessary to calculate Δ_m in order to provide a base deflection

amount for controlling the test machine's actuator for cyclic (reversed) testing. This capacity is defined as the deformation at which the applied load drops, for the first time, below 80% of the load that was applied to the specimen according to ASTM E2126-11 (ASTM 2011). Upon completion of monotonic testing, Δ_m was calculated for each specimen tested. All Δ_m values were averaged according to the connection configuration. The results are presented in Table 4-8 below. Once Δ_m was found, it was multiplied by a reduction factor γ to account for the difference in deformation capacity between monotonic and cyclic testing in which cumulative damage leads to earlier deterioration in strength. A γ value of 0.6 was chosen as recommended by ASTM E2126-11 (ASTM 2011).

Table 4-8: Monotonic Reference Deformation (Δ_m) Values

Connection Configuration	Δ_m (inches)						$0.6\Delta_m$
	Test No. 1	Test No. 2	Test No. 3	Test No. 4	Test No. 5	Avg.	
Spline	-	1.144	1.194	1.199	1.368	1.226	0.736
Half-Lap	0.613	0.467	0.589	0.450	0.537	0.531	0.319
Steel Plate	0.831	0.596	1.222	1.010	1.559	1.044	0.626

A reference deformation value for Spline Test No. 1 (M-SS-1) was not available since testing of that specimen was terminated early as previously mentioned. The highest average Δ_m value was for the surface spline configuration while the lowest average Δ_m was for the half-lap joint. The reported $0.6\Delta_m$ values from Table 4-8 were used as the reference deformation capacity for cyclic (reversed) testing described in Section 3.4.2.

4.3 Objective 2 Results: Comparison of Results to NDS Predictions

4.3.1 NDS Yield Calculations

Yield limit calculations were performed for each of the connection configurations described in Chapter 3. The yield limit equations used are found in NDS Table11.3.1A (AWC 2012). For better comparison of predicted values to experimental results, values for fastener yield bending strength and dowel bearing strength were derived through testing and used as inputs in the yield limit equations. The results of fastener bending strength and dowel bearing strength are described in sections 4.1.1 and 4.1.2. The results of SG testing are found in section 4.1.3. The yield limit equations only consider loading parallel or perpendicular to grain, and not both simultaneously as exists in CLT. Therefore, yield limit calculations were performed for both loading conditions for connections containing lag screws. It was not necessary to calculate parallel and perpendicular lateral design values for the nailed connection since direction of grain is not a factor for fasteners with a diameter of less than 0.17-in. according to NDS Table 11.3.1B.

Yield modes I_m, I_s, II, III_m, III_s, and IV were calculated for each of the tested connection configurations. The minimum yield value of each of CLT connection configuration was chosen as the governing lateral design value, *Z*. The results are presented in Table 4-9. All calculations for connections containing lag screws used a fastener diameter equal to the measured root diameter of 0.178-in. A dowel bearing strength of 4,650 was assumed for the LVL according to NDS Table 11.3.3 (AWC 2012) and utilizing the minimum specific gravity of 0.50 reported by ESR-1210 (ICC-ES 2014) for the product. A dowel bearing strength of 61,850-psi was assumed for the 11-gage ASTM 653 steel side plate according to Footnote 2 of NDS Table 11P (AWC 2012). CLT dowel bearing strength was assumed as 5,170-psi as described in Section 4.1.2.

According to Footnote 1 of NDS Table 11.3.1B (AWC 2012), Reduction Terms (R_d) of 2.28 and 2.85 were calculated for lag screw connections for loading parallel to grain and perpendicular to grain respectively,

Table 4-9: Nominal Lateral Design (Z) Values for Yield Limit Equations

Connection Configuration	Fastener Diameter	I_m (lbs)	I_s (lbs)	II (lbs)	III_m (lbs)	III_s (lbs)	IV (lbs)
Spline //	0.178"	1629	635	535	539	229	**136**
Spline ⊥		1303	508	428	431	183	**109**
Half-Lap //	0.178"	984	1387	498	326	469	**139**
Half-Lap ⊥		758	1110	399	261	376	**112**
Steel Plate //	.162"	1287	547	521	533	**163**	205

Calculated *Z* values were then multiplied by the applicable adjustment factors for dowel-type fasteners from Table 10.3.1 of the NDS (AWC 2012) as well as the Format Conversion Factor (K_F), Resistance Factor (ϕ), and Time Effect Factor (λ) required for the Load and Resistance Factor Design (LRFD) method, to obtain the adjusted lateral design value, Z'. The resulting load (*Z'*) was then multiplied by the number of fasteners in each CLT panel face per the connection configuration in order to obtain the predicted connection strength of the total connection (Table 4-10).

Table 4-10: Adjusted Nominal Design Values and Predicted Connection Strengths

Connection Configuration		Z' Per Fastener (lbs.)	Total Connection Strength (lbs.)
Spline	//	176	527
	⊥	141	422
Half-Lap	//	181	542
	⊥	144	433
Steel Plate		212	1693

4.3.2 Comparison

Table 4-11 lists the average 5% offset yield loads obtained for each connection configuration from testing, the yields after the reduction term was applied, and the NDS predictions. For surface spline connections, adjusted values were lower than what was predicted by the NDS. Actual load in the parallel direction was 13.9% lower than the expected. Similarly, actual load in the perpendicular direction was 13.7% lower than expected according to the NDS prediction. Only one surface specimen, M-SS-1, exceeded the predicted values from NDS calculations. The adjusted values for M-SS-1 were 564-lbs. in the parallel direction, and 451-lbs. in the perpendicular direction. These values showed a 7.0% and 6.9% increase in strength compared to predicted values for the parallel and perpendicular directions respectively. M-SS-2 yielded the lowest adjusted loads for the surface spline group at 360-lbs. in the parallel direction and 288-lbs. in the perpendicular direction. These loads were 31.7% and 31.8% different with respect to the parallel and perpendicular directions. The NDS predicted a Mode IV failure for this configuration which is in line with the findings of the types of failures described in Section 4.2.4. However, several instances of Mode III_s failures were evidenced by fastener rotation also described in that section. Since observed and predicted failure was Mode IV, and since Mode IV failure is characterized by fastener bending and wood crush around the fastener at the connection interface, and not characterized by fastener rotation, it was assumed that the direction of grain of the CLT at the fastener interface governs the failure in the CLT. This seemed a safe assumption as long as there was a sufficient depth of material in that location. Following this assumption, perpendicular values would be the better metric for comparison.

Table 4-11: Average Yield Loads from Testing, Adjusted 5% Offset, and NDS Predictions by Connection Configuration

Connection Configuration	Average 5% Offset Yield Load (lbs.)	Adjusted 5% Offset (lbs.)		NDS Prediction (lbs.)	
		//	⊥	//	⊥
Spline	1,036	454	364	527	422
Half-Lap	1,527	670	536	542	433
Steel Plate	2,555	1,161		1693	

Average adjusted 5% offset values for the half-lap connection exceeded both predictions from the NDS. Adjusted load in the parallel direction was 19.1% higher, and 23.8% higher in the perpendicular direction than the predicted values from the NDS. All half-lap specimens yielded adjusted values higher than predicted. From specific test specimens, these adjusted values ranged from 5.8% to 42.5% higher than predicted. The yield limit equations predicted a Mode IV failure. Although a Mode IV failure does not include fastener rotation, the assumption of the governing layer as previously mentioned, may not be a safe assumption since the depth of the layer at the interface of the half-lap connection may not be sufficient since the depth is less than or equal to half of the depth of the center layer (depth ≤ 0.6875-in.).

The average adjusted 5% offset value for the steel plate connection was 31.4% lower than predicted by the NDS. Only one specimen, M-SP-1, came close to the NDS predicted value at 1,678-lbs., or a reduction in expected strength of only 0.9%. The other specimens ranged from 28.2% to 47.8% lower than predicted. Nail head shear-off could be one possible reason experimental results were much lower than predicted. Another factor contributing to lower values may be the result of the formation of a gap between the steel plate and the face of the CLT during testing as shown in the photograph in Figure 4-17. The NDS predicted a yield mode of III_s for the steel plate configuration, which is characterized by wood crush and fastener bending

in the main member and rotation of the fastener in the side member. Only minimal elongation of the nail holes was visible in the steel plate as seen in Figure 4-18.

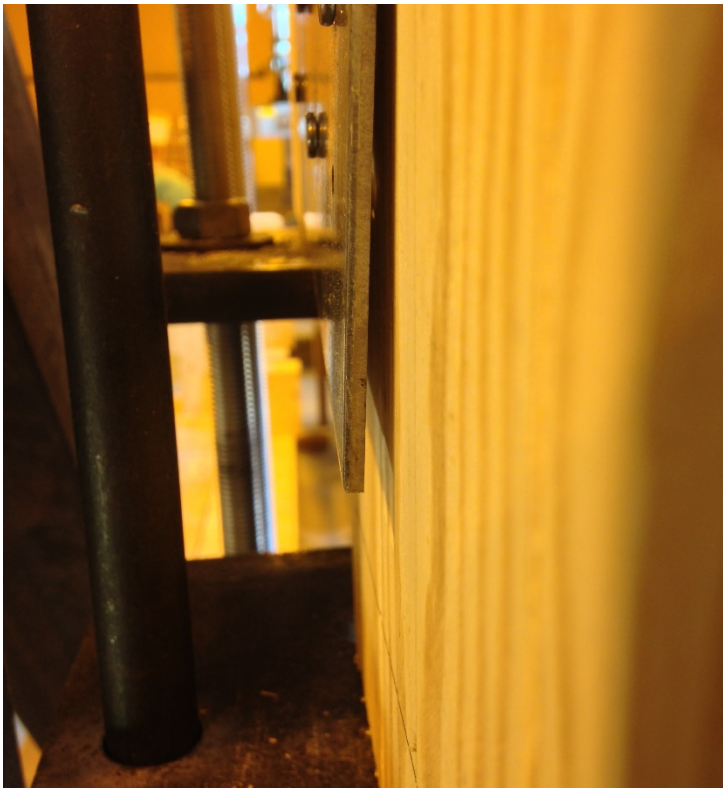

Figure 4-17: Photograph of the Development of a Gap between the Steel Plate and CLT During Testing

Figure 4-18: Elongation of Nail Holes in the Steel Plate

4.4 Objective 3 Results: Cyclic (Reversed) Connection Testing

This section describes the results of the cyclic testing of selected CLT joints. Five connections were tested for each of the three connection configurations for a total of fifteen tests. The testing procedure utilized the CUREE Basic Loading Protocol and the reference deformation capacities obtained from monotonic testing as described in Section 4.2.6. From cyclic testing, values for maximum load, shear stiffness were calculated, envelope curves were drawn, and failures were identified and reported in the following sections.

4.4.1 Load

The average maximum load obtained through cyclic testing for each connection configuration as well as the average maximum load obtained during monotonic testing are listed in Table 4-12. Cyclic maximum load is the maximum absolute value of load observed. The surface spline configuration had a range of cyclic maximum values from 2,025 lbs. to 3,900 lbs. The surface spline connection also had the greatest amount of variation with a COV of 28.1%, which was over twice the COV of the half-lap configuration and more than 7 times the COV of the steel plate. The half-lap configuration had a range of cyclic maximum values of 1,810 lbs. to 2,500 lbs. The steel plate configuration had a range of cyclic maximum values of 5,530 lbs. to 6,100 lbs.

Table 4-12: Average Maximum Load and COV from Cyclic and Monotonic Testing

Connection Configuration	Cyclic		Monotonic	
	Mean (lbs.)	COV (%)	Mean (lbs.)	COV (%)
Spline	2,820	28.1	4,050	26.8
Half-Lap	2,260	11.8	4,260	18.2
Steel Plate	5,780	3.9	4,950	6.5

Average cyclic maximum loads were much lower than the average monotonic maximum loads for the spline connection and the half-lap connection. The surface spline connection showed a reduction in average ultimate strength of 30.6% under cyclic loading. The half-lap connection had the highest average reduction in ultimate strength of 47.0% when subjected to cyclic loading. Conversely the steel plate connection had an increase in average strength of

16.6% when compared to monotonic tests. Trends in COV of maximum loads were similar between cyclic and monotonic results. COV from average cyclic maximum loads with the surface spline configuration, increased of 4.9% from monotonic results. Both the half-lap and steel plate configurations decreased in variation of 35.2% and 40.0% respectively when subjected to cyclic loads.

Lower average maximum values in cyclic testing were speculated to result from earlier fastener deterioration due to the effect of full-reversal cyclic loading. The greater cyclic average strength for the steel plate connection was due to the ability of the nail to resist deterioration and the visco-elastic response of the wood under a faster loading rate. In general, since wood is a polymer, it has the ability to resist higher loads when quickly loaded than when loaded at a slower rate. Therefore, higher fastener durability and increased wood mechanical properties are believed to be the main factors in the strength increase of the steel plate connection.

4.4.2 Loading Behavior: Hysteresis Curves and Envelope Curves

Upon completion of cyclic testing, load-deformation, or hysteresis, curves were generated for each tested specimen. Specimens were tested with two LVDTs, one placed on the front face and one placed on the back face near the connection. Deflection was taken as the average of the two deflections as recorded by the LVDTs. Once the hysteresis curves were modelled from load and deflection, envelope curves were generated for each specimen. Envelope curves were created by plotting the locus of extremities of the load-deformation hysteresis loops, which contains the maximum loads from the first cycle of each phase of the cyclic loading and

neglects points where the absolute value of the displacement at the maximum load is less than in the previous phase.

Figure 4-19 is a hysteresis curve with its corresponding envelope curve for a steel plate specimen. All other hysteresis curves can be found in Appendix B. A positive load value was generated by a downward force, while a negative load value was generated by an upward force. Ultimate load of the connections were observed in both the positive and negative load ranges. The points on the envelope curve were then averaged by phases and an average envelope curve was created for each connection configuration. These average envelope curves were then plotted against the composite curves from monotonic data.

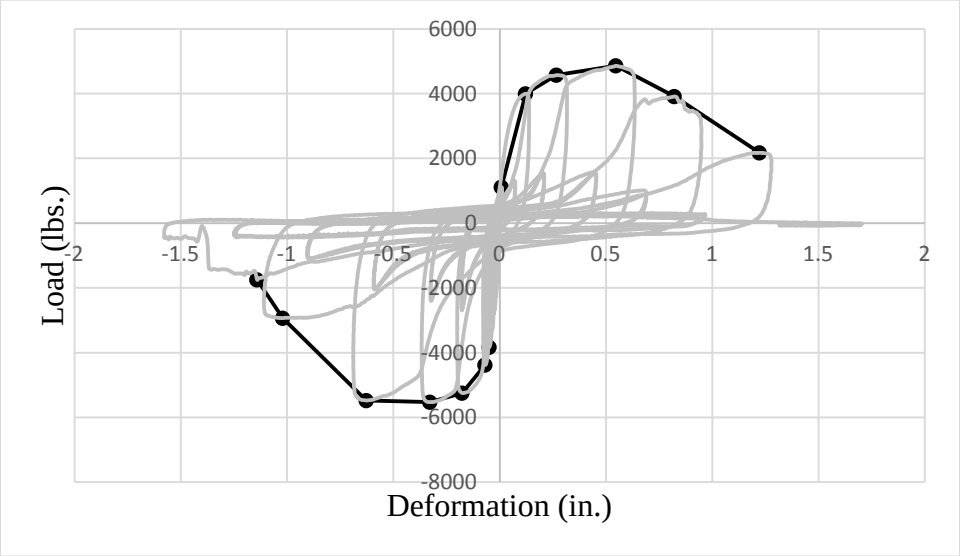

Figure 4-19: Hysteresis Curve and Envelope Curve for a Steel Plate Specimen

These composite monotonic curves were created by averaging the loads and deflections at the proportional limit, 5% offset yield limit, ultimate load, and where the load decreased by 20% of the ultimate load for each connection configuration. Figure 4-20 is graph of the composite monotonic curve against the graph of average cyclic envelope curve for the surface

spline connection. The composite monotonic curve has a higher initial stiffness than the envelope curve. The composite curve reached a higher maximum load than did the averaged envelope curve. The deflection at maximum load was also much higher for the monotonic curve than the deflection at maximum for the cyclic curve. This is evidence of the effect of fastener deterioration caused by cyclic loading. However, a 5% offset line when drawn on the cyclic envelope curve would yield a higher value than the yield loads obtained through monotonic testing. This is evidence of increased mechanical properties of wood under a faster loading rate as described in the previous section. The second increase in shear stiffness from fastener bending, wood crush and axial stresses acting on the fastener, as discussed in 4.2.2, is apparent in the cyclic curve but is not as prominent as seen in the monotonic curve.

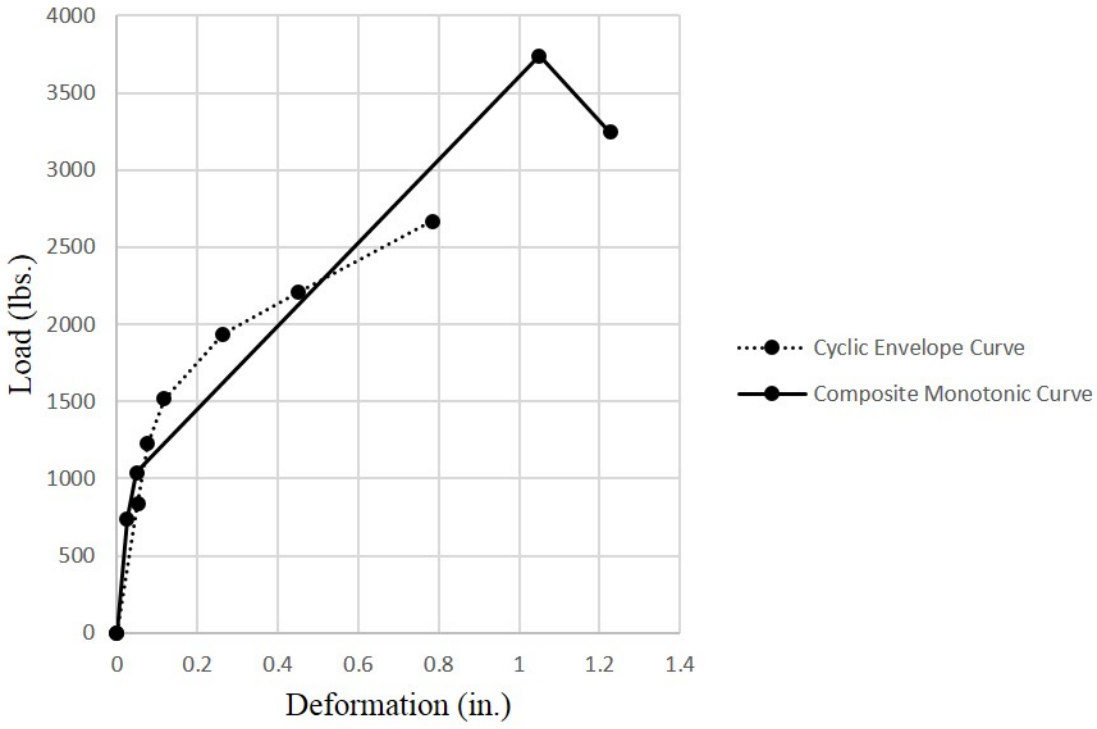

Figure 4-20: Graph of the Composite Monotonic Curve and Average Cyclic Envelope Curve for the Surface Spline Configuration

Figure 4-21 is a graph of the composite monotonic curve against the graph of average cyclic envelope curve for the half-lap connection. Several cyclic half-lap specimens experienced reduced load values at the second and third primary loops as seen in Figure 4-21. It is unclear what may have caused this to happen. Again, the monotonic curve reaches a higher maximum load value at a higher amount of deflection than the cyclic curve. Furthermore, the second increase in shear stiffness seen in the monotonic curve was not as pronounced in the cyclic specimens. According to Figure 4-21, shear stiffness, discussed in more depth in Section 4.4.3, of the two curves was very similar.

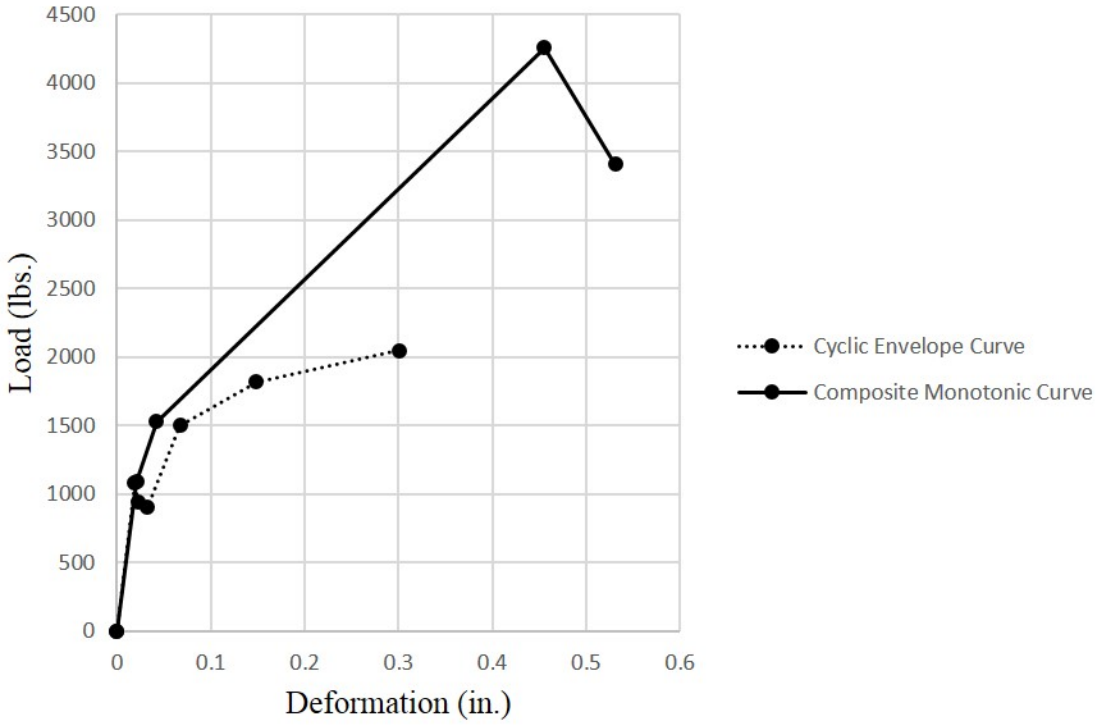

Figure 4-21: Graph of the Composite Monotonic Curve and Average Cyclic Envelope Curve for the Half-Lap Connection

Figure 4-22 is a graph of the composite monotonic curve against the graph of average cyclic envelope curve for the steel plate connection configuration. Unlike the spline and half-lap connections, the cyclic steel plate specimens experienced higher maximum loads than the monotonic specimens. Deflection amounts at ultimate loads were similar at 0.58-in. for cyclic testing and 0.63-in. for monotonic testing. Initial shear stiffness, discussed in Section 4.4.3, for cyclic steel plate specimens was greater than the average shear stiffness from monotonic testing. Again, this is most likely due to increased wood mechanical properties from a quicker load rate.

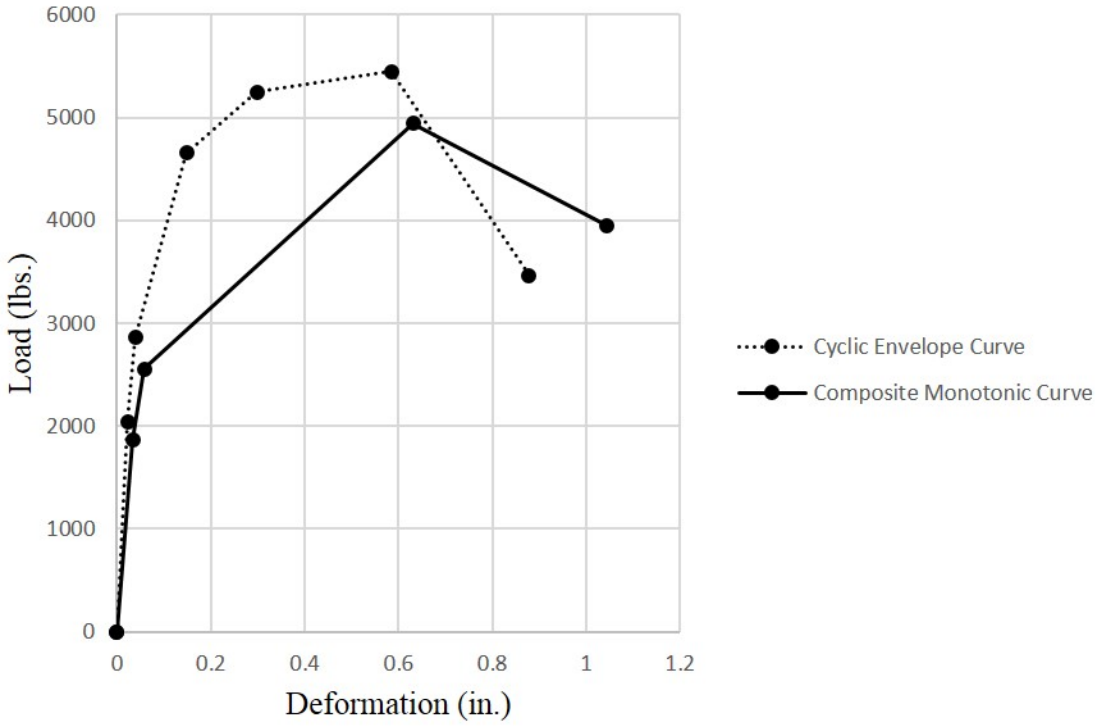

Figure 4-22: Graph of the Composite Monotonic Curve and Average Cyclic Envelope Curve for the Steel Plate Connection

4.4.3 Connection Stiffness

The average connection stiffness and the COV for each connection configuration from cyclic testing and monotonic testing are listed in Table 4-13. Connection stiffness of cyclic specimens was found by averaging the values of the positive and negative envelope curves. The resulting average was then plotted and shear stiffness was taken as the slope of the elastic region of the resulting load-deformation curve. Connection stiffness of monotonic specimens was found previously in Section 4.2.3.

Table 4-13: Average Connection Stiffness for Cyclic and Monotonic Connection Tests

Connection Configuration	Cyclic		Monotonic	
	Mean (lb. /in.)	COV	Mean (lb. /in.)	COV
Spline	24,800	48.3 %	33,200	55.6%
Half-Lap	57,100	47.7%	42,700	24.6%
Steel Plate	96,600	15.8%	58,100	38.2%

Average shear stiffness for cyclic spline specimens decreased by 25.3% over monotonic results. This reduction is due largely in part of specimen C-SS-4 which had a shear stiffness of only 6,200 lbs./in. Excluding this data set would give an average shear stiffness of 29,400 lbs./in. or a decrease of 11.3%. Both the half-lap and steel plate connections saw an increase in shear stiffness from cyclic testing. The half-lap experienced an increase of 33.5% while the steel plate experienced the greatest increase at 66.2%. COV between cyclic and monotonic spline specimens were similar. The half-lap connection had a COV nearly twice that reported for monotonic specimens. The steel plate specimen had a decrease in COV of more than half of the monotonic COV reported in Table 4-12. However, as discussed in Section 4.2.3, excluding data

set M-SP-5 would cause the remaining specimens to have a COV of only 10.2%. In this case, cyclic specimens would have experienced a higher degree of variation under cyclic loads.

4.4.4 Connection Failures

Upon completion of testing for each specimen, the resulting damage was observed and recorded. The observed failures for the cyclic spline specimens listed in Table 4-14. The two types of failures that occurred were splitting of the LVL due to the low resistance of shear parallel to grain in wood, and fastener failure. Fastener failure was due to the combination of fastener bending and the addition of axial stresses, in this case tension, acting on the fastener. Figure 4-23 a. and b. are photographs of damage from specimens C-SS-1 and C-SS-2.

Table 4-14: Observed Failures in Cyclic Surface Spline Specimens

Surface Spline Specimen	Observed Failures
C-SS-1	LVL split (shear parallel to grain).
C-SS-2	LVL split (shear parallel to grain)
C-SS-3	Fastener failure
C-SS-4	Fastener failure. LVL splitting began to occur
C-SS-5	Fastener failure

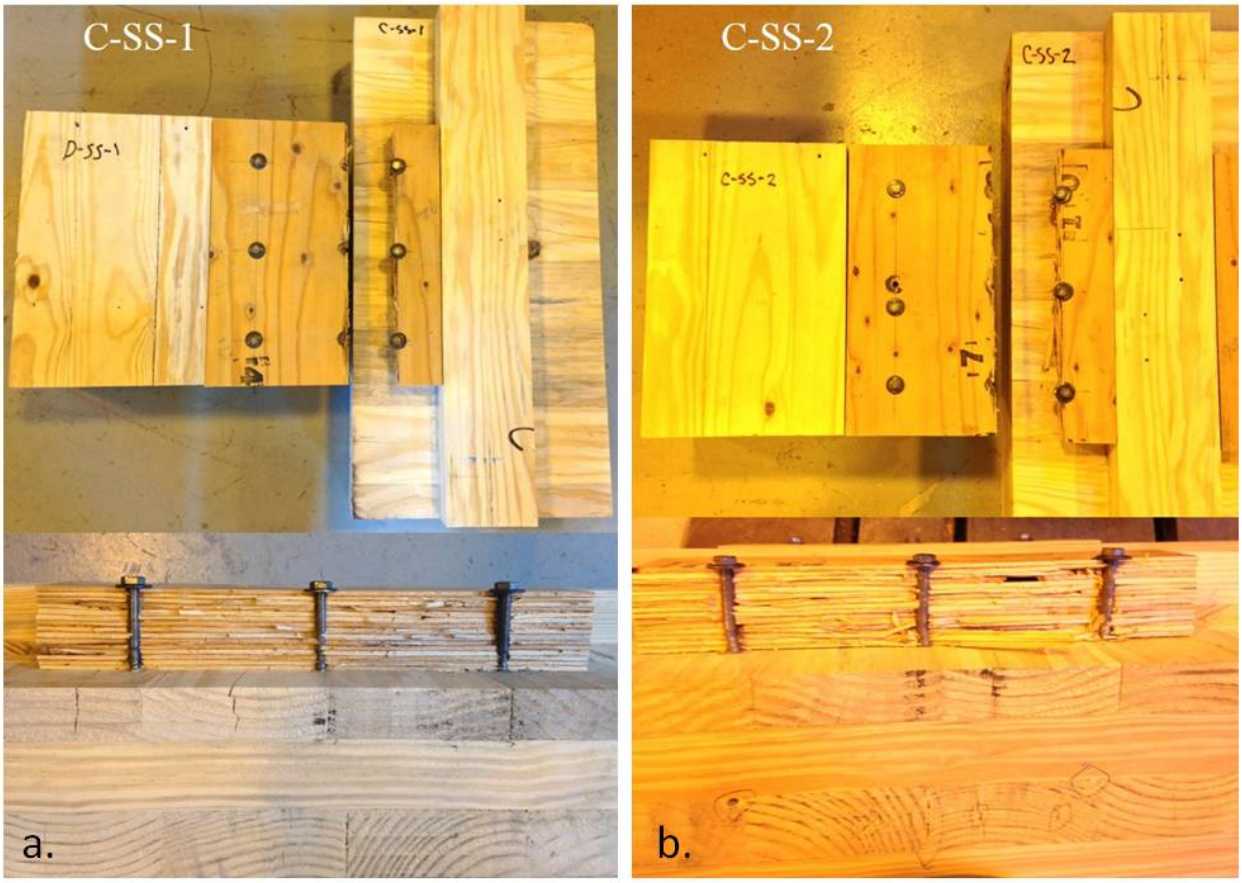

Figure 4-23: Photographs of Damages from Specimens C-SS-1 and C-SS-2

Cyclic spline specimens C-SS-3,4 and 5 all failed due to fastener failure. As the shear force caused the CLT panle to slide against the LVL spline, the wood around the fastener begins to crush and the fastener begins to bend. As deflection increases, the lag screw enters withdrawal mode. Resistance due to embedment of fastener threads in the wood, causes tension to develop in the fastener. This tension combined with cyclic fastener bending, causes deterioration of the fastener and eventually failure occurs. Figure 4-24 a. and b. are photographs demonstrating this type of failure in the cyclic spline specimens. Slight splitting of the LVL in C-SS-4 is apparent (Figure 4-25), however, this specimen ultimately failed due to fastener failure.

Figure 4-24: Observed Fastener Failure in Cyclic Spline Specimens

Figure 4-25: Partial Shear Parallel to Grain Failure in LVL Spline for C-SS-4

All cyclic half-lap specimens tested failed due to fastener failure. However, unlike other monotonic and cyclic specimens, this failure often resulted in fastener failure at two locations. Figure 4-26 is a photograph of segments of threaded fastener that was caused by the failure of the fastener in two different locations. This dual failure is evidence of the formation of two plastic hinges. NDS yield calculations discussed in Section 4.3.1 predicted a Mode IV yield for this connection configuration. The observed dual fastener failure is evidence that yield Mode IV is what occurred in cyclic tested half-lap specimens.

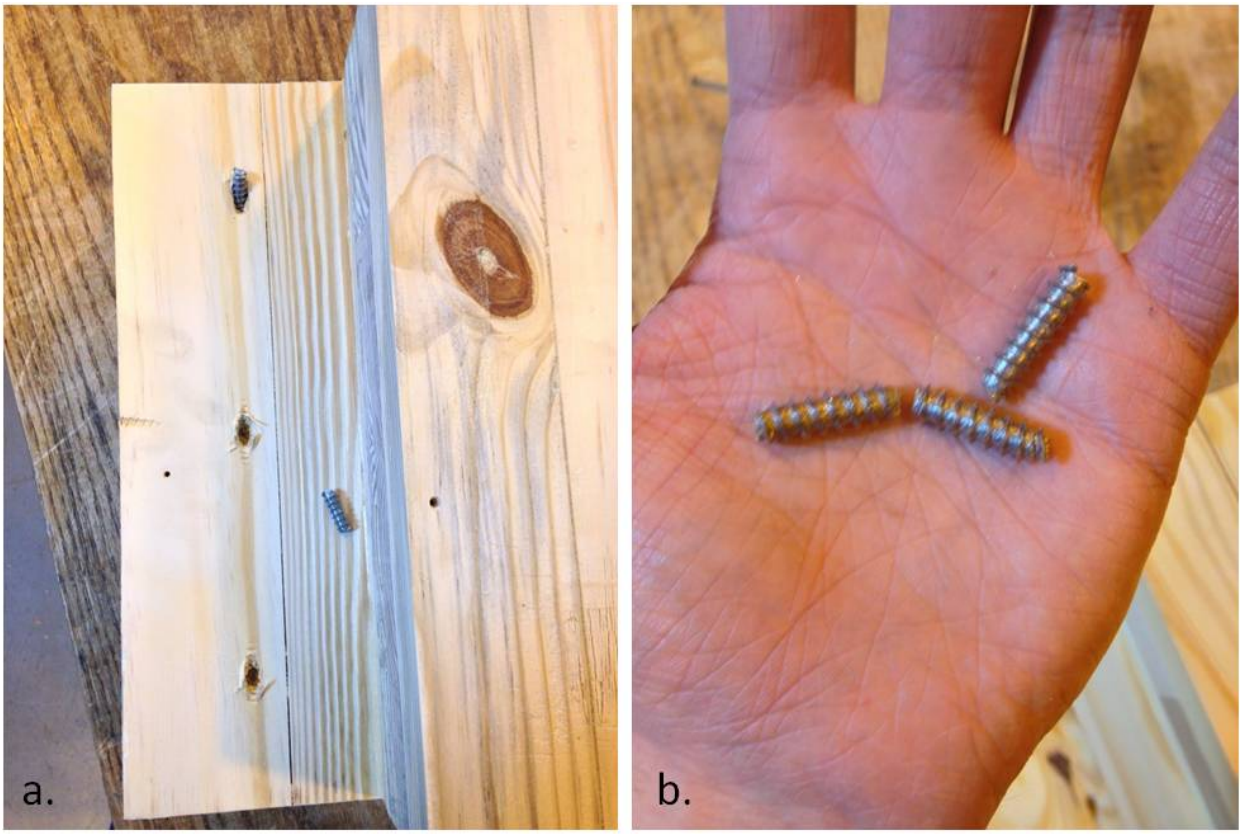

Figure 4-26: Photograph of Segmented Lag Screws from Cyclic Half-Lap Specimens

Cyclic steel plate specimens all experienced similar failures. Rotation of the steel plate from the cyclic shear force resulted in wood crushing at an angle to the grain direction in the face layer of the CLT as shown in Figure 4-27. This rotaion generated a shear force that acted perpendicular to the axis of the nail. This force was great enough to cause the nail heads to be sheared off at location of the steel plate. Nail heads were sheared off in much greater quantities from cyclic testing than monotonic testing. This can be attributed to the higher maximum loads obtained through cyclic testing, as well as the effect of fastener deterioration from cyclic loading. Figure 4-28 a. and b. are photographs depicting nail head shear-off. Red circles indicate locations where nail heads were sheared off. In three cases, C-SP-2,C-SP-3 and C-SP-5, the back and forth

sliding of the CLT panel against the steel plate caused a ratcheting effect that lead to fastener withdrawal. In the cases of C-SP-2 and C-SP-3, nail withdrawal was less than 0.5-in. However, C-SP-5 experienced complete withdrawal of one fastener. Figure 4-29 is a collection of photographs demonstrating this phenomenon.

Figure 4-27: Photograph of Diagonal Wood Crush Caused by Plate Rotation

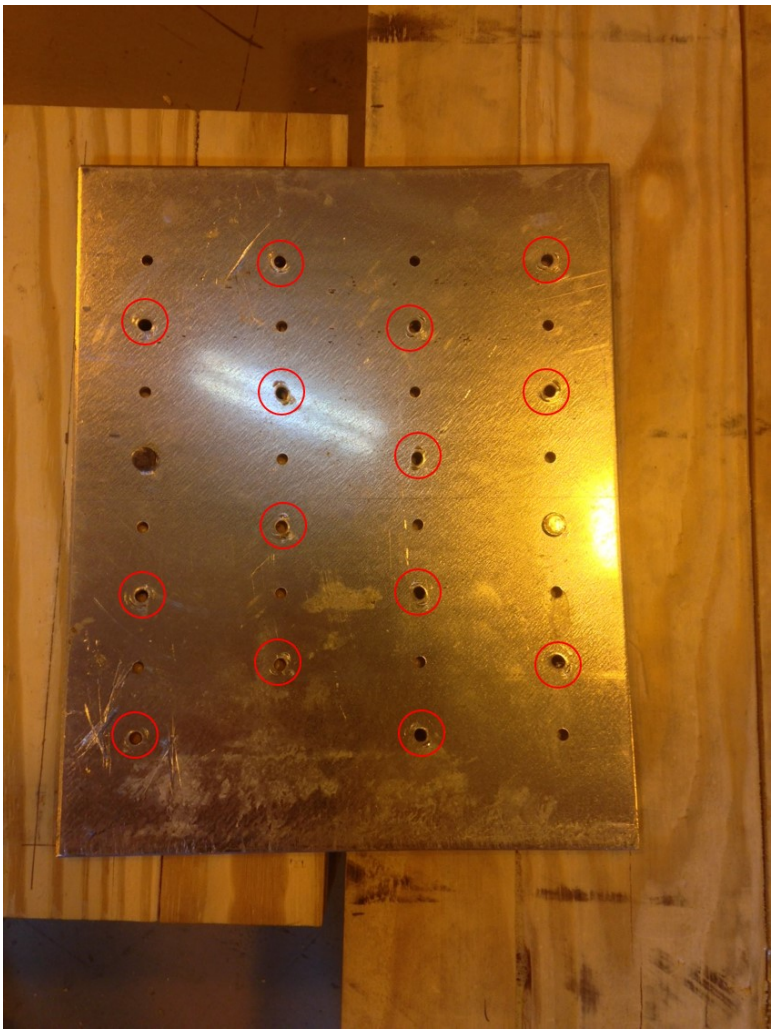

Figure 4-28: Photograph of Nail Head Shear-off in Cyclic Steel Plate Specimens

Figure 4-29: Photographs of Fastener Withdrawal from Steel Plate Specimens

Chapter 5: Summary and Conclusions

5.1 Summary

An investigation of lateral resistance of CLT connections was performed by measuring load and stiffness of three connection configurations: LVL surface spline, half-lap joint, and butt joint with a nailed steel plate. Connections were subjected to shear forces through monotonic and cyclic loading. Experimental results were then compared to predicted values from mathematical models presented in the NDS (AWC 2012). There were three main objectives for this research: (1) evaluate connection shear strength and shear stiffness of selected CLT joints through monotonic mechanical testing; (2) compare results of monotonic testing to predicted values from the NDS (AWC 2012); and (3) evaluate connection shear strength, shear stiffness and ductility of selected CLT joints through cyclic mechanical testing. Five specimens were tested for each of the three connection configurations for a total of 15 monotonic tests. From these results, ultimate load, 5% offset (yield) load, shear stiffness, failure type, ductility ratios and monotonic reference deformation was recorded. Yield loads were compared to corresponding predicted values from the NDS (AWC2012). Additionally, five specimens for each connection configuration were tested through cyclic loading for a total of 15 tests. Experimental results were compared to monotonic test results.

5.2 Conclusions

5.2.1 Monotonic Tests

In general, the butt joint with the steel plate connector demonstrated the most favorable results of the three connections. The yield load for the steel plate connection was 2.5 times

greater than the yield load for the LVL surface spline connection. Failure of the steel plate connection was much more delayed than the spline and half-lap connections and offered the least the amount of variation in the results. Conversely, the LVL surface spline yielded relatively poor results. Splitting of the LVL spline occurred often, resulting in a catastrophic failure type. Catastrophic failures were also observed for the half-lap connection due to snapping or shearing-off of fasteners at the connection interface.

5.2.2 Comparison to NDS Predictions

Adjusted loads from monotonic testing were approximately 14% lower than that predicted by the NDS (AWC 2012) for the surface spline connection. Likewise, adjusted values for the steel plate connection averaged approximately 31% lower values than that predicted by the NDS (AWC 2012). Only the half-lap connection exceeded NDS predictions with adjusted values averaging 21% greater than predicted. Predicted yield modes were similar to actual yielding in most cases with the exception of a few surface spline connections where a mix of yield modes were observed within a single specimen. In all, it would appear that the NDS (AWC 2012) values are not conservative enough for predicted CLT connections since actual loads were much lower than predicted. However, further research on the effects of moment from the test set-up used for this research should be investigated.

5.2.3 Cyclic Tests

Similar to monotonic results, the steel plate connection demonstrated better lateral resistance and better ductility than the surface spline and half-lap connections. Maximum loads for cyclic testing were much lower than loads for monotonic testing for the spline and half-lap connections. This was expected due to early fastener deterioration from full reversal loading. The

steel plate connection saw an increase in ultimate loads of nearly 17%. This increase is speculated to be the result of the ability of the nail to resist deterioration and the faster loading rate associated with the cyclic loading program. The surface spline specimen saw a reduction in shear stiffness when compared to monotonic results, while the half-lap and steel plate specimens experienced an increase in shear stiffness.

5.3 Limitations of Research

- Only one diameter and length of lag screw was tested.
- Only one diameter, length and shank type of nail was tested.
- Connection profiles in the CLT were “homemade” and not milled in a factory with precise tolerances.
- Only one type/brand of LVL was tested.
- Only one species of timber was tested.
- Effects of moment due to test set-up unknown.
- Only lag screws placed in-line were tested.
- Only one fastener spacing design was tested.
- Only specimens with a narrow range of moisture content were tested.
- Sample sizes were limited to five specimens per connection type.
- Only one load rate for monotonic testing was conducted.
- Only one cyclic loading protocol was conducted.
- No models for choosing fastener deterioration reduction factor available for computing monotonic reference deformation. (γ=0.6 used based on ASTM recommendation)
- Monotonic and Cyclic specimens were different sizes.

- Only dowel bearing for the parallel direction was used in calculations.
- Only tested panels with the outer face aligned parallel to one another.

5.4 Recommendations for Future Research

- Testing of connections using other diameters of lag screws.
- Examination of the effects of layer thickness on connection behavior. Does alternating grain direction matter after beyond a certain thickness?
- Examination of the effects of grain direction at the connection interface on connection behavior. Do the face layers at the connection govern behavior?
- Testing of different species of timber.
- Examination of the effects of different fastener spacings.
- Comparison of cyclic testing of connections to the NDS.
- Development of equivalent energy elastic-plasitc (EEEP) curves.
- Full scale monotonic testing of CLT wall panels conducted with non-proprietary fasteners and ASTM protocols.
- Full scale cyclic testing of CLT wall panels conducted with non-proprietary fasteners and ASTM protocols.
- Examination of the effects of various fastener threaded length on connection behavior.
- Adequate models needed for predicting CLT connection strength and stiffness.
- Explore the potential effects of moment from test set-up on experimental results.
- Testing of panels aligned perpendicular to one another.

References

Albright, D.G. 2006. The Effects of Bolt Spacing on the Performance of Single-Shear Timber Connections Under Reverse-Cyclic Loading. M.S. Thesis. Virginia Polytechnic Institute and State University. Blacksburg, VA, USA.

American Wood Council (AWC). 2012. National Design Specification for Wood Construction. American Wood Council, Leesburg, VA.

American Wood Council (AWC). 2014. General Dowel Equations for Calculating Lateral Connection Values - Technical Report 12. American Wood Council, Leesburg, VA.

ASTM D1761-12. 2012. Standard Test Methods for Mechanical Fasteners in Wood. ASTM International, West Conshohocken, PA.

ASTM D2395-14. 2014. Standard Test Methods for Density and Specific Gravity (Relative Density) of Wood and Wood Based Materials. ASTM International, West Conshohocken, PA.

ASTM D4442-07. 2007. Standard Test Methods for Direct Moisture Content Measurement of Wood and Wood-Base Materials. ASTM International, West Conshohocken, PA.

ASTM E2126-11. 2011. Standard Test Methods for Cyclic (Reversed) Load Test for Shear Resistance of Vertical Elements of the Lateral Force Resisting Systems for Buildings. ASTM International, West Conshohocken, PA.

Billings, M.A. 2004. Optimization of Spacing Between Bolts in a Row in a Single-Shear Timber Connection Subjected to Monotonic and Reverse Cyclic Loading. M.S. Thesis. Virginia Polytechnic Institute and State University. Blacksburg, VA, USA.

Blass, H. J., Fellmoser, P. 2004. Design of Solid Wood Panels With Cross Layers. World Conference on Timber Engineering, 2004. Vol. 14, No. 17.6, p.

Ceccotti, A. 2008. New Technologies for Construction of Medium-Rise buildings in Seismic Regions: The XLAM case, *Journal of the International Association for Bridge and Structural Engineering*, pages 156-165.

Dujic, B., Pucelj, J., Zarnic, R. 2004. Testing of Racking Behavior of Massive Wooden Wall Panels. Proceedings of the 37th CIB-W18 Meeting, Edinburgh, Scotland.

Gavric, I., Fragiacomo, M., & Ceccotti, A. 2012. Strength and Deformation Characteristics of Typical X-lam Connections. World Conference on Timber Engineering,2012. Auckland, New Zealand.

Hindman, D.P., Vaalnijarov, A., Richardson, B. L. 2015. Dowel Bearing Strength of Southern Pine Cross Laminated Timber Panels. Journal of Materials in Civil Engineering. In Preparation.

International Code Council – Evaluation Service (ICC-ES). 2014. ESR -1210: RigidLam Laminated Veneer Lumber (LVL) and RigidRim LVL Rimboard.

Johansen, K. W. 1949. Theory of Timber Connection. International Association for Bridge and Structural Engineering Publication, Vol. 9, 249-262.

Joyce, T., Smith, I., & Ballerini, M. 2011. Mechanical Behaviour of In-plane Shear Connections Between CLT Wall Panels. In Proceedings of the CIB Working Commission W18– Timber Structures. 44th meeting, Alghero.

Kennedy, S., Salenikovich, A., Williams Munoz, M. M., & Sattler, D. 2014. Design Equations for Dowel Embedment Strength and Withdrawal Resistance for Threaded Fasteners in CLT. World Conference on Timber Engineering, 2014. Québec, QC, Canada.

Lauriola, M., Sandhaas, C. 2006. Quasi-Static and Psuedo-Dynamic Tests on XLAM Walls and Buildings. *Cost E29 International Workshop on Earthquake Engineereing on Timber Structures*, pages 119-133, Coimbra, Portugal, 2006.

Mohammad, M., Muñoz, W. 2011**. "**Connections in Cross-Laminated Timber Buildings – Chapter 5" CLT Handbook – Cross Laminated Timber, FPInnovations Special Publication SP-528E, Canadian Edition.

Moosbrugger, T., Guggenberger, W., & Bogensperger, T. 2006. Cross-Laminated Timber Segments Under Homogeneous Shear – With and Without Openings. World Conference on Timber Engineering, 2006. Portland, Oregon. USA.

Muñoz, W., Mohammad, M., & Gagnon, S. 2010. Lateral and Withdrawal Resistance of Typical CLT Connections. World Conference on Timber Engineering, 2010. Riva del Garda, Italy.

Popovski, M., Schneider, J., & Schweinsteiger, M. 2010. Lateral Load Resistance of Cross-Laminated Wood Panels. World Conference on Timber Engineering, 2010. Riva del Garda, Italy.

Soltis, L.A.,Wilkinson, T. L. 1987. Bolted-Connection Design. General Technical Report FPL-GTR-54, USDA, Forest Service, Forest Products Laboratory, Madison, WI.

Soltis, L. A., Wilkinson, T.L. 1991. "United States Adaptation of European Yield Model to Large-Diameter Dowel Fastener Specification." Proceedings of the 1991 International timber engineering conference; 1991 September 2-5; London. London: TRADA; 3.43-3.49. Vol. 3.

Trayer, G.W. 1932. The Bearing Strength of Wood Under bolts. Technical Bulletin No. 332. USDA. Washington, D.C

Uibel, T., & Blaß, H. J. 2006. Load Carrying Capacity of Joints With Dowel Type Fasteners in Solid Wood Panels. In Proceedings. CIB-W18 Meeting.

Uibel, T., & Blaß, H. J. 2007. Edge Joints With Dowel Type Fasteners in Cross Laminated Timber. In Proceedings. CIB-W18 Meeting.

Vessby, J., Enquist, B., Petersson, H., & Alsmarker, T. 2009. Experimental Study of Cross-Laminated Timber Wall Panels. *European Journal of Wood and Wood Products*, *67*(2), 211-218.

Appendix A – Monotonic Load-Deflection Curves

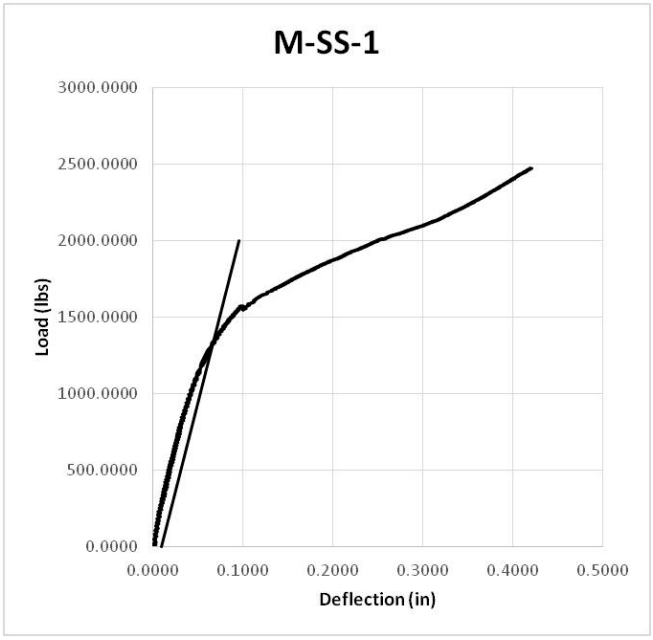

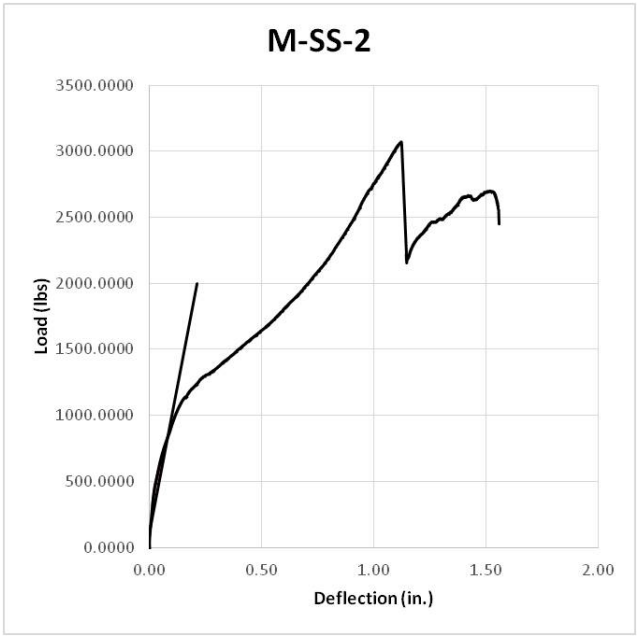

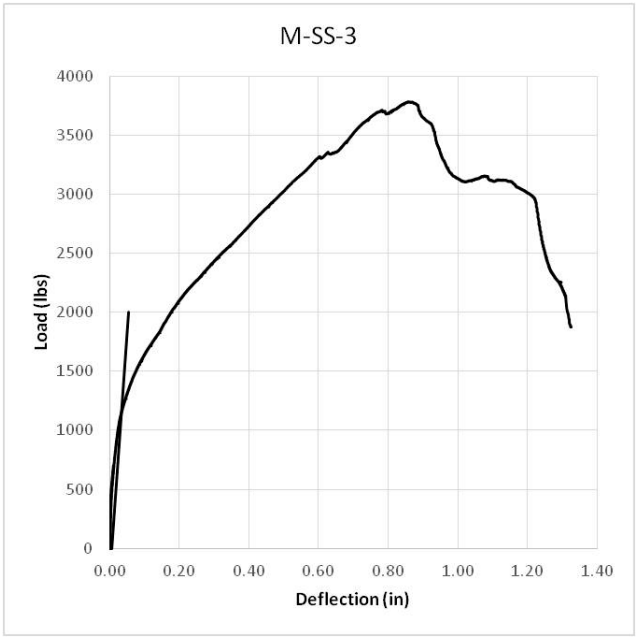

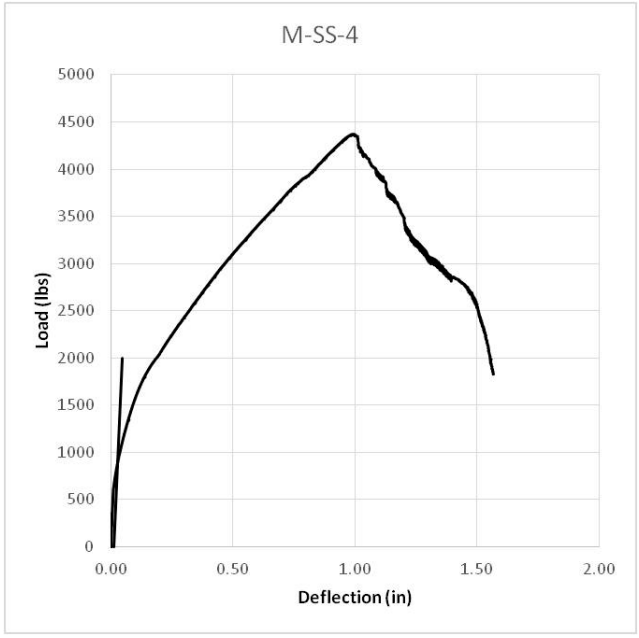

Appendix A – Monotonic Load-Deflection Curves (cont.)

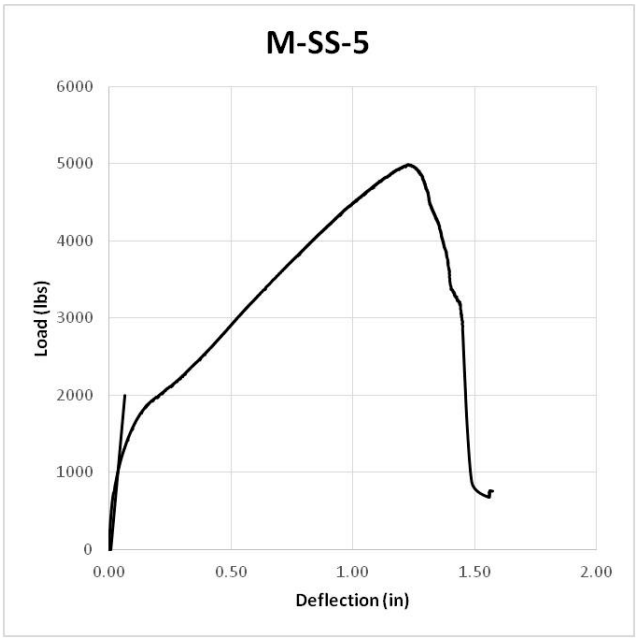

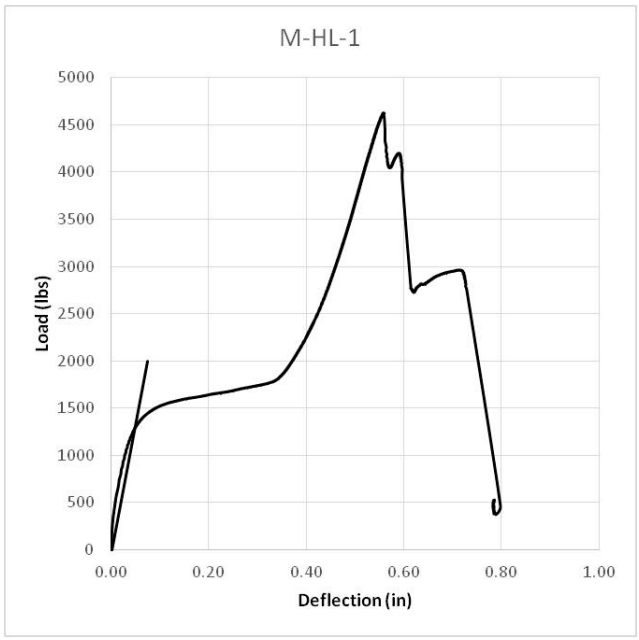

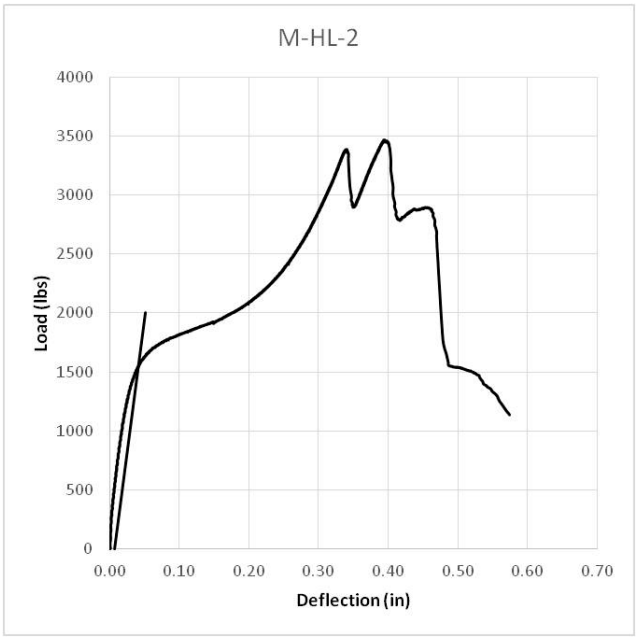

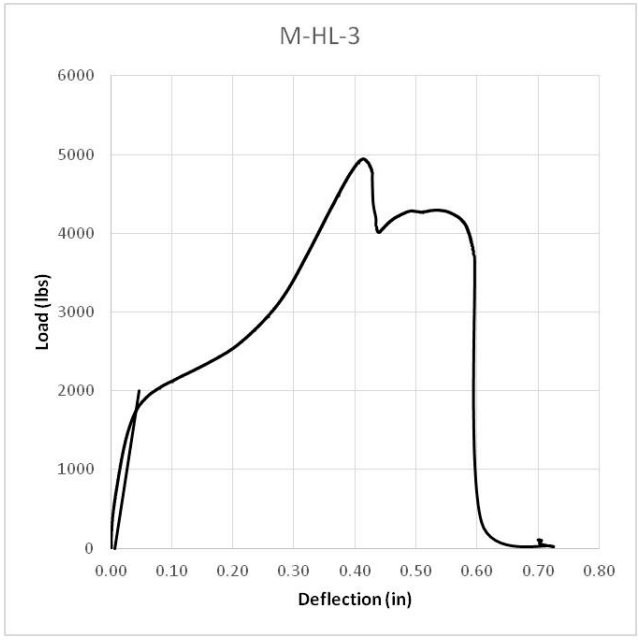

Appendix A – Monotonic Load-Deflection Curves (cont.)

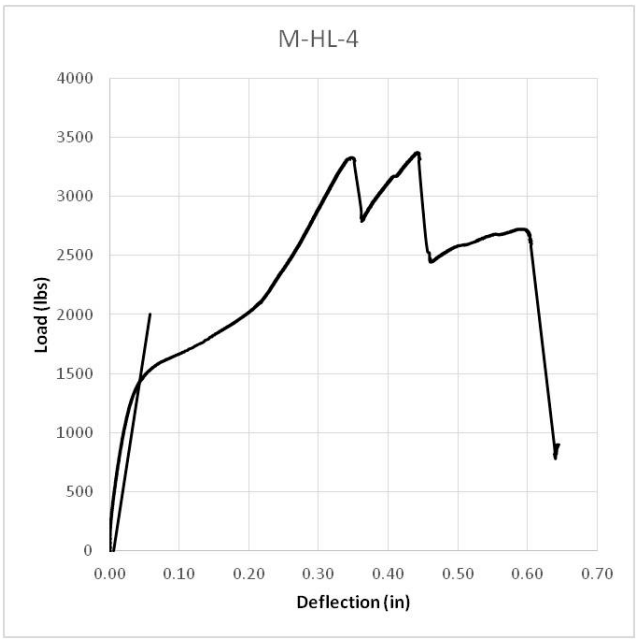

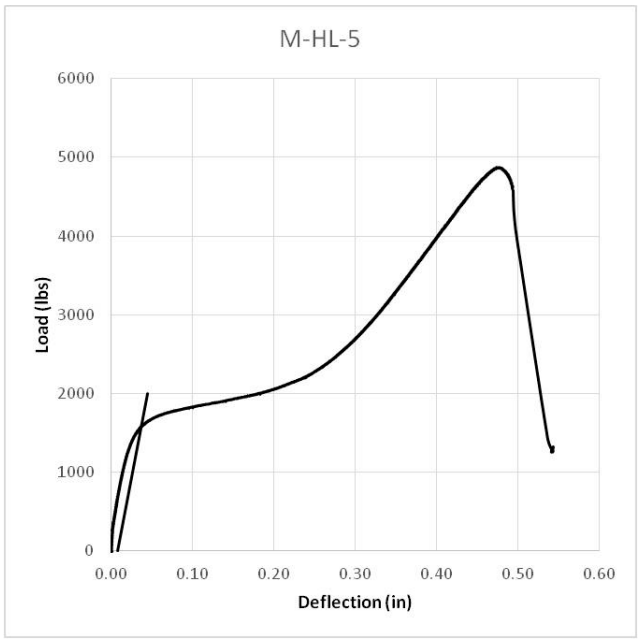

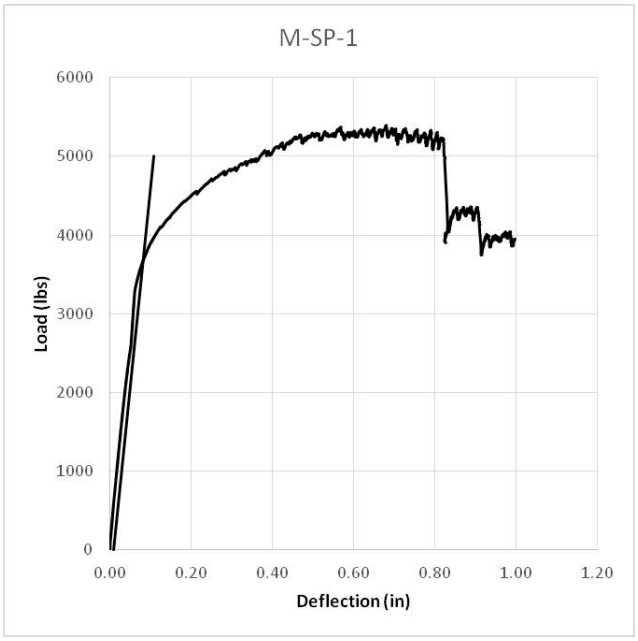

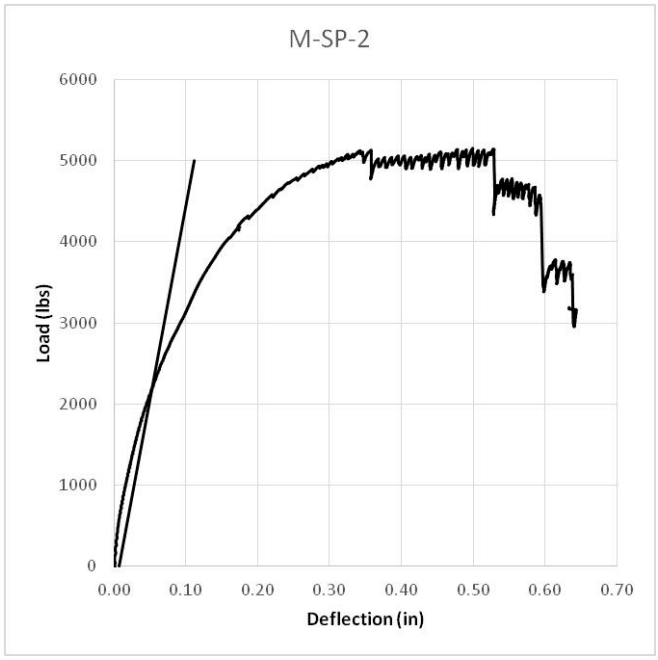

Appendix A – Monotonic Load-Deflection Curves (cont.)

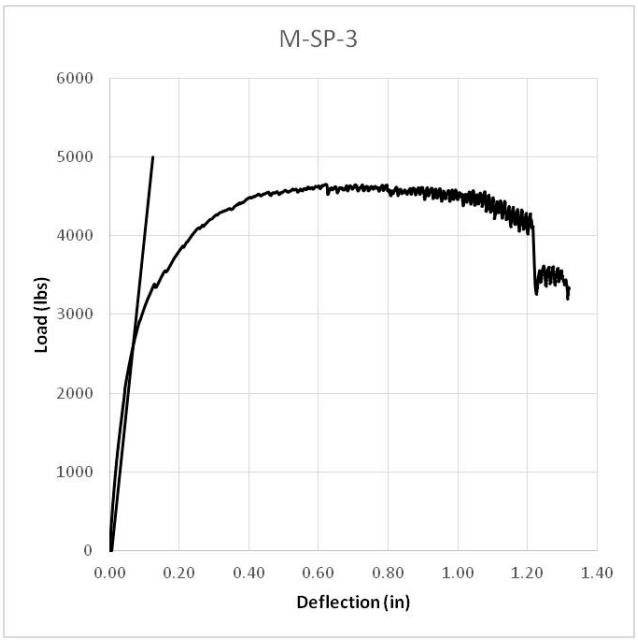

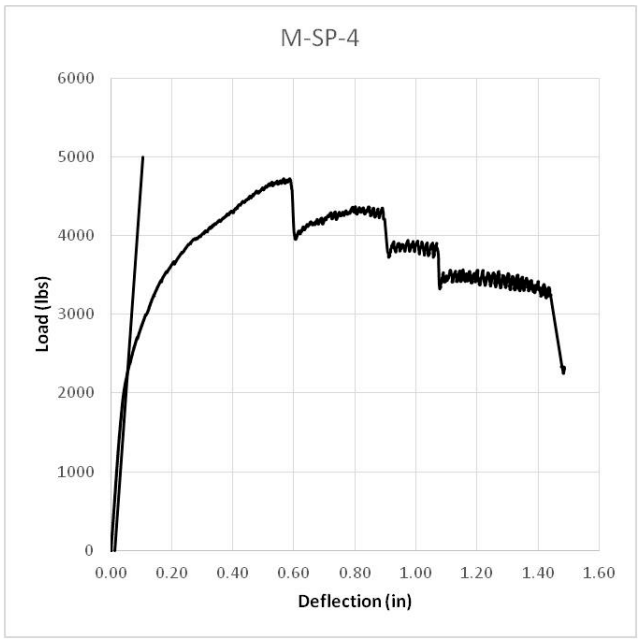

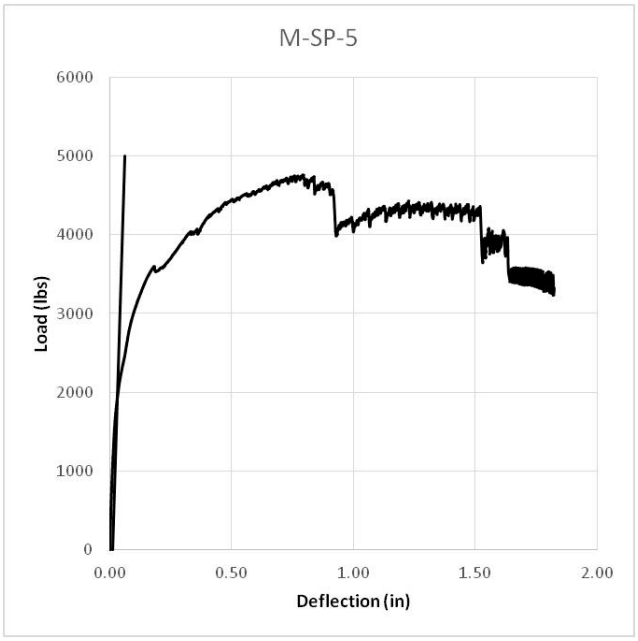

Appendix B – Cyclic Hysteresis Curves

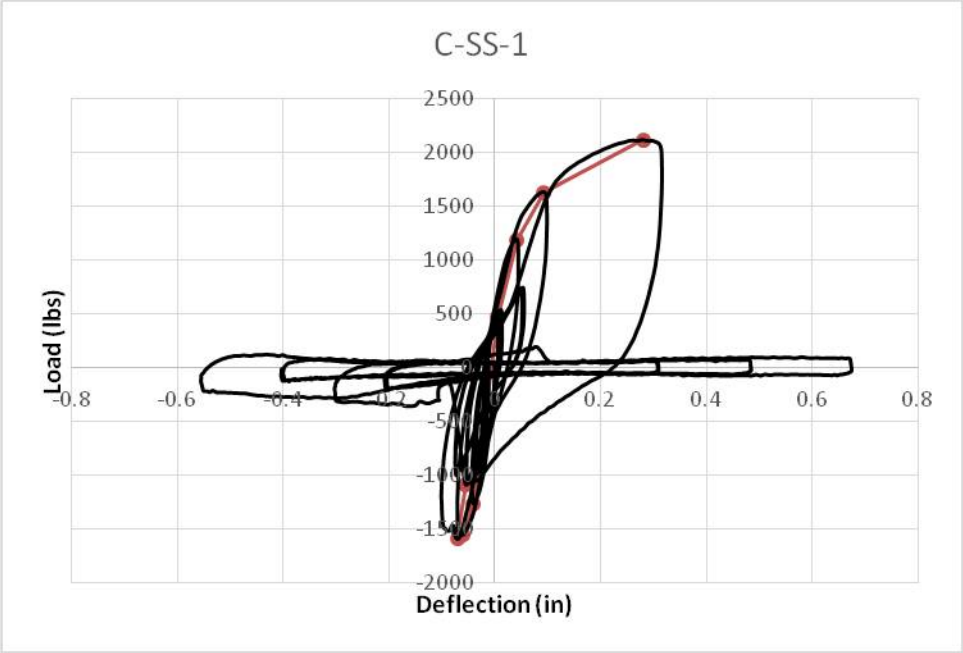

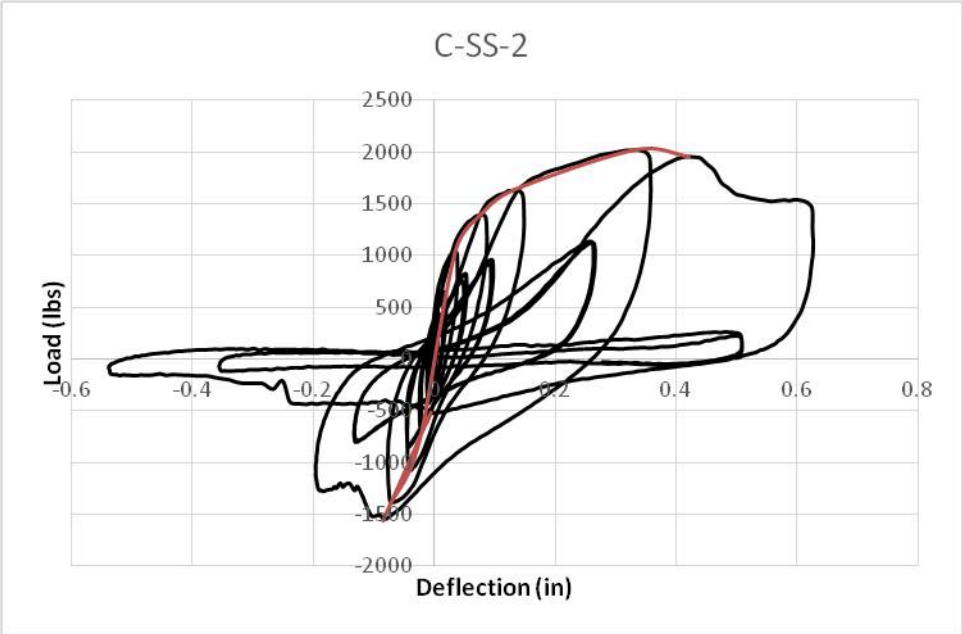

Appendix B – Cyclic Hysteresis Curves (cont.)

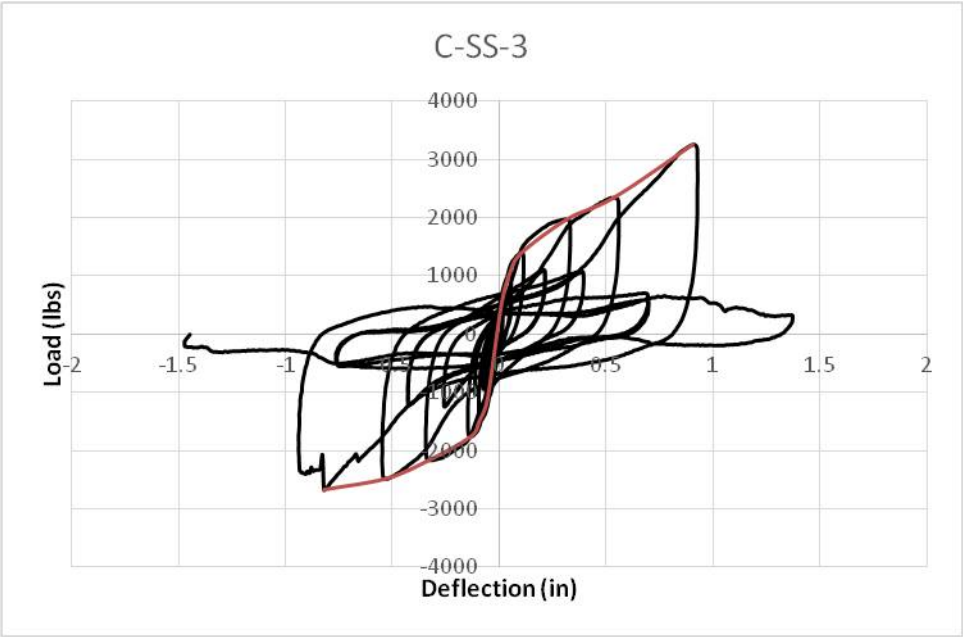

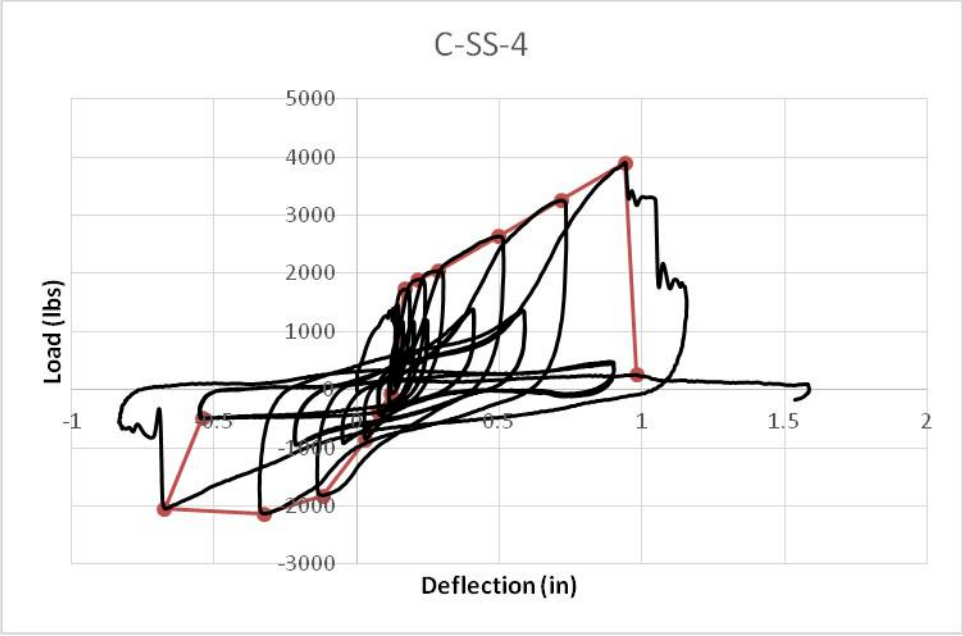

Appendix B – Cyclic Hysteresis Curves (cont.)

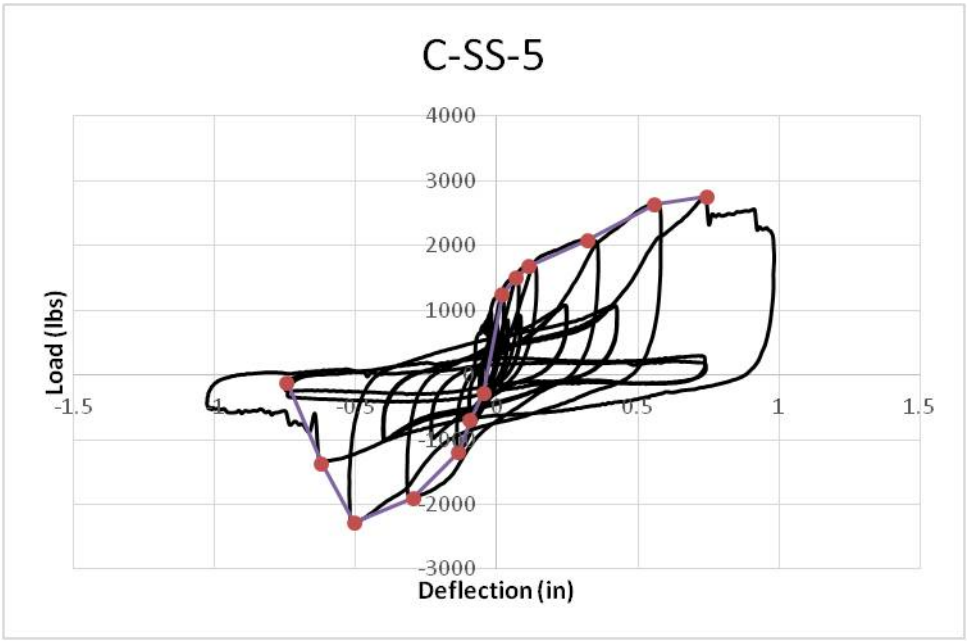

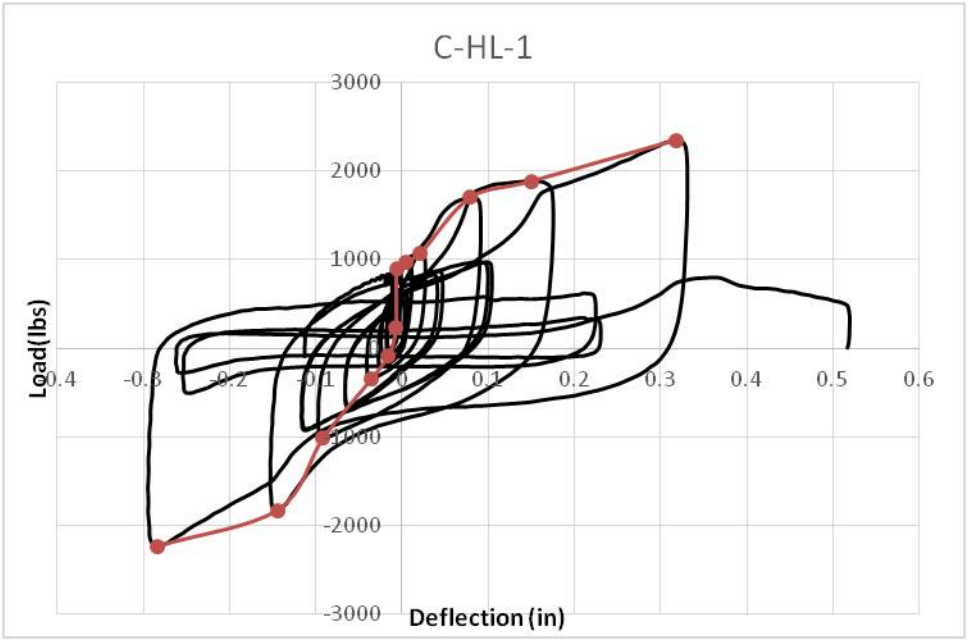

Appendix B – Cyclic Hysteresis Curves (cont.)

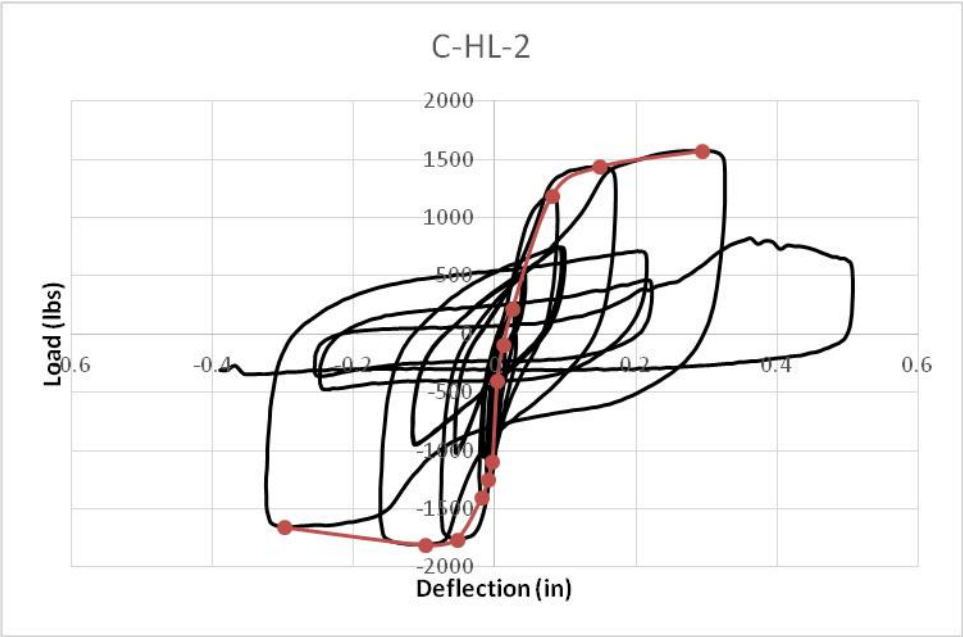

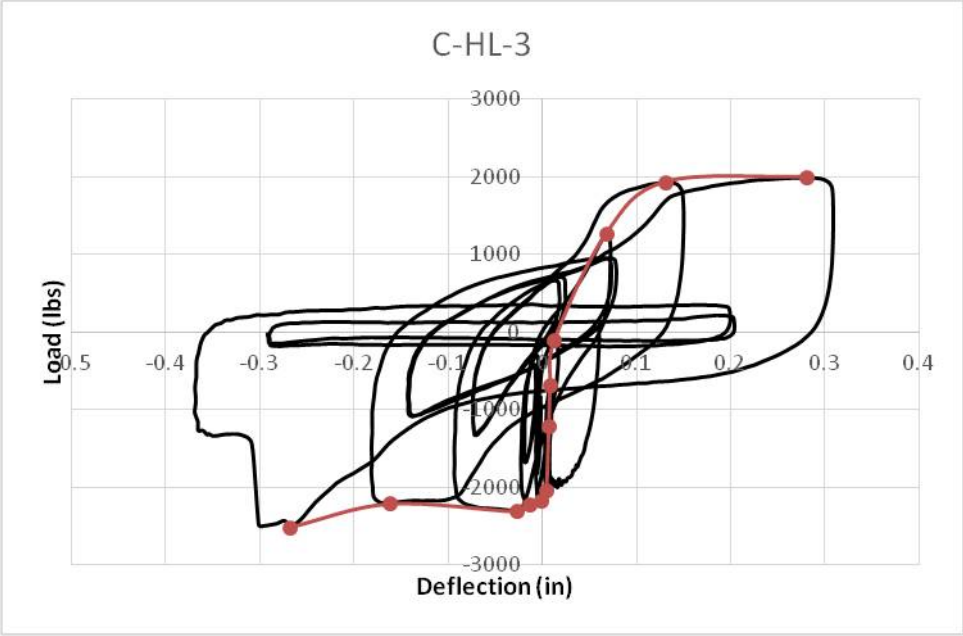

Appendix B – Cyclic Hysteresis Curves (cont.)

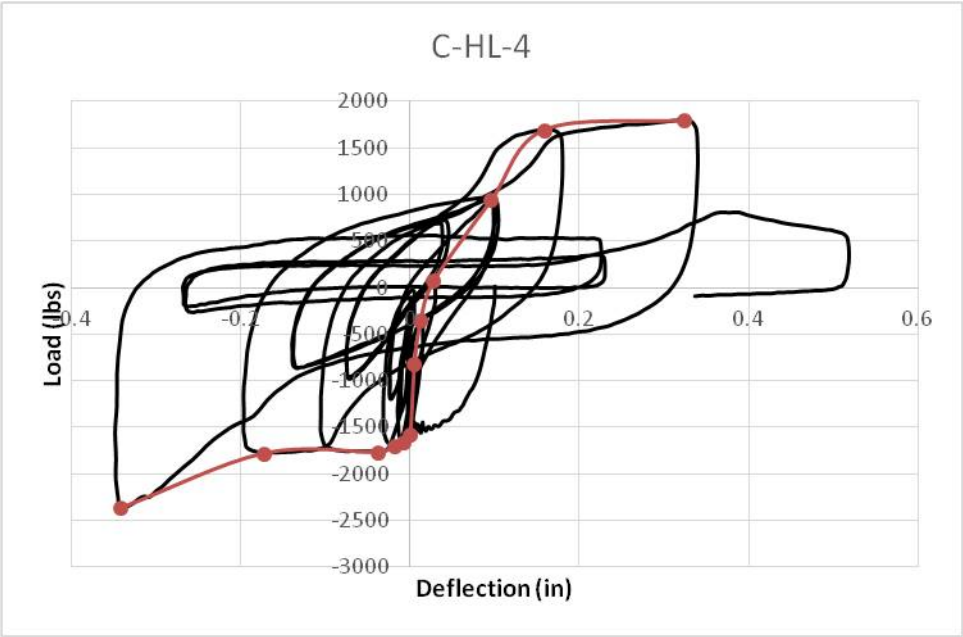

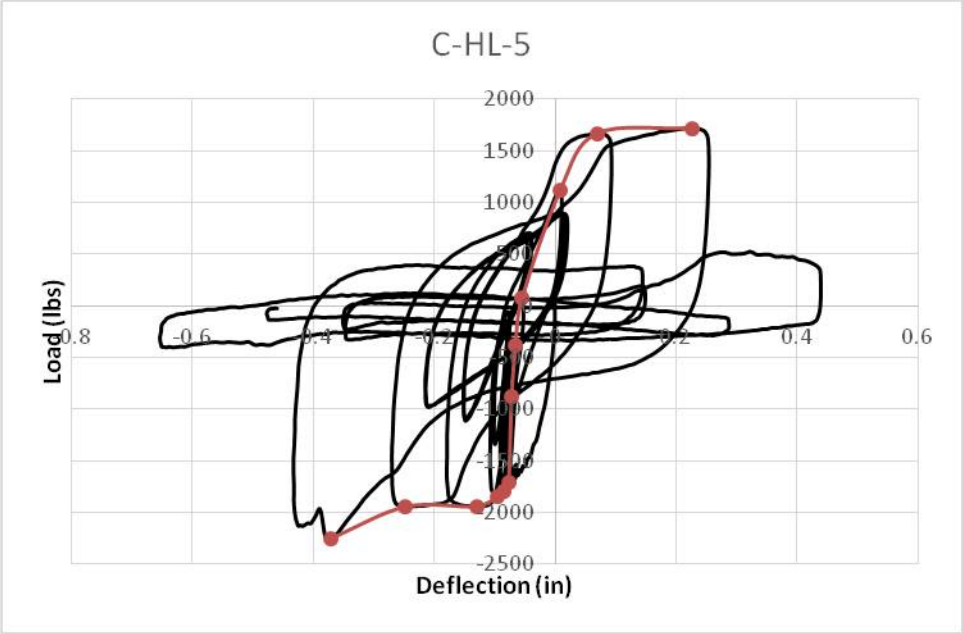

Appendix B – Cyclic Hysteresis Curves (cont.)

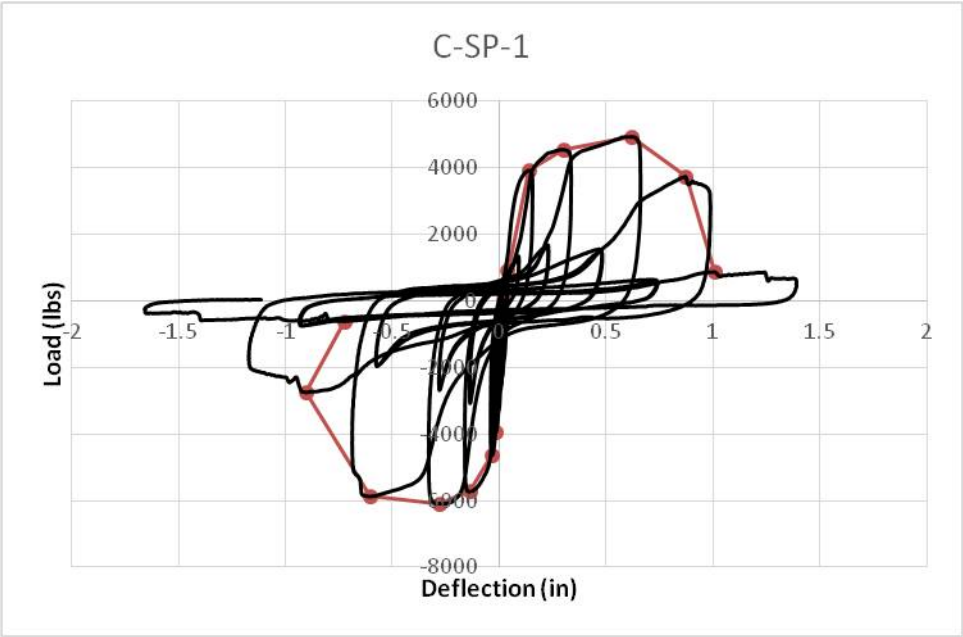

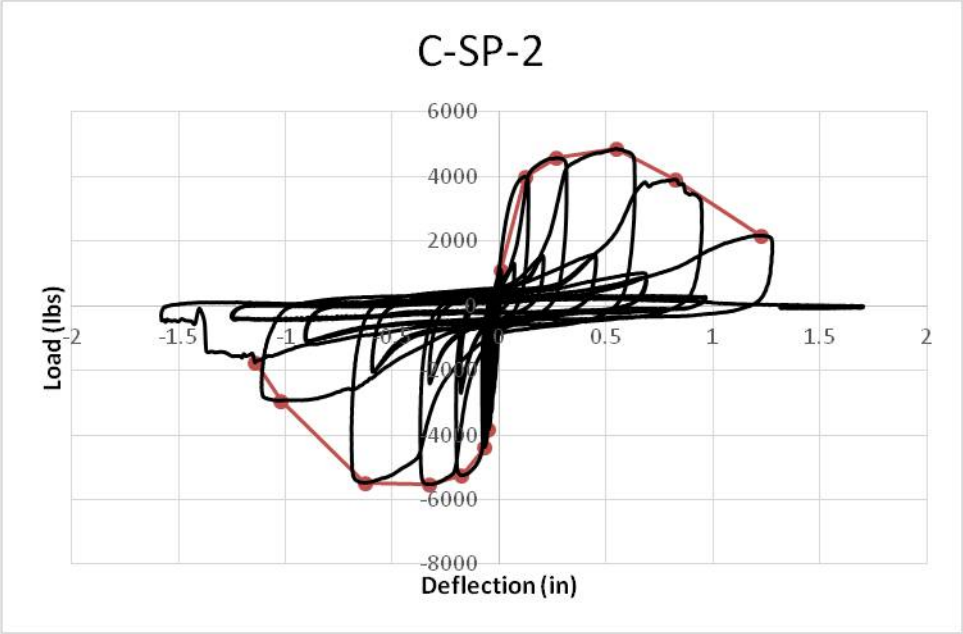

Appendix B – Cyclic Hysteresis Curves (cont.)

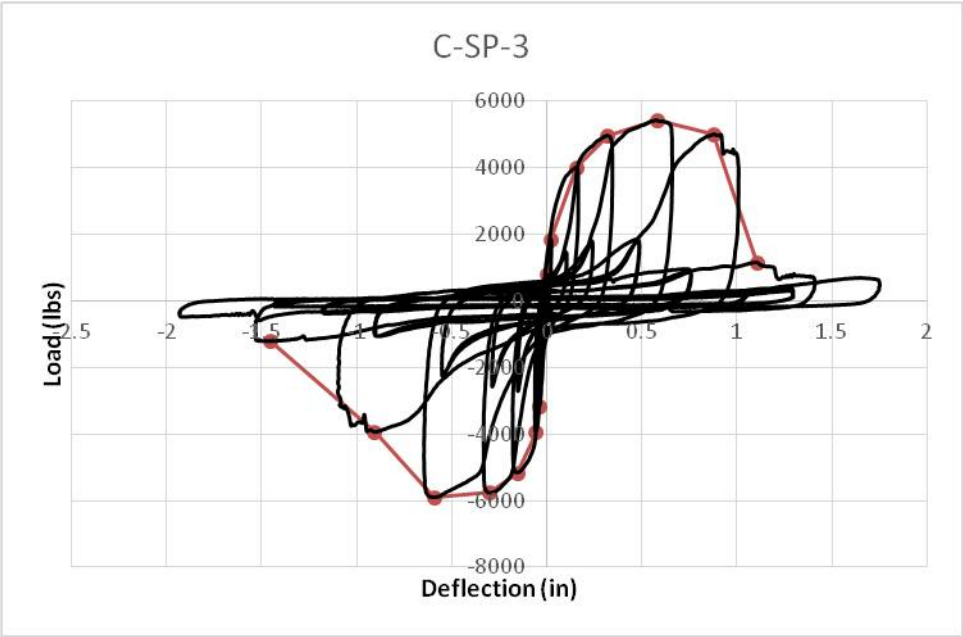

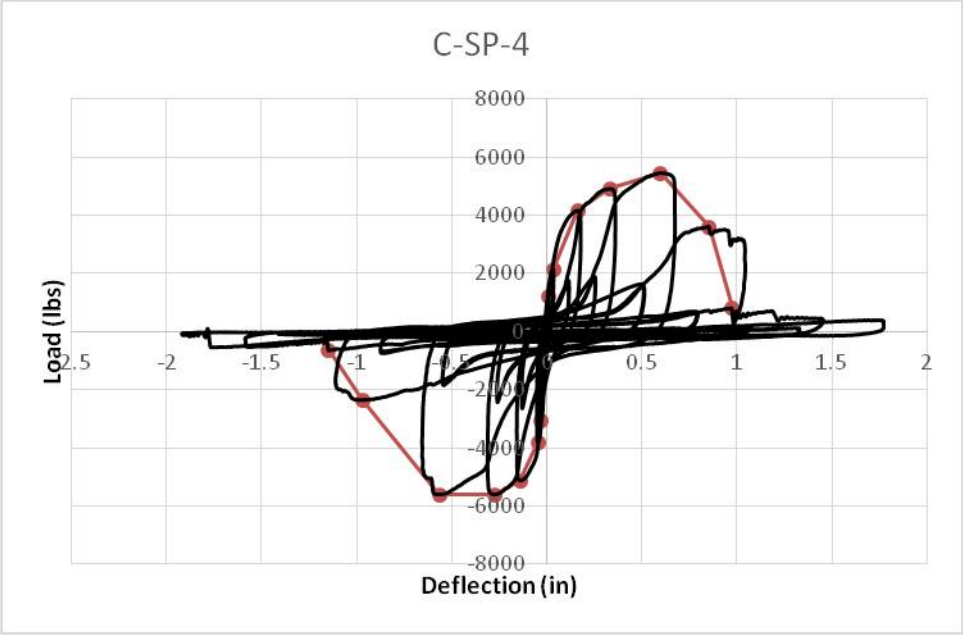

Appendix B – Cyclic Hysteresis Curves (cont.)